THE UNIVERSITY OF
SYDNEY

Mechanisms of photoprotection by 20-hydroxyvitamin D_3, a naturally occurring 1α25-dihydroxyvitamin D_3 analogue

Sally Eloise Carter

The Skin and Bone Research Group

Department of Physiology

Supervisor: Professor Rebecca Mason

Associate Supervisor: Dr Mark Rybchyn

"This thesis is presented as part of the requirements for the

award of the Degree of

Master of Philosophy (Medicine)

from the

University of Sydney"

January 2014

STUDENT PLAGIARISM: COMPLIANCE STATEMENT

I certify that:

I have read and understood the University of Sydney Plagiarism: Coursework Policy and Procedure;

I understand that failure to comply with the University of Sydney Plagiarism: Coursework Policy and Procedure can lead to the University commencing proceedings against me or potential student misconduct under Chapter 8 of the University of Sydney By-Law 1999 (as amended);

This work is substantially my own and to the extent that any part of this work is not my own I have indicated that it is not my own by acknowledging the source of that part of or those parts of the work

Name: Sally Carter

Signature: Sally Carter 29th August 2014

ABSTRACT

The active metabolite of vitamin D_3, 1, 25 dihydroxyvitamin D ($1,25(OH)_2D$) is produced in the skin following exposure to UVR. UVR also produces DNA damage in the form of premutagenic cyclobutane pyrimidine dimers (the majority of which are thymine dimers) and 8oxodG, and also causes immunosuppression. UVR-induced DNA lesions and immunosuppression eventually lead to photocarcinogenesis. It has previously been shown that $1,25(OH)_2D$ reduces direct DNA damage in a process that requires the non-genomic actions of ligand binding to the vitamin D receptor, including the opening of chloride channels. Mice with an ablated vitamin D receptor gene are more susceptible to photocarcinogenesis, however mice that do not contain the gene required to hydroxylate 25-hydroxyvitamin D to active $1,25(OH)_2D$ do not show greater susceptibility to produce UVR-induced skin tumours, suggesting the possibility of other photoprotective $1,25(OH)_2D$-like molecules present in the skin. Recently an alternate vitamin D metabolism pathway has been found in the skin involving CYP11A1 that produces 20-hydroxyvitamin D (20(OH)D), a vitamin D-like molecule that can bind to the VDR without producing the genomic effects of $1,25(OH)_2D$. Furthermore, previous reports show that tetrahydrocurcumin (THC), a metabolite of the spice curcumin, is an effective anti-oxidant at micromolar concentrations, but may potentially have $1,25(OH)_2D$-like photoprotective effects at nanomolar concentrations.

The current study tested whether 20(OH)D and THC would reduce UVR-induced DNA damage in primary human keratinocytes and Skh:Hr1 mice, and inflammatory oedema and immune suppression in Skh:Hr1 mice. Furthermore, the mechanism of photoprotection of $1,25(OH)_2D$ and 20(OH)D was tested using DIDS, a chloride channel inhibitor, shown to inhibit vitamin D non-genomic actions, as well as an inhibitor of Wnt, a procarcinogenic signalling protein.. Photoprotection with $1,25(OH)_2D$ was also assessed using Skh:Hr1 mice and oestrogen receptor-β knock out (ERβKO) mice, to examine whether firstly UVR-induced immunosuppression differed between males and females, and secondly whether the photoprotective effects of $1,25(OH)_2D$ and 20(OH)D were affected by gender.

20(OH)D and THC were as photoprotective as $1,25(OH)_2D$ against UVR-induced DNA damage in both primary human keratinocytes (8oxodG and thymine dimers) and Skh:Hr1 mouse skin (thymine dimers), 3 hours following UVR exposure. In primary human keratinocytes, use of DIDS reversed the protective effect of both $1,25(OH)_2D$ and 20(OH)D against thymine dimers The Wnt inhibitor alone was protective against UVR-induced thymine dimers, and did not cause reversal of the photoprotection by $1,25(OH)_2D$ and 20(OH)D. 20(OH)D was as effective as

$1,25(OH)_2D$ in reducing UVR-induced skin inflammation and immunosuppression in Skh:Hr1 mice. UVR-induced immunosuppression and DNA damage was greater in males than females, and at high doses $1,25(OH)_2D$ caused immunosuppression on its own. ERβKO mice were more susceptible to UVR-induced immunosuppression than wild type controls and the photoprotective effect of $1,25(OH)_2D$ and 20(OH)D was reduced.

This study showed for the first time that 20(OH)D is photoprotective against UVR-induced DNA damage, inflammation and immunosuppression, in the same non-genomic way as $1,25(OH)_2D$. Furthermore, the results show $1,25(OH)_2D$ mediated photoprotection is more pronounced in the presence of a functional ERβ, suggesting a potential interaction between ERβ and the actions of VDR ligands.

ACKNOWLEDGEMENTS

I would like to thank everyone who has helped and guided me through this research project.

First and foremost I would like to sincerely thank Professor Rebecca Mason for taking me on as a student and for her words of wisdom throughout this project. I am very grateful her support and understanding, especially during the labours of writing. This thesis was one of the hardest things I have ever had to do, and I am so lucky to an accomplished woman to look up to for constant inspiration.

Thank you to Dr Mark Rybchyn, my laboratory lifeline, who was always there to answer my many questions and aid in any mishaps! Thank you to Associate Professor Vivienne Reeve for the use for the animal house, her mice, and the proffering of her extensive knowledge, I would not have half this thesis if not for her. Thanks must also go to Dr Clare Gordon-Thomson for getting me started with the cells, and for always making time to help me when I needed it.

To Anna, I owe a huge thank you for all the time and energy she gave to help with the mice. I am so thankful for her friendship and I wish her the best of luck with her thesis.

Finally I would like to thank my friends and family for their understanding and support. Thanks must go to the Robinson family, without whom I would not be where I am today. To Mum, Dad, Hugh, Henry and Annabelle, thank you so much for your encouragement, love and support (both financial and moral), I am so lucky to have such a wonderful family.

TABLE OF CONTENTS

LIST OF FIGURES

LIST OF TABLES

1 INTRODUCTION

1.1 SKIN

1.1.1 Structure and function of the skin

As the largest organ of the adult human body, the skin is the body's first line of defence from stressors such as ultraviolet radiation (UVR) in the external environment. Making up 6% of total body weight with a thickness fluctuating between 1.5 and 4.0mm in different areas of the body, it consists of two layers, an external epithelium called the epidermis and an internal connective tissue called the dermis (Tobin, 2006), as shown in figure 1.1. There is an additional layer underlying the dermis known as the hypodermis connecting the skin underlying organs of the body. Each layer is made up of different cell types which have unique properties allowing for the holistic protective abilities of the skin.

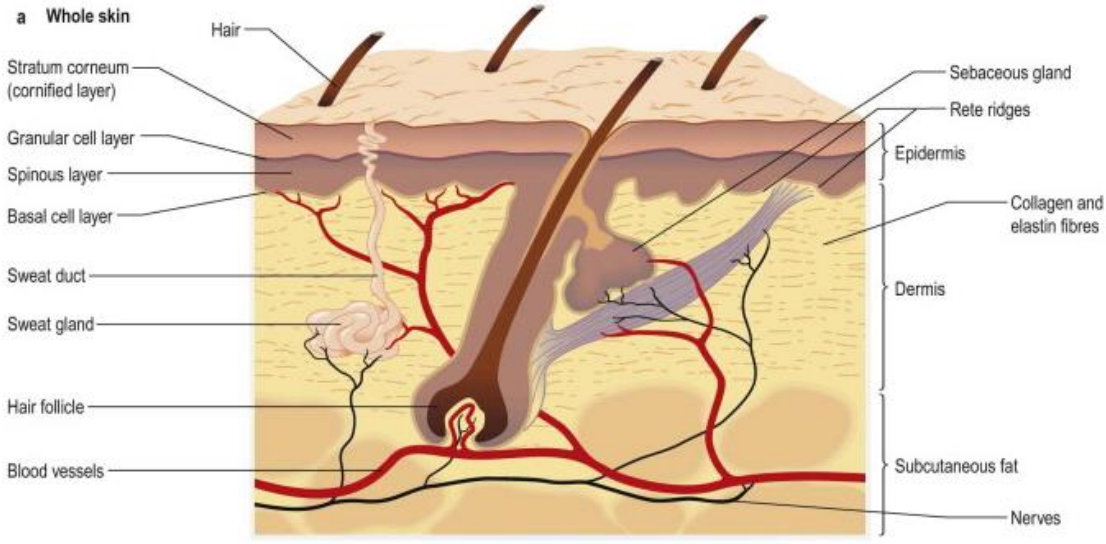

Figure 1.1 Structure of the whole human skin (Kumar and Clarke, 2012).

1.1.2 Epidermis

The epidermis consists of a specialised architecture of different cell types. As a protective epithelium, the epidermis is stratified; it has a stratum of four stacked layers of keratinocytes in a variety of morphologies, the most abundant cell type within the epidermis (~90%), as can be seen in figure 1.2. The remaining 10% of epidermis is made up of Langerhans cells, melanocytes and granstein cells which are dispersed amongst the four layers of keratinocytes (Kanitakis, 2002). From the bottom to top, these continuous layers of epidermal cells are known as the stratum basale, stratum spinosum, stratum granulosum and stratum corneum.

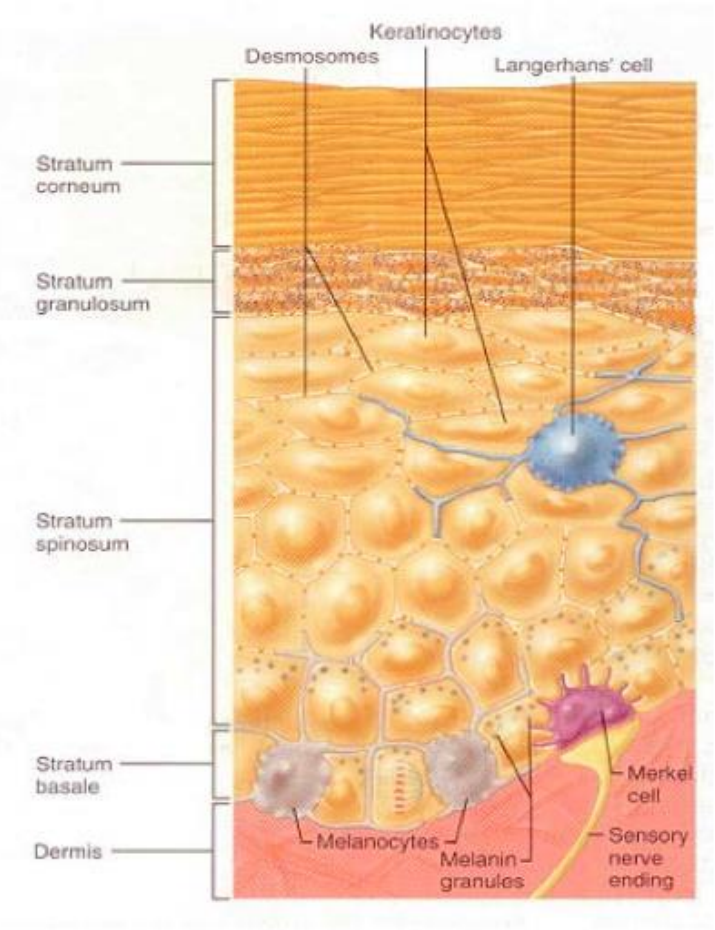

Figure 1.2 Structure of the epidermis (Marieb and Hoehn, 2012).

1.1.2.1 Keratinocytes

Basal layer keratinocytes are cubical in structure and lie anchored to the basement membrane which itself is connected to the vascularised dermis. These cells derive from mitotic divisions of stem cells and express proliferation antigens, which ensure constant renewal and growth. Newly divided basal keratinocytes undergo morphological differentiation and push older cells away from blood supply towards the superficial stratum corneum. Lack of oxygen and nutrients results in degeneration of the nucleus. At the stratum granulosum, keratinocytes develop protein rich keratin filaments and lamellar lipid filaments giving them a "grainy" appearance. In the process of self-directed destruction, the nucleus is digested and the cytoplasm is expelled. Keratin filaments form a tight cross-linked cytoskeletal structure covalently bonded with lipids resulting in cells with a flattened hexagonal cornified cell envelope which ultimately forms the impermeable stratum corneum (Baroni et al., 2012). This process of proliferation and desquamation gives keratinocytes a short life span of 25-45 days (Baroni et al., 2012). The rate of keratinocyte differentiation is largely dependent on application of pressure and friction, thus the soles of the feet contain thicker layers of cells than the eyelids or forehead (Baroni et al., 2012).

Additionally, it is well established that keratinocytes self-mediate growth and proliferation, and play a role in the skin immune response by the production of regulatory chemokines, cytokines, namely interleukins (IL) IL-1, -6, -7, -8, -10, -12, -15, -20 and tumour necrosis factor-α (TNF-α), growth factors such as epidermal

growth factor (EGF), and interferons (IFN) IFN-α, -β, and -γ (Williams and Kupper, 1996, Christensen and Haase, 2012). Whilst some mediators are released constitutively to a small extent in intact skin, production is stimulated following changes to the cutaneous environment, such as physical insult or irritant exposure (Corsini and Galli, 2000, Lippens et al., 2005) supporting the theory that the skin contains links between the multifactorial humoral immune system and cell-mediated immune system (Williams and Kupper, 1996).

1.1.2.2 Melanocytes

Melanocytes are distributed evenly amongst the basal layer of the epidermis and synthesise melanin, the most expressed pigment of the skin (Kanitakis, 2002). The production of melanin occurs within membrane bound melanosomes, as a result of the enzymatic activity of tyrosinase. Melanin granules reach neighbouring keratinocytes via transport along the melanocyte's dendritic processes and seek to accumulate on keratinocyte nuclei to protect from ultraviolet radiation (UVR) (Tobin, 2006).

Melanin pigmentation varies greatly amongst racial and ethnic origin, and it has been reported than there is an inverse relationship between melanin content in the skin and UVR- induced DNA damage (Tadokoro et al., 2003). Interestingly, albino epidermis contains melanocytes deficient in tyrosinase. Lack of tyrosinase-induced melanin production is manifest in the characteristic "white" skin highly prone to damage by UVR exposure.

1.1.2.3 Langerhans cells

These cells originate from haemopoietic stem cells of the bone marrow and migrate to the stratum spinosum of the epidermis. Also known as epidermal dendritic cells for their capacity to form a network through their dendrites, Langerhans cells remove and process invading antigens to present them to helper T-cells which then initiate a cell mediated immune response (Kanitakis, 2002). This part of the barrier protection of the skin is highly affected by exposure to UVR. UVR exposure initiates DNA damage of the Langerhans cell, altering antigen presenting functionality and ultimately suppression of local and systemic immune responses.

1.1.2.4 Merkel cells

Merkel cells are located in the basal layer of the epidermis and derive from the neural crest. These mechanoreceptors form synaptic junctions with free nerve endings arising from the dermis (Kanitakis, 2002).

1.1.3 Dermis

Beneath the basement membrane of the epidermis, lies a highly vascularised elastic connective tissue known as the dermis. It consists of dermal proteins, primarily collagens and elastins, fibroblasts, nerve endings, blood vessels and immune cells such as macrophages and mast cells. Most importantly, the dermis functions to support the epidermis with its elastic properties, and supply via its vascular network, oxygen and nutrients to the epidermis (Tobin, 2006). Like the epidermis, thickness of the dermis is highly dependent on pressure and anatomical location (Kanitakis, 2002).

1.1.3.1 Fibroblasts

The most abundant cell type in the dermis is the spindle-shaped fibroblast.

1.1.4 Hypodermis

This is the deepest layer of the skin and consists primarily of adipocytes, or "fatty cells". Ultimately, whilst the hypodermis provides a connection between the skin and underlying aponeuroses, it also provides insulation, protection from injury and a site for nutrient storage (Kanitakis, 2002).

1.1.5 Parallels in human and murine epidermal structure

Epidermal structure of the skin is generally uniform across mammalian species. In particular, humans and mice show similar hallmarks of keratinocyte mediated barrier formation and protection (Jane et al., 2005). Taking advantage of these similarities by using *in vivo* murine models of biological reactions of the skin has been hugely beneficial in understanding possible mechanisms of skin cancer formation in human skin, where *in vivo* models are not so readily available.

1.2 ULTRAVIOLET RADIATION (UVR)

1.2.1 Sources and types of UVR

Making up around 5% of terrestrial sunlight, UVR spans the electromagnetic spectrum between wavelengths of 100-400nm (Diffey, 2002, Pfeifer and Besaratinia, 2012). Due to the high variation in biological effects of wavelengths in the UV portion, UVR is further subdivided into three components increasing in energy; UV-A (320-400nm), UVB (280-320nm) and UVC (100-280nm) (Diffey, 2002). Stratospheric ozone filters out higher energy wavelengths below 290nm. However, since the 1970's evidence has arisen suggesting that the ozone layer is depleting, especially above Australia, leading to increased surface UVR levels (Makin, 2011).

UVR wavelength is inversely proportional to energy, however energy of the wavelength is directly proportional to its potential to cause DNA damage (Muthusamy and Piva, 2010). As shown in figure 1.3, UV-B wavelengths that reach the earth penetrate the depth of the epidermis and are known to cause direct damage to cellular DNA. On the other hand, long length UV-A radiation penetrates deeper into the dermis, altering metabolic mechanisms which ultimately result in indirect DNA damage. In the laboratory setting, UV-C wavelengths are absorbed by DNA 100 fold more readily than wavelengths of the UV-B range between 290 and 305nm (Besaratinia et al., 2011).

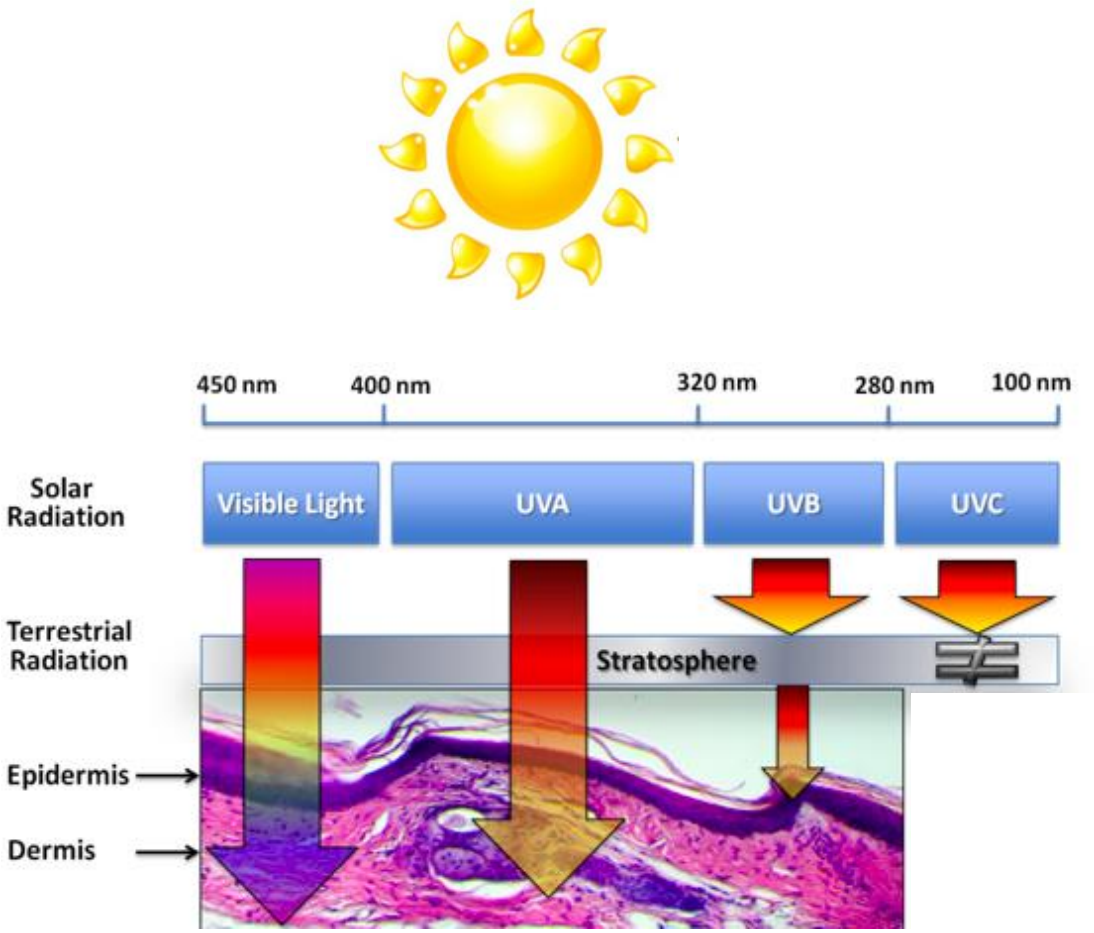

Figure 1.3 UVR penetrates different layers of the skin depending on the wavelength (modified from (D'Orazio et al., 2013))

1.2.2 Photoresponse to acute UVR exposure

1.2.2.1 Erythema (sunburn)

One of the more familiar skin reactions following exposure to acute doses of UVR in fair skin is the appearance of redness and erythema (inflammation) of the skin, characteristic of the common "sunburn" (Matsumura and Ananthswamy (2004). Erythema is a delayed biphasic photoresponse occurring around 2 to 48 hours after UVR exposure and may persist for several days, depending on the dose of wavelength of the spectral light. Irradiation from the UV-B kind causes faint

inflammation, which subsides more rapidly than its UV-A counterpart, which induces blister formation and extends the duration of its effect (Warin, 1978a).

It has been postulated that the mechanism of action of UV radiation on the formation of erythema is via prostaglandin (PG) activation in the skin and in dermal blood vessels increasing vasodilation (Warin, 1978a, Clydesdale et al., 2001).

1.2.2.2 Cornification

In addition to the rapid onset of UVR-induced skin inflammation, another skin photoresponse to an acute UVR exposure is the hyperplasia and cornification of the epidermis, in particular, the stratum corneum (Lippens et al., 2009, de Winter et al., 2001). From around 2 hour to 48 hours following insult, keratinocytes undergo an amplified process of cornification whereby suprabasal cells form the keratinic filament networks and become corneocytes. Basal keratinocytes differentiate at a more rapid rate to replace the resulting in hyperplasia of the epidermis. Cornification and hyperplasia eventuate into a thickening of the epidermis, evidently occurring as a form of photoprotection to decrease the diffusion of UVR reaching vulnerable cell layers in subsequent exposures (de Winter et al., 2001). Eventually the cornified cells are shed, commonly known as “peeling” (de Winter et al., 2001).

1.2.2.3 Melanogenesis

Along with defensive epidermal thickening, the skin stimulates melanin synthesis to protect against the damaging effects of UVR. Melanin production following UV radiation exposure is biphasic, with an initial immediate pigment darkening (IPD)

occurring within minutes of UVR exposure, and a delayed tanning response seen 2-3 days later (Park et al., 2009, Kadekaro et al., 2003). The IPD response is induced primarily by UV-A portion, resulting in oxidation and redistribution of pre-existing melanin, forming nuclear caps over threatened keratinocytes (Matsumura and Ananthaswamy, 2004, Kadekaro et al., 2003). During the DT photoresponse to UV-B, melanocytes increase in number and activity, increase dendritic spread, with an additional increase in tyrosinase mRNA activity, producing suprabasal amounts of melanin (Matsumura and Ananthaswamy, 2004). Increased presence of melanin granules results in hyperpigmentation of the epidermis, known commonly as a "tan". Melanin is chromophoric, absorbing and scattering UV light and acts a rudimental, natural "sunscreen" for the skin (Kadekaro et al., 2003).

1.2.3 UVR-induced DNA damage

UVR is known to induce DNA damage via both direct and indirect insults to DNA conformation. DNA absorption of UVR leads to direct changes in nucleobase formation, resulting in cyclobutadipyrimidines or cyclobutane pyrimidine dimers (CPDs), and pyrimidine (6-4) pyrimidone photoproducts (Matsumura and Ananthaswamy, 2002, Cadet et al., 2005). Moreover, the primary DNA damage from UV-A radiation eventuates via oxidative stress to form the 8-oxo-7,8-dihydro-2'-deoxyguanosine (8-oxodG) DNA lesion (Pattison and Davies, 2006).

1.2.3.1 Direct DNA damage

DNA damage resulting from the absorption of UVR occurs at the site of two adjacent pyrimidines at the 5-6 carbon (C5-C6) double bond, generally between tandem cytosines or thymines (Brash, 1997). If the photoexcitation of the bond opens completely, the double bonds form a stable four membered cyclobutane ring with a neighbouring pyrimidine (e.g. T<>T thymine dimer), known as a CPD (Matsumura and Ananthaswamy, 2002, Ravanat et al., 2001). CPD formation is shown in figure 1.4. On the other hand, if the C5 bond opens and undergoes orientation rearrangement, this may form a single bond between the C5-C6 double bond of the 5'-end pyrimidine and the C4 group of the 3'-end pyrimidine, a 6-4PP (Ravanat et al., 2001, Brash, 1997). CPDs are the most prevalent DNA photoproduct from UV-B irradiation, produced several times more often than 6-4PPs (Ravanat et al., 2001, Matsumura and Ananthaswamy, 2002).

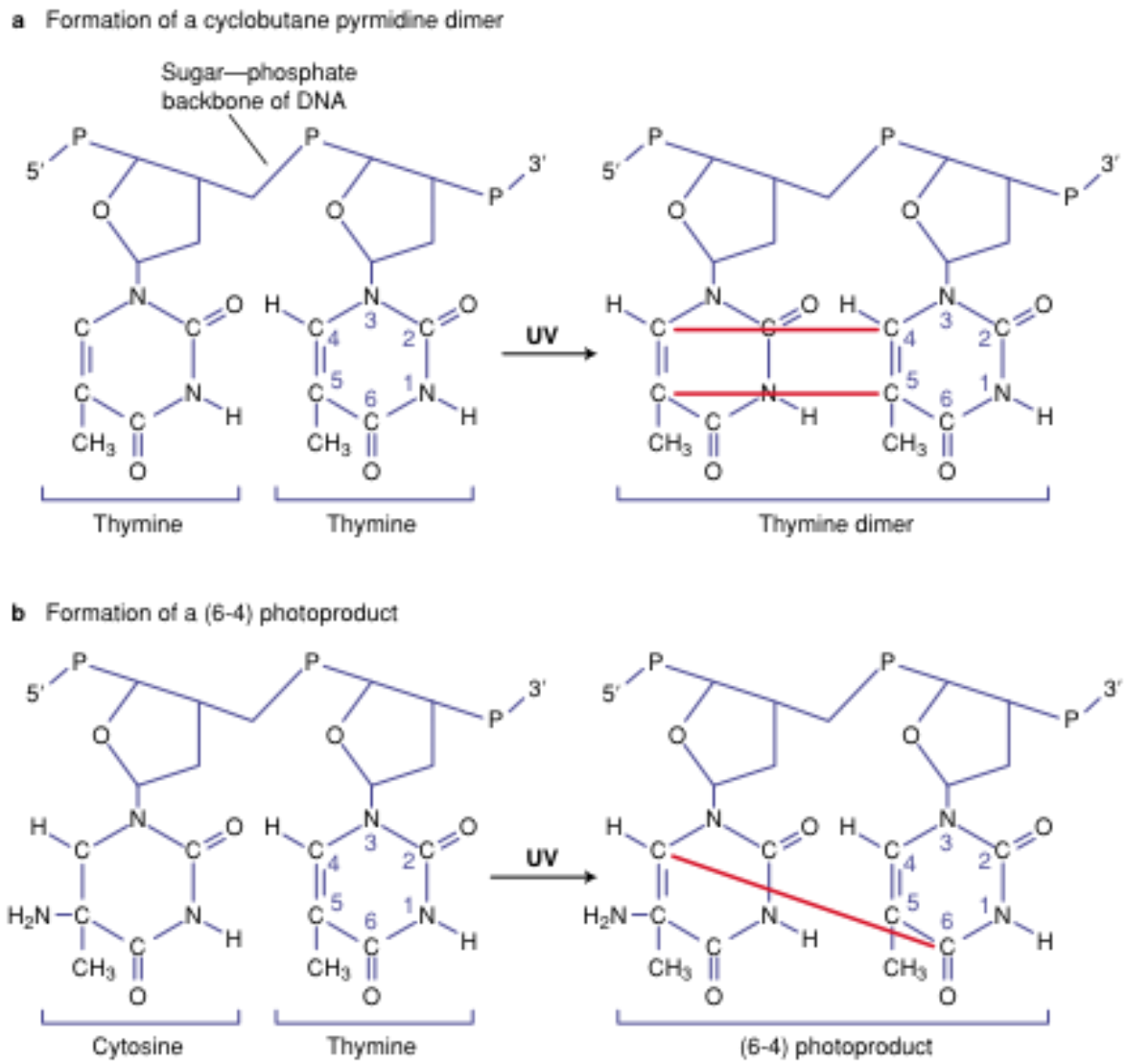

Figure 1.4 Formation of UVR-induced DNA photoproducts (Matsumura and Ananthaswamy, 2002).

Frequency in appearance of these DNA lesions is dependent on wavelength, most prevalent after exposure to high-energy wavelengths in the UV-C and lower portion of UV-B range. However, CPDs are also formed following the longer wavelengths at the border of the UV-B/UV-A spectrum, albeit at a decreased amount. Location of the CPD is an indication of the type of UVR exposure received (Pfeifer and Besaratinia, 2012). UV-A generated CPDs are found in the basal layer of the epidermis, whilst CPDs formed in the suprabasal layers are an offspring of UV-B or UV-C radiation (Halliday and Cadet, 2012).

Unrepaired DNA lesions become incorporated into DNA sequences by the DNA polymerase substitution of an adenine nucleobase opposite the unrecognisable photoproduct (Brash, 1997). Generally, 6-4PPs are more readily repaired compared to their CPD counterpart and are often less mutagenic (Matsumura and Ananthaswamy, 2002).

1.2.3.2 Indirect DNA damage

In addition to its direct absorption by DNA, UVR facilitates DNA damage by the generation of a myriad of reactive oxygen species (ROS) such as singlet oxygen, superoxide anions and hydrogen peroxide (H_2O_2) (Cadet et al., 2005). In addition, it is well established that UVR increases nitrative products, nitric oxide (NO) (Villiotou and Deliconstantinos, 1995). These products may then undergo further reactions to form hydroxyl anions and peroxynitrate, which are, along with singlet oxygen,

implicit in the main mechanisms of formation of oxidative and nitrative DNA base lesions (Jena, 2012, Cadet et al., 2003). Oxidative stress occurs naturally in skin, however there is evidence for an association with a UVR-induced increase in concentrations of ROS and nitrogen associated products and increased prevalence of DNA damage (Pattison and Davies, 2006, Pfeifer and Besaratinia, 2012).

Guanine exhibits the lowest ionisation potential of the DNA purines, and is frequently oxidised and nitrated forming mutagenic guanine centred base lesions, the most lethal and reactive of which is 8oxodG, shown in figure 1.5 (Ravanat et al., 2001, Jena and Mishra, 2012). Formation of 8oxodG is through two pathways mediated by hydroxyl radicals or singlet oxygen, respectively. The former requires one electron oxidation of guanine, creating a guanine radical cation (G•+), which reacts with water molecules to form a second reducing radical, 8-hydroxy-7,8-dihydroguanyl (G-OH•). Oxidation of G-OH• forms the 8-oxodG. The latter pathway involves singlet oxygen mediated cycloaddition of which may then undergo significant ring openings to make pairings with tandem bases and become privy to the cellular DNA sequence, ultimately leading to mutations and carcinogenesis (Jena and Mishra, 2012). Development of the 8-oxodG lesion is a hallmark of UVR induced oxidative stress and the most frequent form of DNA damage by UV-A (Pfeifer and Besaratinia, 2012, Cadet et al., 2003).

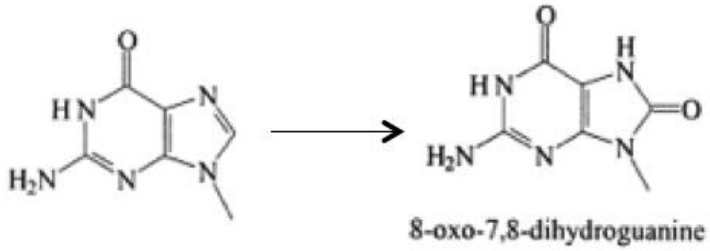

Figure 1.5 Formation of the 8-oxo-7,8-dihydroguanine from the guanine moiety (modified from (Ravanat et al., 2001))

Until recently, the general consensus was that all CPDs are a result of direct UVR absorption by DNA, however studies from our laboratory by Gordon Thomson et al (2012) have shown that a small proportion of these lesions are produced by the indirect metabolic effects of UVR. Using both the classic monoclonal antibody immunohistochemical staining comet assay technique, it was shown that inhibitors of metabolism, such as low temperature (4°C) and sodium azide, reduced the presence of CPDs in UVR-exposed keratinocytes (Gordon-Thomson et al., 2012). Moreover, inhibitors of the nitric oxide synthase pathway attenuated CPD formation following UVR, whilst peroxynitrite donors caused an accumulation of CPDs in unirradiated keratinocytes.

1.2.4 DNA damage repair

Cells exposed to UVR show an upregulation of p53 tumour suppressor gene activity. The p53 gene encodes for a phosphoprotein which plays a role in cell cycle arrest, allowing for increased time for DNA repair and where this is not possible, the induction of apoptotic pathways. Before cells can synthesise DNA in the S-phase of the cell cycle growth is arrested in the G_1 phase where lesions are recognised and

removed via mechanisms involved in DNA damage repair (DDR) (Melnikova and Ananthaswamy, 2005). Amongst the base excision repair (BER) and mismatch repair (MMR) methods of repair, nucleotide excision repair (NER) is the main repair complex associated with direct UVR-induced DNA photoproducts, notably, CPDs and 6-4PPs (Friedberg, 2001). There are two sub pathways of NER, transcription-coupled NER (TC-NER) which directly removes lesions from the transcribed strand of the gene of interest, and the slower, less efficient global genome NER (GG-NER), removing the lesion from the untranscribed chromatin of the whole gene (Hanawalt, 2002).

The mechanism of action of the NER is a five step process which begins at recognition of the damage by the XPC-HHR23B protein complex in GG-NER, or by elongating RNA polymerase II in TC-NER (de Laat et al., 1999). Following identification, the pathways follow identical steps in purging the lesion. DNA is locally unwound at the site of damage, following which ~30 nucleotides surrounding and including the damaged DNA are incised XPF/ERCC1 (excision repair cross-complement gene1) and XPG endonucleases, at the 5' and 3' ends respectively (Shivji et al., 1995). Damaged DNA is removed and de novo synthesis of DNA ligase is formed to replace the excised lesion and allow for safe transcription of the gene (Matsumura and Ananthaswamy, 2002).

Several diseases associated with a faulty NER complex elucidate its vital importance in preventing mutagenesis. Xeroderma pigmentosum (XP) results from a defect in the any one of the eight XP enzymes and associated genes affecting both

subpathways of NER. Phenotypes of the autosomal recessive disease show hypersensitivity to light and predisposition to amplified formation of squamous and basal cell carcinomas and malignant melanomas (Lehmann, 2003). In a similar vein, Cockayne syndrome (CS) is manifest when there is a mutation in the TC-NER associated RNA polymerase recognition signal proteins CS-A and CS-B. CS patients lose the ability to recover from UVR exposure and display increased sensitivity to UVR evident with a severe rubor rash, and developmental and neurological retardation (de Laat et al., 1999).

Oxidative damage lesions resulting from UVR such as 8oxodG are not repaired by NER, rather they are excised and removed by the actions of BER (Melnikova and Ananthaswamy, 2005). In this instance, increase DNA single strand breaks are recognised and cleaved by a DNA glycosylase, which releases separates the N-glycosyl bond between the damaged base and the backbone of the helix. An abasic (apurinic/apyrimidinic (AP)) site is formed and recognised by either an AP endonuclease or AP lyase which cleave and remove the site completely. DNA polymerase β catalyses the release of deoxyribophosphate (dRP) from the one base gap site, which aids in polymerisation of new DNA to fill in the gap, using XRCC1 as a scaffold, whilst also ensuring complete removal of the AP site (Robertson et al., 2009). DNA ligase 3 then forms a nucleotide patch to fill in the DNA strand (Rastogi et al., 2010).

1.2.5 Apoptosis

When DNA damage cannot be repaired, pre-programmed cellular UV responses are initiated to remove the damaged cells and prevent transcription of malignancies in daughter cells, instead forming the apoptotic “sunburn cell” (Lippens et al., 2009, Kulms and Schwarz, 2000). Apoptosis is a complex process involving several signalling pathways which ultimately lead to the activation of caspases, a hallmark of programmed cell death. Following UVR exposure, apoptotic pathways may be activated by direct UVB radiation, or in a p53 way manner from extensive DNA damage or via indirect reactive oxygen species (ROS) generation (Melnikova and Ananthaswamy, 2005, Van Laethem et al., 2009).

There are two procaspase apoptotic pathways, extrinsic (death receptor (DR) associated) initiated by a foreign ligand, and intrinsic (mitochochondria) induced by self-induced intracellular cascades. The intrinsic pathway is initiated following UVB activation of p38 mitogen activated protein kinase (MAPK) signalling. The MAPK signaling cascade includes three distinct stages of protein kinase activation; a mitogen-activated extracellular signal-regulated kinase kinase kinase (MEKK), which activates a mitogen-activated extracellular signal-regulated kinase kinase (MEK) which can subsequently activate a MAPK. MAPKs include c-jun-N-terminal kinase (JNK), extracellular signal-regulated kinase and p38 MAPK. These kinases are widely located in keratinocytes and are targeted by various extracellular stimuli, including UVR (Assefa et al., 2005) as shown in figure 1.6. P38 MAPK causes the translocation of Bax, a proapoptotic protein, from the cytoplasm to the mitochondria

(Muthusamy and Piva, 2010, Van Laethem et al., 2009). Bax makes the mitochondria permeable, releasing cytochrome c and oxygen free radicals (Van Laethem et al., 2009, Kulms and Schwarz, 2002). Expression of apoptosis activating factor 1 (APAF-1) increases which together with cytochrome c forms the apoptosome, recruiting procaspase 9 and 3, leading to the final executioner caspase cascade. Mitochondrial induced apoptosis is heavily regulated by anti- and pro-apoptotic Bcl family proteins (Van Laethem et al., 2005). Additionally, ROS generated by UVR contributes to the activation of p38 MAPK (Van Laethem et al., 2009).

Apoptosis initiated by unrepairable DNA damage occurs via p53 induced upregulation of cytochrome c release from the mitochondria and interaction with Bcl proteins which in turn regulate subsequent caspase pathways. Death receptors are part of the tumour necrosis factor (TNF) superfamily, including TNF-receptor 1, Fas, and TNF-Related Apoptosis-Inducing Ligand receptors 1 and 2 (TRAIL1/2), are located on the cell surface membrane. DRs are activated following exposure to UVB by either a UVB-induced receptor cluster formation on the cell membrane, allowing ligand-independent signal transduction or via their natural ligands, released from the DNA damaged cell (Van Laethem et al., 2009, Kulms and Schwarz, 2000). Subsequent signalling pathways involving Jun N-terminal kinase (JNK) lead to the activation of caspase 3 (Kulms and Schwarz, 2002). Like p38 MAPK, UVR-activated JNK can translocate to the nucleus of the cell to initiate transcription of target genes resulting apoptosis (Assefa et al., 2005, De Haes et al., 2003, Bode and Dong, 2003). Whilst both intrinsic and extrinsic pathways contribute to the induction of

executioner caspases, it has been suggested that UVB-induced apoptosis is mediated mainly by the intrinsic pathway (Kulms and Schwarz, 2002, Van Laethem et al., 2009)

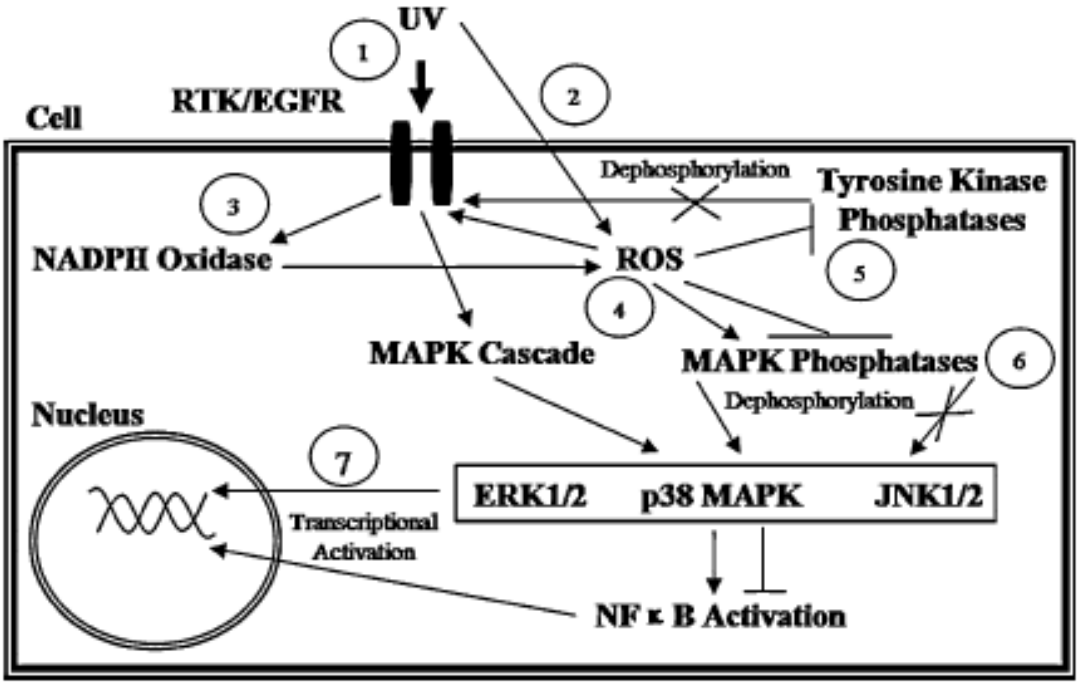

Figure 1.6 Signalling pathways activated by UVR that contribute to apoptosis (Muthusamy and Piva, 2010).

There are several cellular signalling proteins involved in protection against apoptosis. The phosphatidylinositol 3-kinase/Akt (PI3K/Akt) pathway is activated through the MAPK pathway during apoptotic signalling, acting as a balance to prevent apoptosis by inhibition of mitochondrial cytochrome c release and blocking the recruitment of procaspase 9 and 3 allowing progression of the cell cycle (Muthusamy and Piva, 2010, Wang et al., 2003). Extracellular signal regulated kinase (ERK) isoforms are also antiapoptotic by inhibiting the activity of executioner caspase 3. The PI3K/Akt pathway is also basally active at a low level in epidermal

keratinocytes and ERK and Akt are upregulated by UVR (Peus et al., 1999, Wang et al., 2003, Wan et al., 2001). Both ERK and Akt help maintain epidermal cell proliferation and cellular survival in response to extracellular insults (Diker-Cohen et al., 2006). Akt is known to inhibit glycogen synthase kinase-3β (GSK-3β), which then frees β-catenin to induce transcription of proto-oncogenes involved in cell growth (Cross et al., 1995). The significance of this lies in the fact that this may be a pathway for the development of cancerous cells and the progression to photocarcinogenesis. However, the potency of ERK in preventing apoptosis following UVB may be decreased due to its tendency to be down-regulated (Melnikova and Ananthaswamy, 2005). Similarly, activation of JNK by UVR, has been shown to inactivate ERK and Akt, suggesting that the apoptotic pathway dominates survival if UVR dosage is sufficient (Wang et al., 2012b).

"Sunburn" cells exhibit the general morphology of apoptotic cells. Appearing firstly in the proliferative basal layer, sunburn cells exhibit pyknotic nuclei and membrane blebbing. Caspases use keratin and actin filaments as cleavage substrates, which results in cytoskeletal changes that differentiate sunburn cells from cornified cells (Lippens et al., 2005).

1.2.6 Immunosuppression

UVR diminishes the power of the body's immune response, allowing malignant DNA damaged cells to evade normal immunological elimination, leading to the formation of cancerous tumours. Immunosuppression following UVR exposure is often measured using the delayed-type hypersensitivity (DHR) or contact hypersensitivity

(CHS) tests (Rangwala and Tsai, 2011). In both tests, immune responses to a presenting antigen are significantly depressed, both locally, sites previously exposed to UVR, and systemically, non-irradiated sites (Murphy, 2009). It has been postulated that this may be due to disabled T cell-mediated immunity (Reeve, 2002).

UVR causes immunosuppression via a number of different pathways. Firstly, DNA damage is a potent stimulator of immune suppression. Cells containing CPDs unable to be repaired by NER decrease the reaction to CHS (de Gruijl, 2008, Kripke et al., 1992). Secondly, Langerhans cells, the main antigen presenting cells of the epidermis, are vulnerable to distinct changes in their morphology and functionality following even slight UVB exposure. UVB radiation reduces the expression of cell surface markers and damages well established dendritic networks, ultimately depleting Langerhans cell numbers, reducing their antigen presenting capabilities (Aubin, 2003, Murphy, 2009). Lastly, UVR-exposed keratinocytes, particularly those with CPDs directly secrete immunoregulatory cytokines such as interleukin-10 (IL-10), or mediators which stimulate its secretion from other cells (Beissert and Loser, 2008). Once in the bloodstream, IL-10 acts as an immunoregulatory factor, which induces systemic immunosuppression via reducing antigen presentation in Langerhans cells (Aubin, 2003). Furthermore, the reduced immunosurveillance provided by Langerhans cells result in decreased effector T cell proliferation and differentiation and ultimately decreased antitumoural immune protection (Loser and Beissert, 2009). Recently it has been shown in murine epidermis that following UVR exposure, production of RANKL, a TNF family member is upregulated, and

binds to its RANK receptor of Langerhans cells (Beissert and Loser, 2008). RANKL binding increases secretion of IL-10, amongst other immune related cytokines, which contribute to systemic immunosuppression, and formation of skin tumours.

Another contributor to the inhibition of antigen presentation in Langerhans cells is the development of cis-urocanic acid. UCA, an isomer present in the stratum corneum, undergoes photoisomerisation following UVB exposure from stable trans-UCA to cis-UCA, making it a powerful immunosuppressive agent (Hart et al., 2001).

1.2.7 Photocarcinogenesis

While acute UVR photoresponses appear to disappear within a few days, chronic and overexposure to UVR may result in genetic defects leading to the progression of premalignant actinic keratoses (AK) and ultimately squamous cell carcinomas (SCC), known as photocarcinogenesis (Melnikova and Ananthaswamy, 2005), as shown in figure 1.7 In acute UVR exposure, the p53 tumour suppressor gene is highly upregulated, however in UV-induced skin cancers it is commonly mutated and suppressed (Lee et al., 2003). Cells containing p53 mutations do not undergo cell cycle arrest to facilitate DNA repair to remove “UV-signature mutations”, and avoid p53 induced apoptosis. Damaged cells are able to proliferate and graduate onto becoming premalignant AK lesions (Melnikova and Ananthaswamy, 2005). p53 mutations occur early in the development of squamous cell carcinomas, often occurring in seemingly normal UV exposed murine skin months before the appearance of a tumour (Hussein, 2005). Similarly, chronically UVR exposed cells exhibit deregulated and inhibited Fas expression on the surface membrane,

allowing cells to resist extrinsic mechanisms of apoptosis and contribute to the malignant cell population of the skin (Melnikova and Ananthaswamy, 2005). In addition, persistent oxidative damage by chronic UVA radiation may result in the activation of protooncogenes commonly found in skin cancers such as c-fos and c-jun (Nishigori, 2006).

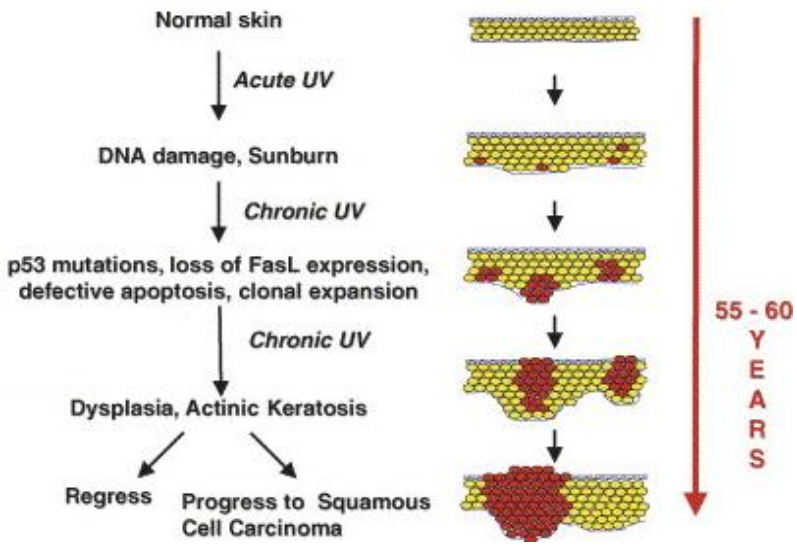

Figure 1.7 UV-induced initiation and progression of a human squamous cell carcinoma (modified from Melnikova and Ananthswamy, 2005).

Skin cancers are generally divided into two groups; melanoma skin cancers (MSC) or non-melanoma skin cancers (NMSC), which include squamous cell carcinomas (SCC) and basal cell carcinomas (BCC). The current study will focus primarily on the events leading to the development of squamous cell carcinomas.

1.2.8 Gender bias in photocarcinogenesis

In general, females with cancer are faced with a better prognosis than males with cancer (Molife et al., 2001). The prevalence of NMSCs, especially SCCs, are generally higher in the male population than in females (Foote et al., 2001, Preston and Stern, 1992). This is particularly evident in the Australian population (Staples et al., 1998, Staples et al., 2006). It is evident that cutaneous melanoma also follows a similar trend, often occurring in the later decades of life, and in higher numbers in men than women (Leiter and Garbe, 2008). In humans, this has been attributed to male susceptibility to be exposed to more sun and not using sun protection, however recent studies have shown that there may be underlying biological characteristics that are involved in increasing proneness for SCCs.

In study by Thomas Ahner and colleagues (2007), using a well established photocarcinogenesis mouse model, it was shown in a laboratory setting that male Skh:Hr1 mice exposed to UVR exhibit a greater number of SCC tumours compared to their female counterparts (Thomas-Ahner et al., 2007). Pro-carcinogenic DNA damage was seen as early as 48 hours following UVR exposure, with 8oxodG production greater in male mice than female mice. In a similar vein, the cutaneous inflammatory reaction to UVB was greater in females compared to males, suggesting that females are less immunosuppressed by UVB, which may be protective against malignant cell growth, progressing to cancer (Thomas-Ahner et al., 2007, Damian et al., 2008).

It has recently been discovered that the predominant steroid receptor in human skin is the oestrogen receptor-β (ER-β), in addition to ER-α, which plays a role in the hair follicle growth cycle (Pelletier and Ren, 2004, Thornton et al., 2003b, Thornton et al., 2003a). Evidence suggests that activation of the ER-β by agonist ligands has several anti-inflammatory and anti-carcinogenic properties (Catley et al., 2008, Cotrim et al., 2013). In addition, ER-β signalling has proven to be effective at reducing immunosuppression in mice following exposure to UVR (Widyarini et al., 2006) and the loss of ER-β results in an increased expression of immunosuppressive cytokine IL-10 (Reeve et al., 2009). Use of both oestrogen and phytoestrogen has proven to be anti-carcinogenic in mice exposed to UVR, whilst disruption of estrogen receptor signalling allowed the growth of transplanted tumours in murine skin (Cho et al., 2010, Widyarini et al., 2006). A very recent paper has suggested that a potential protective mechanism of ER-β signalling is via downregulation of PI3K/Akt phosphorylation subsequently leading to inhibition of Wnt and β-catenin activity which reduces SCC tumour cell survival (Chaudhary et al., 2013).

1.3 VITAMIN D – THE SUNSHINE VITAMIN

1.3.1 Background

Vitamin D exists in two forms, vitamin D_2 (ergocalciferol) and vitamin D_3 (cholecalciferol). This fat soluble secosteroid may be obtained through dietary sources, plant or animal products respectively, or via biological production following skin exposure to UVR. Technically speaking, vitamin D is not a true vitamin, rather a hormone due to its ability to be synthesised in skin (Malloy et al., 1999).

1.3.2 Structure

The molecular structure of the vitamin D compound family, including the active metabolite, 1α,25-dihydroxyvitamin D_3 ($1,25(OH)_2D$), is chemically related to that of classical steroid hormones through its basis around a steroid hormone specific cyclopentanoperhydrophenanthrene 4 ring carbon skeleton (Norman et al., 1999). However, unlike its steroidal relatives, the 9-10 carbon-carbon bond of ring B is un-joined, designating vitamin D into the secosteroid category. This is shown in figure 1.8.

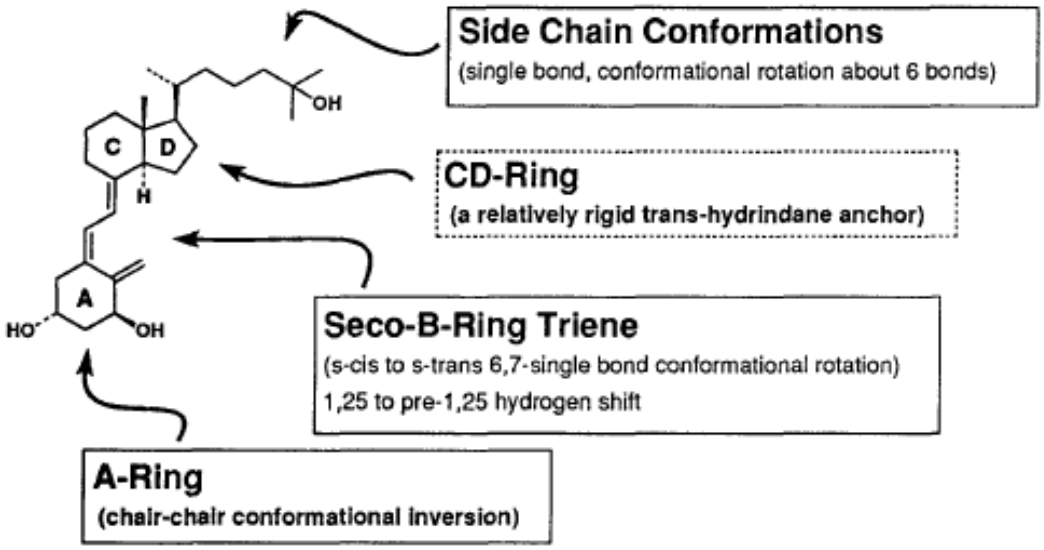

Figure 1.8 Chemical structure of the vitamin D metabolite $1,25(OH)_2D_3$ (Okamura et al., 1995).

In comparison to their classical steroid counterpart, molecules of the vitamin D superfamily are particularly conformationally flexible, due to three major structural regions of its carbon skeleton. Firstly, simple rotation of the 8-carbon side chain about the 5 carbon-carbon single bond allows for a plethora of differing molecular shapes. Additionally, as a result of the 9-10 carbon-carbon breakage, the cyclohexane-like A-ring is liberated from the B-ring and undergoes rapid interconversion between chair-chair conformers. The mobility of the A-ring results in orientation of the 1α-hydroxyl and 3β-hydroxyl to move between axial and equatorial. Finally, the seco B-ring rotates freely around its 6-7 single carbon bond, producing 6-s-cis and 6-s-trans variates of conformation, which may be locked or flexible (Norman et al., 1999, Norman et al., 2001), shown in figure 1.9. It is the conformational flexibility of the vitamin D_3 backbone, which allows for the generation of a vast number of ligand shapes, able to generate different biological responses through the vitamin D receptor (VDR).

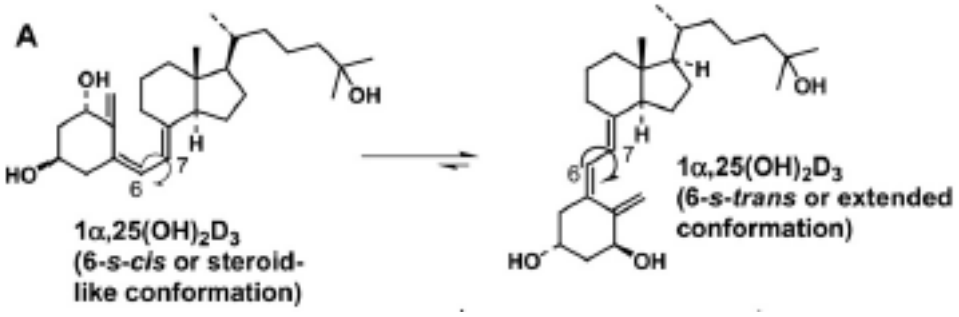

Figure 1.9 Conformational flexibility of 1,25(OH)$_2$D (Haussler et al., 2011)

1.3.3 Synthesis

As sunlight strikes skin cells, epidermal and dermal stores of 7-dehydrocholesterol (7-DHC) absorb UVB photons. Absorption of UV energy results in the cleavage of the 9-10 carbon-carbon bond of the B-ring of 7-DHC to form the thermally unstable pre-vitamin D_3 (pre-D) molecule (Holick et al., 1980). In human skin the highest levels of pre-D following UV irradiation are found in the stratum spinosum and basale cells of the epidermis (Holick, 1981). Pre-D is thermally isomerised over hours and days, at the optimal temperature of 37°C, to vitamin D_3 which is released from the lipid bilayer into the extracellular space. Over exposure to UVR does not result in vitamin D toxicity, as pre- D and vitamin D absorb UVB photons and produce photoproducts such as lumisterol and tachysterol. Such products are thought to be biologically inert, with low calcemic capabilities (Holick, 2004).

Vitamin D_3 binds to the vitamin D-binding protein (DBP) in the dermal capillary bed, moving the biologically inactive vitamin D_3 molecule into the bloodstream to target

organs of the vitamin D endocrine system for metabolism into a more active form (Holick, 2004). Similarly, dietary vitamin D (D_2 or D_3) absorbed through the small intestine and into the circulation is picked up by DBP (Lehmann and Meurer, 2010).

In the liver, vitamin D is hydroxylated by the cytochrome P450 enzyme 25-hydroxylase at the carbon-25 position to form 25-hydroxyvitamin D (25(OH)D). 25(OH)D is transported to the kidney via DBP and undergoes further hydroxylation at the carbon-1α position by 25-hydroxyvitamin D-1α-hydroxylase (1α-hydroxylase) forming the biologically active 1α-25-dihydroxyvitamin D_3 metabolite (1,25$(OH)_2$D; calcitriol) (Lehmann, 2003). In this active form, 1,25$(OH)_2$D is able to induce biological responses throughout the body through organs expressing the vitamin D receptor (VDR). Renal formation of the active 1,25$(OH)_2$D is tightly regulated by serum calcium levels via circulating parathyroid hormone (Lehmann and Meurer, 2010).

In addition to the hepatic/renal production of 1,25$(OH)_2$D, several tissues have recently been discovered to contain either or both the aforementioned hydroxylation enzymes (Holick, 2004, Bikle et al., 1986). In particular it has been shown that epidermal cells contain the whole vitamin D production pathway, beginning with 7-DHC, including both 25-hydroxylase and 1α-hydroxylase enzymes, ending in 1,25$(OH)_2$D. There has also been evidence for fibroblasts containing 25-hydroxylase, thus making more 25(OH)D available to neighbouring keratinocytes (Vantieghem et al., 2006). Such a symbiotic relationship between skin cells suggests that production of 1,25$(OH)_2$D is important in the body's autonomous protection from the sun.

To avoid hypercalcaemia, catabolism of $1,25(OH)_2D$ and 25(OH)D occurs in most cells via negative feedback activation of the 24-hydroxylase enzyme to form inactive metabolites when there are high levels of $1,25(OH)_2D$. This system is inhibited when levels of calcium and PTH are low (St-Arnaud, 2008).

1.3.4 Transduction pathways

$1,25(OH)_2D$ is the predominant structural ligand of the vitamin D_3 endocrine system. It exerts its biological effects via two pathways, shown in figure 1.10; a genomic pathway mediated by the well known nuclear VDR, and a non-genomic/rapid response pathway whose receptor is currently not established (Mizwicki and Norman, 2009, Nemere et al., 1984, Norman et al., 1999, Nemere et al., 1994, Zanello and Norman, 2004a).

1.3.4.1 Vitamin D Receptor (VDR)

As a nuclear receptor of the steroid family, the VDR is found in nucleated cells in most tissues of the human body including the intestine, kidney, bone, skin, parathyroid gland, pancreas, pituitary, cells of the immune and reproductive systems, amongst others (Wang et al., 2012c, Norman, 2008). The VDR is made up of six primary amino acid domains each designated a different functionality, specifically, a variable domain (A/B), a DNA binding domain (C), a hinge (D), a ligand binding domain (E) and a transcriptional activation domain (F) (Norman, 2008).

1.3.4.2 Genomic pathway

The biological responses of $1,25(OH)_2D$ are mediated by the classic genomic pathway through stereospecific ligand binding to the nuclear vitamin D receptor (VDR_{nuc}). The lipophilic $1,25(OH)_2D$ molecule passes through the lipid bilayer of the plasma membrane and binds to the hydrophobic pocket in the ligand binding domain of the VDR_{nuc}. Upon activation, the VDR_{nuc} heterodimerises with a free retinoid X receptor (RXR) forming a VDR-RXR complex. Zinc fingers of the DNA binding domain recognise the VDR-RXR complex, allowing docking with vitamin D response elements (VDREs) in the DNA sequences of vitamin D target genes. Subsequent recruitment of protein comodulators assists interaction with the general transcription apparatus wherein gene transcription is promoted or repressed (Haussler et al., 2011). Resulting physiological effects are latent manifestations of genetic alterations.

1.3.4.3 Non-genomic pathway

The non genomic pathway activated by $1,25(OH)_2D$ generates a biological response within seconds to minutes through a number of intracellular signalling pathways (Norman et al., 1999, Haussler et al., 2011, Norman, 2008). These include the opening of chloride and calcium channels, mitogen activated protein kinases (MAPKs), protein kinase C, phosphatidylinositol 3-kinase (PI3K), phospholipase C, and subsequent g-protein coupled second messenger systems such as cyclic monophosphate (cAMP). Activated messenger systems may cross talk with the nucleus to contribute to gene transcription (Norman, 2008).

The location of a binding protein/receptor via which 1,25$(OH)_2$D exerts its rapid response effects is still under examination. There is evidence for a rapid response binding protein for 1,25$(OH)_2$D, first identified in the basolateral membrane of chick epithelium, involved in rapid calcium perfusion from the duodenum (Nemere et al., 1994). Subsequent purification of the protein led to its definitive identification as the 66kD membrane-associated rapid response steroid binding (MARRS) protein, identical to ERp57/PDIA3 (Nemere et al., 2000).

In the last decade, it has been proposed that the rapid actions of 1,25$(OH)_2$D may occur via a putative alternative ligand binding pocket within the ligand binding domain of the VDR (Mizwicki et al., 2004). Through molecular modelling, the natural 6-s-cis locked analogue of 1,25$(OH)_2$D, 1α,25 dihydroxylumisterol$_3$ (JN) which has weak genomic activity but equivalent 1,25$(OH)_2$D rapid signalling, was shown to dock on the classic VDR through a pocket other than the genomic pocket to elicit its non-genomic cellular responses. The flexible 1,25$(OH)_2$D molecule was found to have a high affinity for both, with differing modes of binding. It is thought that vitamin D sterol binding at the VDR occurs kinetically through the AP, whilst in a thermodynamic manner at the GP, and thus subsequent responses are highly dependent on the conformation and orientation of the ligand present (Mizwicki et al., 2004, Mizwicki and Norman, 2009). The AP prefers the planar 6-s-cis locked non-genomic agonist vitamin D sterols, such as JN, whilst the bowl shaped GP binds 6-s-trans conformed isomers of 1,25$(OH)_2$D. The conformationally flexible 1,25$(OH)_2$D molecule can take up both structures, thus making it the most potent agonist for both genomic and non-genomic biological responses. The AP forms complexes with

an array of 1,25$(OH)_2$D molecule conformations, whilst the GP is more restricted with its binding affinity (Mizwicki and Norman, 2009).

Evidence for a bi-functional VDR comes from a study showing increased 1,25$(OH)_2$D induced rapid chloride fluxes in wild type mouse osteoblasts, whilst mouse osteoblasts lacking a functional VDR showed no response (Zanello and Norman, 2004a). The VDR-KO mouse strain used in the aforementioned study were previously reported to exhibit genetic defects similar those seen in human vitamin D-resistant rickets type II, such as alopecia, growth retardation, impaired bone formation and rickets, amongst many others (Yoshizawa et al., 1997).

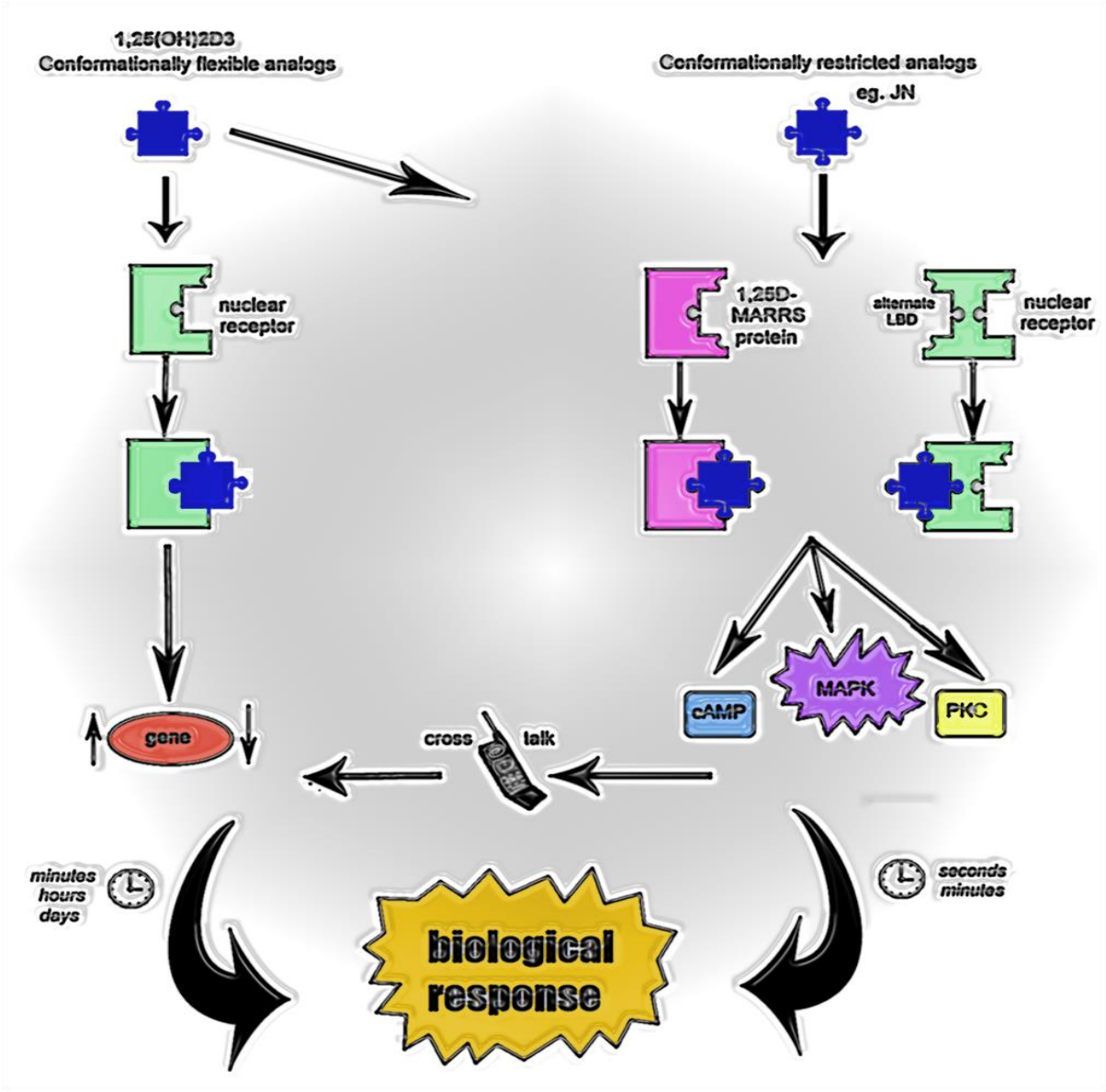

Figure 1.10 The genomic and non-genomic pathways of vitamin D actions (Mason, 2010)

1.3.5 Actions

The classic role of $1,25(OH)_2D$ is to work synergistically with parathyroid hormone (PTH) to maintain normal calcium homeostasis. When serum calcium levels fall below normal levels, PTH stimulates the formation of $1,25(OH)_2D$ from the kidney

to act on the small intestine to increase intestinal absorption of calcium. In turn $1,25(OH)_2D$ encourages the maturation of osteoclasts resulting in bone resorption (St-Arnaud, 2008). $1,25(OH)_2D$ also facilitates healthy skeletal growth and mineralisation by increasing absorption of phosphate, and promoting osteoblastogenesis (Marie and Kassem, 2011, Bikle, 2012). Additionally, $1,25(OH)_2D$ prevents apoptosis in osteoblasts (Vertino et al., 2005). In skin $1,25(OH)_2D$ regulates keratinocyte proliferation, stimulates differentiation and maintains normal hair follicle cycling (Bikle, 2011a). Immunologically, the adaptive immune response is inhibited by $1,25(OH)_2D$, which in turn prevents autoimmunity and the diseases that follow. In a similar vein, $1,25(OH)_2D$ stimulates innate immunity to aid in the prevention of infectious diseases (Bikle, 2011b). $1,25(OH)_2D$ maintains an antiproliferative effect on most cells by slowing cell cycle progression at the G1 phase, which make it a novel candidate for the treatment of diseases involving uncontrolled malignant cell growth such as cancer (Samuel and Sitrin, 2008).

1.4 PHOTOPROTECTION BY VITAMIN D

The use of $1,25(OH)_2D$ as a chemoprotective agent has been reported and accepted in several cancer types. In particular, over the last decade research into the use of vitamin D compounds to combat the formation of skin cancers has boomed, due to the depletion of the ozone layer and increasing number of worldwide skin cancer cases.

1.4.1 $1,25(OH)_2D$ mediated protection against UVR-induced DNA damage, apoptosis and immunosuppression

Studies from the Mason group have shown that application of $1,25(OH)_2D$ at physiological concentrations (10^{-9}) to cultured keratinocytes either before, or immediately following UVR exposure (200 mj/cm^2 UVB and 1170 mj/cm^2 UVA) significantly reduces the formation of thymine dimer CPDs as early as 0.5-3 hours post-UVR, when compared to vehicle treated skin cells, detected using immunohistochemistry (Gupta et al., 2007, Wong et al., 2004, Sequeira et al., 2012b). In addition to this, *in vivo* experiments in hairless mice from the group have supported these findings, and provided a novel photocarcinogenesis study showing evidence for $1,25(OH)_2D$ prevention of SCCs in murine skin (Dixon et al., 2011).

Using immuno dot-blot densitometric analysis, De Haes and colleagues were also able to show a significant reduction in CPD formation following UVR when cells were pre-incubated with $1,25(OH)_2D$ for at least 18 hours prior to irradiation. In this study, maximal protection occurred at the pharmacological concentration of 10^{-6} (De Haes et al., 2005). Whilst the data support the work of the Mason group, use of

pharmacological concentrations may not be viable in humans due to the hormone's hypercalcaemic toxicity.

In vivo and *in vitro* results from several groups have exposed a role for 1,25$(OH)_2$D in the reduction of apoptotic sunburn cells and enhancement of keratinocyte survival following UVR (Manggau et al., 2001, Gupta et al., 2007, De Haes et al., 2004a, Lee and Youn, 1998, De Haes et al., 2003, Dixon et al., 2011). On the other hand, one study by Benassi and colleagues using TUNEL assays, suggests that application of 1,25$(OH)_2$D on keratinocytes increases apoptosis to a similar extent as UVB radiation (Benassi et al., 1997). This study however used high concentrations of 1,25$(OH)_2$D and did not test the extent of apoptosis of when the two variables were combined.

UVR increases the formation of NO in skin, which interacts with ROS such as the superoxide anion generated by UVR to form peroxynitrite (Ravanat et al., 2001). Peroxynitrite belongs to the reactive nitrogen species (ROS) known to cause single strand DNA base mutations. In addition, presence of NO in skin cells prevents the repair of CPDs following UVR (Bau et al., 2001). The Mason group explored the effect of physiological doses of 1,25$(OH)_2$D on combating the effects of indirect DNA damage by UVR-instigated ROS and RNS. In one study, using the Griess assay to detect nitrite levels it was found that application of 1,25$(OH)_2$D following UVR exposure significantly increased the stable metabolite, in turn decreasing available NO products, as well as reducing CPD and sunburn cell formation (Gupta et al., 2007).

More recently it was established using comet assays and immunohistochemical staining that 1,25$(OH)_2$D reduces the appearance of 8oxodG mutations in keratinocytes as early as 0.5 hours following UVR (Gordon-Thomson et al., 2012). The same study showed that topical application of a physiological dose of 1,25$(OH)_2$D to hairless albino mouse skin significantly reduced appearance of 8oxodG positive keratinocytes. Human skin explants exposed to UVR equivalent to Australian summer sun for 5-10 minutes showed significant decreases in the formation of CPDs, 8oxodG and 8-nitroguanosine mutations with the application of 1,25$(OH)_2$D at 1nM when compared to their vehicle counterparts at various time points following UVR (Song et al., 2012).

Dixon and colleagues have shown that topical application of 1,25$(OH)_2$D on hairless albino mice following UVR reversed systemic immunosuppression seen in untreated mice, 2 weeks after UVR (Dixon et al., 2007).

1.4.2 Mechanisms of 1,25(OH)2D

It is generally accepted that photoprotection by 1,25$(OH)_2$D occurs substantially via the non-genomic pathway (Mason et al., 2010). In the *in vivo* and *in vitro* studies by Dixon and colleagues, 1α,25-dihydroxylumisterol (JN), a vitamin D analogue, with only the ability to induce the rapid response pathway decreases the formation of CPDs and apoptosis at the same physiological concentration of 1,25$(OH)_2$D following UVR, with statistically equivalent potency (Dixon et al., 2007, Dixon et al., 2005, Dixon et al., 2011).

Use of non-genomic antagonists completely reversed photoprotection by $1,25(OH)_2D$ whilst antagonists of the genomic pathway had no effect (Dixon et al., 2007).

Previous studies from this laboratory have shown that $1,25(OH)_2D$-mediated photoprotection against UV irradiation occurs via a non-genomic pathway (Dixon et al., 2007, Dixon et al., 2005, Wong et al., 2004, Sequeira et al., 2012a, Sequeira et al., 2012b). A number of reports on the actions of $1,25(OH)_2D$ binding to a putative mVDR suggest that $1,25(OH)_2D$ activates rapid ionic and molecular signalling pathways. These include the induction of protein kinase C, the mitogen activated protein kinase (MAPK) and phosphatidylinositol 3-kinase (PI3K) pathways and the opening of chloride and calcium channels (Norman et al., 2001).

The role of the VDR in the non-genomic pathway is not completely understood, however recent evidence to suggest the location of the classic nuclear VDR present within plasma membrane caveolae which binds $1,25(OH)_2D$, and mediates its non-genomic activity (Huhtakangas et al., 2004, Norman et al., 2002). Molecular modelling experiments identified alternative ligand-binding pockets within the VDR, distinct from the classic ligand binding domain, which have a high affinity for both trans- and cis-locked ligand shapes of $1,25(OH)_2D$ and analogues (Mizwicki et al., 2004).

Additionally, it is well established that some non-genomic actions of specific $1,25(OH)_2D$ occur via specific 6-cis-locked molecular shapes binding to a membrane

associated rapid response steroid binding protein (MARRS), also known as ERp57. It has recently been shown through co-immunoprecipitation that the VDR and ERp57 are physically linked. Sequeira and colleagues (2012b) found that in terms of photoprotection, blockade of ERp57 by Ab099, a neutralising antiserum, reduced the effectiveness of $1,25(OH)_2D$ in reducing thymine dimer formation in UVR-exposed fibroblasts (Sequeira et al., 2012b). This shows strong evidence for the role of the non-genomic pathway in photoprotection by $1,25(OH)_2D$ and $1,25(OH)_2D$ -analogues.

Previous reports have established that diisothiocyanatostilbene-2,2'-disulfonic acid (DIDS) inhibits $1,25(OH)_2D$ non-genomic activation of chloride currents (Mizwicki et al., 2010, Zanello and Norman, 2004b, Zanello and Norman, 1997, Zanello and Norman, 1996, Zanello and Norman, 2006, Zanello and Norman, 2003). One recent study from the Mason group showed that in keratinocytes, the presence of DIDS completely abolished $1,25(OH)_2D$ -mediated reduction of thymine dimers following UVR, but had no effect on its own (Sequeira et al., 2012b). This suggests that the photoprotective effects of $1,25(OH)_2D$ are mediated by the opening of these DIDS-sensitive non-genomic chloride channels.

Both UVR and $1,25(OH)_2D$ enhance the expression of p53 in both melanocytes and keratinocytes as seen in studies by Gupta et al. (2007) and Sequeira et al. (2012a). This suggests that cells undergo longer cell cycle arrest, to allow for increased time to repair DNA damage, by XPC and DDB2 nucleotide excision repair enzymes, and reduce the need to form sunburn cells (Gupta et al., 2007). However, since the

study by Sequeira et al (2012b) demonstrated that p53 expression remained high in VDR null and ERp57 antiserum Ab099 treated fibroblasts, and displayed high numbers of thymine dimers following treatment with $1,25(OH)_2D$ after UVR exposure, this hints at the presence of an alternate mechanism of thymine dimer reduction (Sequeira et al., 2012a).

Studies by de Haes and colleagues used pathway inhibitors to show evidence for $1,25(OH)_2D$ induced inhibition of mitochondrial cytochrome c release, the JNK stress activated pathway and the production of IL-6, which led to a partial reduction in apoptotic cells post UVR (De Haes et al., 2003). In addition, $1,25(OH)_2D$ activated anti-apoptotic PI3K/Akt and ERK signalling pathways and Bcl_2 proteins from basal levels to enhance cell survival following UVR (De Haes et al., 2004a, De Haes et al., 2003). The application of pharmacological inhibitors of ERK and PI3K somewhat reversed photoprotection against UVR-induced apoptosis, suggesting that $1,25(OH)_2D$ is photoprotective via the MEK/ERK and PI3K/Akt signalling pathways (De Haes et al., 2004a). Additionally, Western blotting showed that $1,25(OH)_2D$ causes downregulation of JNK signalling following UVR, preventing JNK activated apoptosis (De Haes et al., 2003). While, on the other hand, UVR induced p38 activation was not affected in the presence of $1,25(OH)_2D$ (De Haes et al., 2003).

Another proposed mechanism of photoprotection by $1,25(OH)_2D$ is through the induction of metallothionein (MT) mRNA to reduce cell apoptosis (De Haes et al., 2004b, Lee and Youn, 1998). One study noted that the reduction in apoptotic cells treated with $1,25(OH)_2D$ following UVR resulted from the recruitment of

metallothionein, a free radical scavenger, to reduce ROS molecules contributing to apoptosis (Lee and Youn, 1998). Mice lacking MT genes are generally more susceptible to UVR-induced immunosuppression, sunburn inflammation and apoptotic sunburn cells (Hanada et al., 1998, Reeve et al., 2000, Wang et al., 2004). Similarly, application of $1,25(OH)_2D$ to skin cells induced sphingosine-1-phosphate (S1P), which is a regulator of cell survival by increasing Bcl-2 to reduce apoptosis (Manggau et al., 2001).

In terms of $1,25(OH)_2D$ and its immunomodulatory actions with UVR, there are mixed reports. Firstly, topical application of $1,25(OH)_2D$ on Skh:Hr1 mice has been shown to prevent UVR-induced immunosuppression in mice, without having any basal immunosuppressive actions (Dixon et al., 2011, Dixon et al., 2005, Dixon et al., 2007). On the other hand, there is evidence to suggest that $1,25(OH)_2D$ at high doses is immunosuppressive in humans (Damian et al., 2010). Additionally, when used following UVR-exposure, it had no effect on immunosuppression whilst also providing protection from UVR-induced DNA damage and apoptosis (Damian et al., 2010). In agreement with this, De Haes et al. (2003) and Mason et al. (2010) showed that $1,25(OH)_2D$ suppressed levels of IL-6, a pro-inflammatory cytokine, in skin cells and mice respectively. IL-10 secretion, an immunosuppressive cytokine released from UVR-damaged cells is upregulated upon $1,25(OH)_2D$ application, as is the IL-10 receptor on keratinocytes (Yu et al., 2011). Furthermore, $1,25(OH)_2D$ suppresses the secretion of another pro-inflammatory cytokine, IL-12, from macrophages and dendritic cells, which then suppresses the activity of the T-helper cells involved in the acquired immune response (Bikle, 2009). An in vivo study has shown that

immunosuppressive T-regulatory cells are upregulated by $1,25(OH)_2D$ (Gorman et al., 2007). $1,25(OH)_2D$ also inhibits B cell proliferation and differentiation, and immunoglobulin production (Chen et al., 2007). Thus the evidence leans towards $1,25(OH)_2D$ being immunosuppressive rather than protecting against immunosuppression in humans, which therefore shows the importance of finding a photoprotective analogue.

1.5 VITAMIN D-LIKE COMPOUNDS AND ANALOGUES

Due to the fact that 1,25$(OH)_2$D readily causes hypercalcaemia and because of its expensive price, the use of 1,25$(OH)_2$D as a photoprotective agent in sunscreens is not viable. Thus it has become of increasing interest to discover alternative agents that are inexpensive and have low calcaemic activity.

1.5.1 20$(OH)D_3$

Recent studies in vitamin D metabolism have exposed a novel role for a cytochrome P450 enzyme (CYP11A1) in the hydroxylation of vitamin D_3 and its precursor 7-DHC. Known mostly for its role in oxidation and cleavage of the side chain on cholesterol to form pregnenolone, CYP11A1 also cleaves the side chain of 7-DHC and hydroxylates the side chain of vitamin D_3 to produce over ten novel products, as shown in figure 1.11 (Slominski et al, 2012; Slominski et al, 2005; Guryev et al, 2003). 20-hydroxyvitamin D_3 (20(OH)D) has been identified as the main reaction product (Slominski et al., 2005).

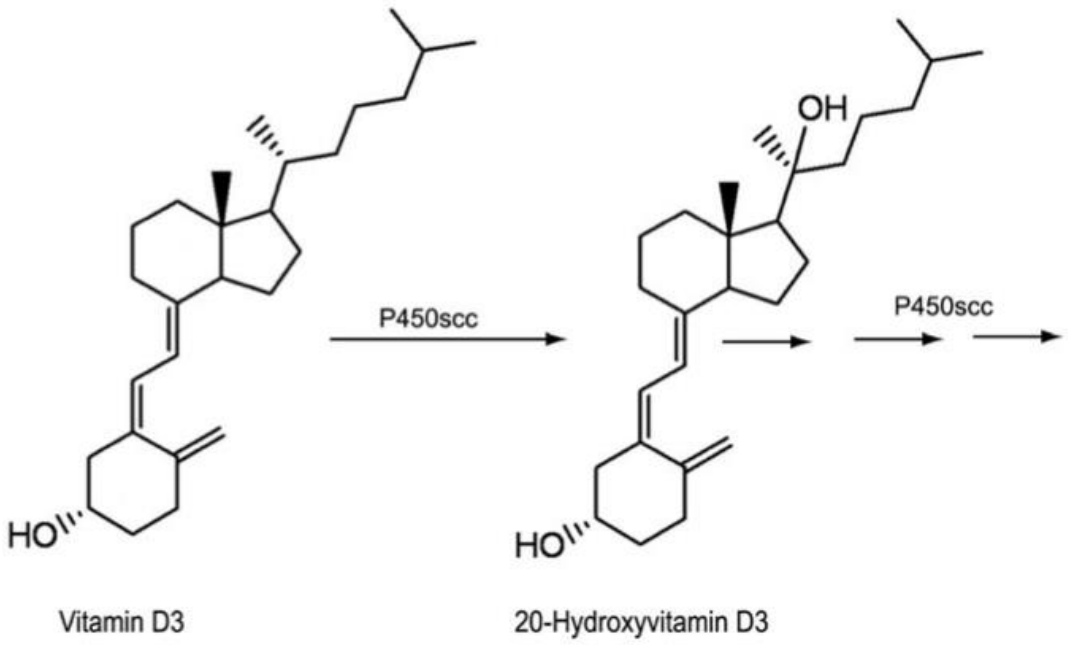

Figure 1.11 CYP11A1 metabolism of vitamin D3 to 20(OH)D3 (Janjetovic et al., 2009)

Slominski et al (2012) provided *in vivo* evidence this novel pathway, using HPLC techniques, further identifying 20-hydroxyvitamin D_3 (20(OH)D) as the major product of vitamin D_3 metabolism by CYP11A1 in areas of the body expressing high levels of P450cc, such as the steroidogenic adrenal glands, placenta and germ cells which suggests it may produce systemic effects (Slominski et al, 2012). Furthermore, the CYP11A1 system has been shown to exist in the epidermal layer of the skin (Slominski et al., 1996, Slominski et al., 2004) and is upregulated upon UVB/UVC radiation (Skobowiat et al., 2011).

20(OH)D is biologically active through binding to the VDR (Zbytek et al., 2008b, Tuckey et al., 2008b) however, knowledge of its biological significance is limited. Upon binding to the VDR, 20(OH)D can initiate heterodimerisation with the RXR to

increase inhibitor proteins for proliferation (Janjetovic et al., 2011b). It has been shown that 20(OH)D stimulates keratinocyte differentiation (Zbytek et al., 2008b) and decreases nuclear factor-κB (NK-κB) a transcription factor involved in the inflammatory response and the progression of cancer in cells (Janjetovic et al., 2009).

The anti-cancer effects of 20(OH)D have been shown in hepatocellular carcinoma and breast cancer cell lines, with the same effectiveness of 1,25$(OH)_2$D at reducing colony numbers. Additionally, melanoma cell proliferation was inhibited with application of 20(OH)D due to targeting and blockade of NK-κB activity (Wang et al., 2012a). It has therefore been acknowledged that 20(OH)D has anti-proliferative activity (Janjetovic et al., 2011b). The advantage of 20(OH)D over 1,25$(OH)_2$D use as an anti-cancer agent is that whilst both have antiproliferative effects, 20(OH)D produces none of the hypercalcemic effects of 1,25$(OH)_2$D, as seen in mice and rats (Janjetovic et al., 2011b, Slominski et al., 2010). However, it should be noted that whilst 20(OH)D is a poor substrate for CYP27B1 hydroxylation *in vivo*, the enzyme which activates 25$(OH)_2$D to 1,25$(OH)_2$D, the product 1,20-dihydroxyvitamin D_3 has some mild calcemic effects (Slominski et al., 2010).

1.5.2 1,25(OH)2D independent actions of the VDR, potential for 20(OH)D in photoprotection

Mice containing an ablated CYP27B1 gene that encodes for the 1α-hydroxylase enzyme are unable to form active 1,25$(OH)_2$D. In a study by Ellison and colleagues CYP27B1 -/- mice showed no increase in susceptibility to DMBA chemically induced

tumours compared to wildtype control mice whilst mice lacking full VDR functionality showed increased DMBA-induced carcinogenesis (Ellison et al., 2008). In the same study, VDR-KO mice exposed to UVR were shown to have decreased thymine dimer repair and enhanced photocarcinogenesis, whilst the effects of UVR on CYP27B1 -/- mice were not investigated. The authors suggested that it is the 1,25(OH)2D-independent action of the VDR rather than 1,25(OH)2D ligands that mediate protection from skin carcinogenesis (Ellison et al., 2008). In a recent study by the Bikle group, CYP27B1 -/- mice did not develop tumours with chronic exposure to UVR (Bikle et al., 2013, Teichert et al., 2011). Such findings suggest that there may be other ligands which activate the VDR, produced by a different pathway from the classic CYP27B1 hydroxylation of $25(OH)_2D$.

In regards to skin manifestations, 1α-hydroxylase knockout mice exhibit a phenotype almost identical to their wildtype counterparts, with the exception of small disruptions in epidermal keratinocyte differentiation, and delays in recovery of normal barrier function (Bikle et al., 2004). In contrast VDR-KO mice develop thickened skin with an abnormal morphology, long curved nails, and alopecia (Zinser et al., 2002).

Furthermore, the recent discovery of 20(OH)D which does not require 1α-hydroxylase to become biologically active provides evidence of alternate endogenous products which may mediate the non-genomic effects of the VDR, where $1,25(OH)_2D$ is not available (Slominski et al., 2005, Slominski et al., 2012, Tuckey et al., 2008a, Guryev et al., 2003). Such an endogenously produced

compound may provide a bridge between the findings of Ellison and Tiechert, and Dixon, Wood and Kensler (Dixon et al., 2011, Ellison et al., 2008, Kensler et al., 2000, Wood et al., 1983).

1.5.3 Tetrahydrocurcumin

Several bodies of evidence suggest that curcuminoids may be great anti-cancer agents due to their antioxidant properties (Naito et al., 2002, Osawa et al., 1995). In particular, curcumin is already well established as an anti-cancer, anti-neurodegenerative and anti-inflammatory agent, however is rapidly metabolised following digestion, limiting its effectiveness (Wu et al., 2013).

THC is an inexpensive, colourless *in vivo* metabolite of the turmeric spice-derived yellow curcumin (diferuloylmethane) (Sugiyama et al., 1996). As seen in figure 1.12 THC is formed by the hydrogenation of curcumin at the conjugated double bonds of the carbon skeleton which increases its antioxidant effectiveness (Somparn et al., 2007).

Figure 1.12 Hydrogenation of curcumin produces tetrahydrocurcumin (Sugiyama et al., 1996).

It has been suggested that the anti-cancer properties of THC may be due to the presence of the β-diketone moiety (Sugiyama et al., 1996). A recent study has shown that THC inhibits the PI3K/Akt pathway in a leukaemia cell line, and increases activity of the apoptotic ERK and JNK pathways, leading to cell death (Wu et al., 2011).

Conformational binding studies show that THC's precursor curcumin can bind to both genomic and alternate pockets of the VDR, however it preferentially activates the latter (Mizwicki et al., 2010). In addition, at pharmacological concentrations, curcumin not only has an affinity for binding at the VDR, but also for activating genomic transcription (Jurutka et al., 2007, Bartik et al., 2010). The binding of THC to the VDR has not been studied as extensively as curcumin, and since hydrogenation of double bonds on the carbon chain does not change the planar shape, it might be assumed that THC acts in a similar way at the VDR. Despite the probability of curcuminoid transcriptional capabilities via the VDR, use of THC in mice has been shown to have no effect on weight, and is not cytotoxic at pharmacological doses (Naito et al., 2002).

1.6 AIMS AND HYPOTHESES

1.6.1 Aims

The aims of this project are:

- To test whether THC, a component of the spice turmeric, known to have antioxidant effects at micromolar concentrations, is photoprotective at nanomolar concentrations against UVR-induced DNA damage in keratinocytes
- To test whether 20(OH)D, a novel 1,25$(OH)_2$D analogue reduces DNA damage in UVR-exposed fibroblasts and keratinocytes to a similar extent as 1,25$(OH)_2$D, and whether this photoprotection may be mediated by chloride channel opening.
- To investigate possible molecular mechanisms involved in 1,25$(OH)_2$D mediated photoprotection from UVR, in particular to determine the effects of inhibiting the Wnt signalling pathway on DNA damage in UVR-exposed keratinocytes.
- To test whether 20(OH)D is photoprotective against UVR-induced DNA damage and immunosuppression to an immune response-eliciting antigen in Skh:Hr1 hairless mice and whether this is sex-specific.
- To determine whether the estrogen receptor β (ERβ) is involved in photoprotection from UVR, using ERβ-knockout mice, and whether this effects the function of 20(OH)D.

1.6.2 Hypotheses

The hypotheses to be tested are:

- That 20(OH)D and THC in nanomolar concentrations are photoprotective to a similar extent as $1,25(OH)_2D$
- That if 20(OH)D is photoprotective it exerts its effects via induction of chloride channel opening, as seen in $1,25(OH)_2D$ -mediated photoprotection.
- That inhibition of UVR-induced Wnt signalling pathways modifies UVR-induced DNA damage, alone and in the presence of $1,25(OH)_2D$.
- That 20(OH)D is photoprotective *in vivo*, in particular that it reduces UVR-induced DNA damage following UV exposure. Additionally, that 20(OH)D has no effect on the basal immune response to a novel antigen but reduces UVR-induced immune suppression against a novel antigen.
- That photoprotection by 20(OH)D from UVR-induced DNA damage and immunosuppression is greater in females than males, and that this may be a result of presence of the ERβ gene.

2 METHODOLOGY

2.1 MATERIALS

2.1.1 General reagents and materials

Unless otherwise stated, all reagents, chemicals and salts were purchased from Sigma Aldrich (St Louis, MO, USA). Seventy-five cm^2 Falcon™ culture flasks and welled culture plates were purchased from Becton Dickinson Labware (Franklin Lakes, NJ, USA). Dulbecco's Phosphate buffered saline (D-PBS) was purchased from Sigma-Aldrich (St Louis, MO, USA), whilst high glucose containing Dulbecco's Modified Eagle Medium (DMEM) with and without calcium were from Invitrogen Life Technologies (NY, USA). Heat-inactivated foetal bovine serum was from SAFC Bioscience. MilliQ H_2O was purified and supplied by the system supplied by the Molecular Biology Facility within the University of Sydney (Sydney, Australia). Antimycotic and antibiotic solutions were purchased from Invitrogen Life Technologies (NY, USA). Poly-L-lysine hydrobromide used in coating coverslips was obtained from Sigma-Aldrich (St Louis, MO, USA). Betadine antiseptic, 20 ml sterile centrifuge tubes and 50 ml sterile sample jars were bought from Livingstone International (Sydney, Australia). Cell-scrapers and cell culture and bacteriological grade Petri dishes were from Sarstedt Ag & Co. (Numbrecht, Germany).

2.1.2 General equipment

General cell culture and experimentation was undertaken using sterile techniques within a biohazard laminar flow hood purchased from Gelman Sciences Pty (Sydney, Australia). A water-jacketed incubator acquired from Forma Scientific (Sydney,

Australia) was used to maintain live cells at 37°C and 5% CO_2. Cells were cryopreserved under liquid nitrogen in a Dewar purchased from Taylor-Wharton (Albury, Australia). The centrifuge was purchased from Hettich Zentrifugen (Tuttlingen, Germany). Cells were viewed using a phase-contrast microscope from Olympus Optical Co Ltd (Tokyo, Japan) and counted manually with a Neubauer bright-line haemocytometer purchased from Weber Scientific International Ltd (Sussex, England). The MSE Micro-Centaur centrifuge was obtained from Lab Supply (Perth, Australia). The plate shaker was purchased from Flow Laboratories (Sydney, Australia) and the vortex mixer was from Thermolyne Corporation (Dubuque, IA, USA). The electronic balance was obtained from A&D Co. Ltd. (Tokyo, Japan), and the PHM80 portable pH meter was purchased from Radiometer Cophenhagen (Paris, France).

2.1.3 Equipment used in UV irradiation

The solar simulator used in the *in vitro* studies contained a FS20T12 UVB lamp and a FL20SBL UVA lamp from Phillips (Amsterdam, Holland). To ensure these lamps were emitting the desired spectral irradiance for experimentation, a calibrated OL754 spectroradiometer from Optronics Laboratories Inc (Orlando, FL, USA) was utilised to measure the light. *In vivo* studies employed the use of six 40W F40T 10/BL UVA tubes from Hitachi (Tokyo, Japan) and a TL 100W/12 UVB tube from Phillips (Eindhoven, Holland). To filter out irradiation below 290 nm a cellulose tri-acetate sheet (thickness = 0.125 mm), purchased from Eastman Chemical Products (Kingsport, TN, USA) was used for both *in vivo* and *in vitro* experiments and used for no more than 4 hours total.

2.1.4 Vitamin D compounds

1α,25 dihydroxyvitamin D_3 (1,25$(OH)_2$D) was purchased from Cayman Chemical Co. (Ann Arbour, MI, USA). Dr Robert Tuckey School of Biomedical, Biomolecular and Chemical Sciences, University of Western Australia, Crawley, Australia generously supplied the 20-hydroxyvitamin D_3 (20(OH)D). Tetrahydrocurcumin (THC) was purchased from SAMI labs Ltd. (India). 1,25$(OH)_2$D, 20(OH)D and THC were dissolved in spectroscopic grade 100% ethanol and stored under argon at -80°C. The integrity of these compounds was tested prior to each experiment using a Nanodrop ND-1000 spectrophotometer purchased from Thermo Fisher Scientific (Australia) supplied by the Bosch Molecular Facility within the University of Sydney, Spectral scans of the compounds are shown in Figure 2.1. The concentration was calculated from their peak absorbance values divided by the molar extinction coefficient of each test compound (see Table 2.1).

Table 2-1 Spectrum peak at which the absorbance was recorded and extinction coefficient for each compound used to calculated their concentration, a measure of their integrity whilst in storage.

Compound	Spectrum peak at which absorbance was read	Extinction coefficient (ε) at spectrum peak
$1,25(OH)_2D$	265	18200
20(OH)D	263 (Janjetovic et al., 2009, Zbytek et al., 2008b)	18000
THC	281 (Khopde et al., 2000)	15460

a.

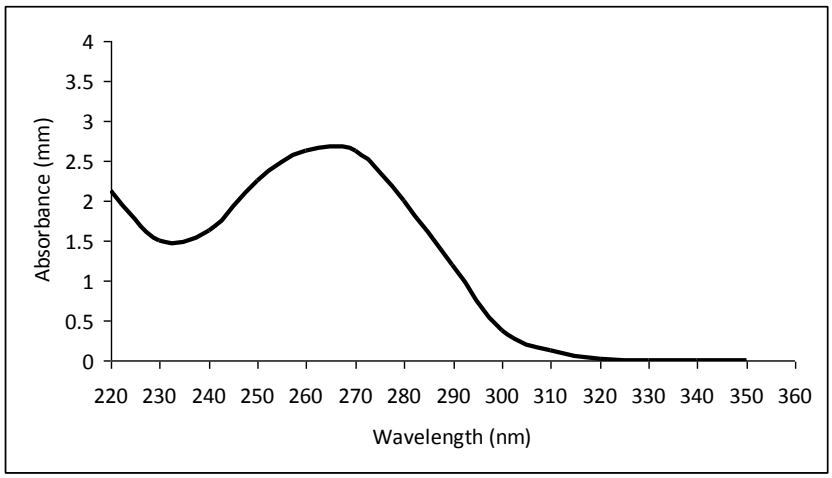

b.

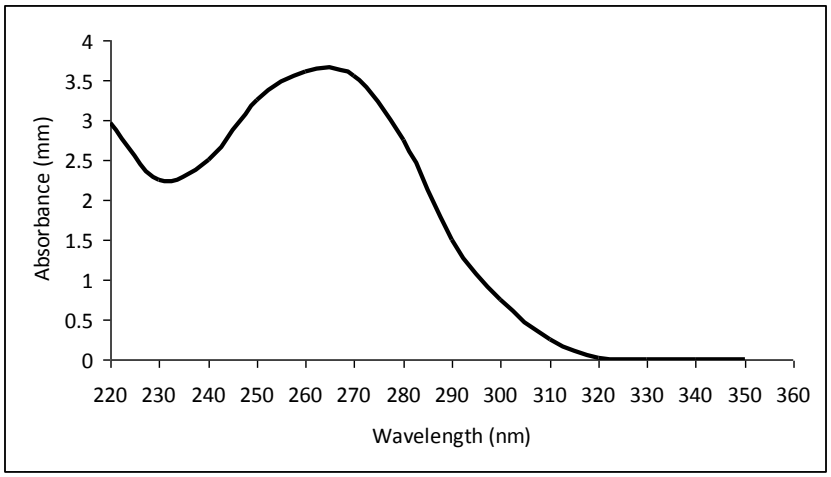

c.

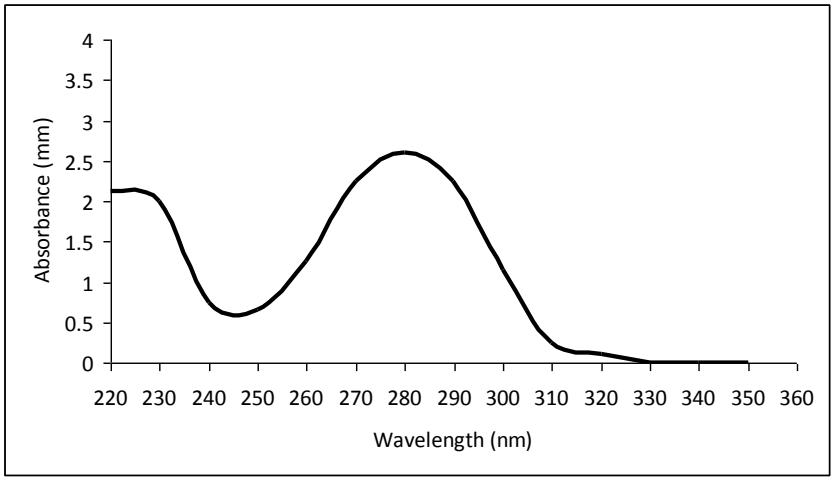

Figure 2.1 Spectral scans of (a) 0.1 mM 1,25(OH)$_2$D$_3$, (b) 0.1 mM 20(OH)D and (c) 0.1 mM THC

2.1.5 Inhibitors of Wnt signalling pathway and chloride channels

4,4'-Diisothiocyanatostilbene-2,2'-disulfonic acid disodium salt, DIDS, a chloride channel antagonist was purchased from Sigma-Aldrich (St Louis, MO, USA) and stored in spectroscopic grade DMSO under argon at room temperature. The Wnt inhibitor IWR-1-endo was purchased from Cayman Chemical Co. (Ann Arbour, MI, USA).

2.1.6 Materials used in immunohistochemistry

The mouse monoclonal IgG_1 anti-thymine dimer antibody H_3 (Roza et al., 1988) was obtained from Sigma-Aldrich, whilst the mouse monoclonal anti-8-oxodG clone 2E2 (Soultanakis et al., 2000) was purchased from Trevigen Inc. (Gathersburg, MD, USA). The DAKO LSAB kit and diaminobenzidine (DAB) were purchased from DAKO (Glostrup, Denmark). Images of the stained cells were acquired using the Nikon Eclipse E800 Macro-Imaging Microscope from Nikon Instruments Inc. (Melville, NY, USA) in conjunction with Leica DFC500 colour camera and LAS imaging software purchased from Leica Microsystems Ltd (Switzerland). Image analysis was undertaken using MetaMorph Imaging System, supplied by the Advanced Microscopy Facility of the Bosch Institute.

2.1.7 Materials used in genotyping

The REDExtract-N-Amp Tissue PCR kit and primers were purchased from Sigma-Aldrich (St Louis, MO, USA). Use of the Hybaid PCR thermal cycler and UVP agarose gel digital imaging system were kindly provided by the Bosch Molecular Biology Facility (Sydney, Australia).

2.1.8 Materials used in animal studies

All animal studies were approved by The University of Sydney Animal Ethics Committee. Female and male Skh:hr1, albino, inbred mice were obtained from the University of Sydney Veterinary Pathology colony. The ethics approval number used for these experiments was K22/1-2011/3/5457. Oestrogen receptor β knockout (ERβKO) mice originally designed by Krege and colleagues (Krege et al., 1998) and C57B1/6 mice used for wildtype comparison were manufactured by A/Prof Vivienne Reeve. Mice were housed in wire topped plastic boxes at temperatures between 23-25°C, maintained by yellow lighting, with a continual supply of fresh H_2O from a sipper. All conditions were facilitated and provided by A/Prof Vivienne Reeve, Photobiology Laboratory, Faculty of Veterinary Science within The University of Sydney. Mice were kept on Shepherds Premium Corn Cob bedding, (Techniplast), and fed with Gordon rat and mouse pellets (Yandeera, Australia). Polyethylene glycol and 4-ethoxymethylene-2-phenyl-2-oxazolin-5-one (oxazolone) (w/v) were purchased from Sigma-Aldrich (St Louis, MO, USA). The spring micrometer was sourced from Interapid (Zurich, Switzerland).

2.1.9 Compositions of media, buffers and solutions

Keratinocyte Growth Medium (KGM)

To promote cell growth, without differentiation, keratinocytes in culture are grown in a low calcium medium. Human keratinocytes were grown in KGM containing DMEM without calcium, 2.2 g/L $NaHCO_3$, 0.293 g/L glutamine, 2.385 g/L HEPES and 500 μg/L hydrocortisone. For isolation of cells from primary tissue, 0.03 g/L penicillin and 0.05 g/L streptomycin was added to the KGM. In culture of

keratinocytes 5000 ng/L epidermal growth factor (EGF), 10 nM cholera toxin with 5% v/v sterilised fetal bovine serum (FBS) was included in the KGM. Henceforth these are referred to as supplements.

0.25% Trypsin

0.3525 g/L, $NaHCO_3$, 2.5 g/L trypsin in MilliQ H_20.

0.1% Trypsin/0.02% EDTA

0.2 g/L EDTA, 1 g/L D-glucose, 0.4 g/L KCl, 8 g/L NaCl, 0.580 g/L $NaHCO_3$ and 1 g/L trypsin in MilliQ H_20.

Martinez buffer solution

Proteins contained in cell medium may absorb some UV radiation during experimentation thus cells may not receive equal amounts of treatment. Thus clear Martinez solution is applied to cells for irradiation as it contains enough glucose for cellular metabolism, without absorbing UV radiation. Martinez solution was made up in MilliQ H_2O and contained 0.4738 g/L NaCl, 0.41 g/L KCl, 0.244 g/L $MgCl_2.6H_2O$, 0.1872 g/L $NaH_2PO_4.2H_2O$, 1.9523 g/L NaHEPES, 1.7873 g/L HEPES, $CaCl_2.2H_2O$, 1.8016 g/L D-glucose.

2.2 *IN VITRO* METHODS

2.2.1 Primary cell culture

The current project had approval from The University of Sydney Human Ethics Committee, using the ethics approval number as in 2.1.8. Primary human keratinocytes and fibroblasts were isolated from neonatal foreskins donated to the laboratory by a paediatric surgeon. Samples were provided only after informed consent from a parent or guardian was obtained. Each sample was processed separately and aseptically within a laminar flow biohazard hood. Upon arrival into the laboratory, the foreskin was maintained in medium containing the antibiotics penicillin and streptomycin, but no foetal calf serum at 4°C for 48 hours post-surgery until cell culture processing was performed. The antibiotics were essential for the prevention of any bacterial contamination. The foreskin was then washed with 70% ethanol twice and submerged in Dulbecco's phosphate buffered saline (DPBS) containing the aforementioned antibiotics for 3 minutes. The foreskin was then washed and submerged in PBS for a further 3 minutes. The fatty hypodermis and blood vessels were removed and discarded.

2.2.2 Isolation of keratinocytes

The remaining skin containing the dermis and epidermis was dissected into 3 mm by 3 mm pieces and rinsed in antiseptic Betadine. PBS was then used to wash the samples. The skin pieces were then transferred to a centrifuge tube containing 0.1% (w/v) sterilised dispase in DPBS with antibiotics and kept at 4°C for 24 hours.

Dispase is a protease which cleaves fibronectin to dissociate the dermis from the epidermis.

The following day, the epidermis was isolated from the dermis and submerged in 0.1% trypsin/0.2% EDTA solution at 37°C for 16-20 minutes with intermittent agitation to stimulate the reaction. The trypsin reaction was stopped by the addition of an equal volume of KGM with 5% (v/v) FBS. After cells were mechanically separated by agitation with a sterile transfer pipette, cells were centrifuged at room temperature for 5 minutes at 2000 rpm. The supernatant media was discarded and the cell pellet was resuspended in KGM growth medium. Cells were plated in 75 cm^2 culture flasks and incubated at 37°C with 5% CO_2 and media was replaced with fresh KGM growth medium after 24 or 48 hours to remove unattached cells and promote growth and proliferation. KGM growth media was changed and refreshed every 2 to 3 days until 70% confluency was achieved.

2.2.3 Passaging cell cultures

Cells were passaged upon reaching 70-90% confluence in the culture flask. Medium was decanted from the culture flask and the flask was rinsed once with DPBS. 0.1% trypsin/0.02% EDTA in DPBS was added to the flask and decanted after 10 seconds. “Dry” trypsinisation ensures that cells are allowed to round, and detach individually from the flask without forming a “sheet” which will not re-attach in a new flask or plate (Dr Mark Rybchyn, personal communication). Following trypsin exposure, the flask was left to incubate for 8 minutes for keratinocytes and 4 minutes for fibroblasts at 37°C. At 5 minutes, the flask was agitated to ensure cells were successfully detaching from the bottom of the flask. After cells had lifted, KGM with

supplements for keratinocytes was added to neutralise the reaction. The resulting cell suspension was evenly reflasked into two or more culture flasks or plated for an experiment.

2.2.4 Cryopreservation

Upon reaching 70-90% confluence, cells that were not required for experimentation were frozen down and preserved. Cells were detached from the bottom of the culture flask as in 2.2.1.2, however the reaction was neutralised by the addition of the ice-cold 5% (v/v) DMSO in FBS freezing medium. The remaining cell suspension was transferred to cryovials and stored at -80°C for approximately 24 hours. After this time, cryovials were stored in liquid nitrogen for long term preservation.

2.2.5 Retrieval of cells from cryopreservation

Cryovials were removed from the liquid nitrogen when required for experimentation and thawed briefly in a 37°C waterbath. The cells were then transferred to a centrifuge tube containing KGM with 5% FBS and centrifuged for 5 minutes at 1500 rpm at room temperature. The remaining supernatant was decanted and the cell pellet was gently resuspended in KGM with supplements and transferred to a 75 cm^2 flask.

2.2.6 Poly-l-lysine coating coverslips

Cells will not adhere to glass, thus poly-L-lysine is used to coat the coverslips so that cells may be stained during immunohistochemistry. Glass coverslips (5mm diameter) were autoclaved and dried in a scintillation vial to ensure sterility. Under sterile conditions, 0.01% poly-L-lysine was added to the vials. The vial was

continuously agitated for 5 mins so that all coverslips were exposed to the polymer. The poly-L-lysine was removed and coverslips were rinsed with sterilised MilliQ H_2O three times and then dried in sterile glass Petri dishes for at least 6 hours. The coated coverslips were stored in sterile sample jars at room temperature.

2.2.7 Plating for experimentation

Passage 2-5 cells were used for experimentation. As in 2.2.1.2 cells were passaged and resuspended in cell specific media. Ten μl of the cell suspension was obtained and cell density was calculated using the haemocytometer. For use in whole cell immunohistochemistry in 96 well plates, keratinocytes were seeded onto poly-L-lysine coated coverslips placed in each well, in quadruplicate for each treatment.

For experiments using keratinocytes, 24 hours after plating, and at least 24 hours prior to experimentation, media was changed to supplement-free KGM with 5% FBS. This is to ensure that normal quiescent cell signalling pathways were restored before experimentation, as the supplements stimulate proliferation.

2.2.8 Ultraviolet irradiation

Cells were irradiated under aseptic conditions within a laminar flow hood, using the solar simulator described in 2.1.3. All cells received the same treatment with the exception of sham cells which were covered in aluminium foil so they did not absorb any UVR. Before irradiation media in both sham and UVR treatment groups was aspirated and replaced with Martinez buffer solution containing glucose to support cellular metabolism without absorbing UVR. The UVR setup inside the laminar flow hood is depicted in Figure 2.2.

UV irradiation below 290 nm was removed through a cellulose tri-acetate sheet used no more than 4 hours of irradiation in total. Plates were placed on a turn table and at exactly halfway through irradiation were turned 180° so that cells received even exposure of UVR. Post UVR, Martinez buffer solution was aspirated and media containing treatments was added to the wells.

Figure 2.2 *In vitro* irradiation set up

2.2.9 UV lamps

Output of the UVA and UVB lamps was checked to ensure cells were receiving identical UVR doses throughout experimentation. A calibrated OL754 spectroradiometer was used to measure spectral irradiance. Duration of irradiation (70 minutes) was calculated using the measured values so that cells received a UVR dose of 2138 mJ/cm^2 of UVA and 610 mJ/cm^2 of UVB. This is equivalent to approximately three times the minimal erythemal dose (MED) from sunlight. One MED produces mild redness of the skin. For the duration of experimentation, irradiance in the UVC range below (290nm) were filtered out using cellulose triacetate sheets, to reflect the natural filtering effect of the ozone layer. Figure 2.3 represents the irradiances taken from UV lamps with and without the cellulose triacetate filter and from sunlight at midday in March in Sydney, Australia.

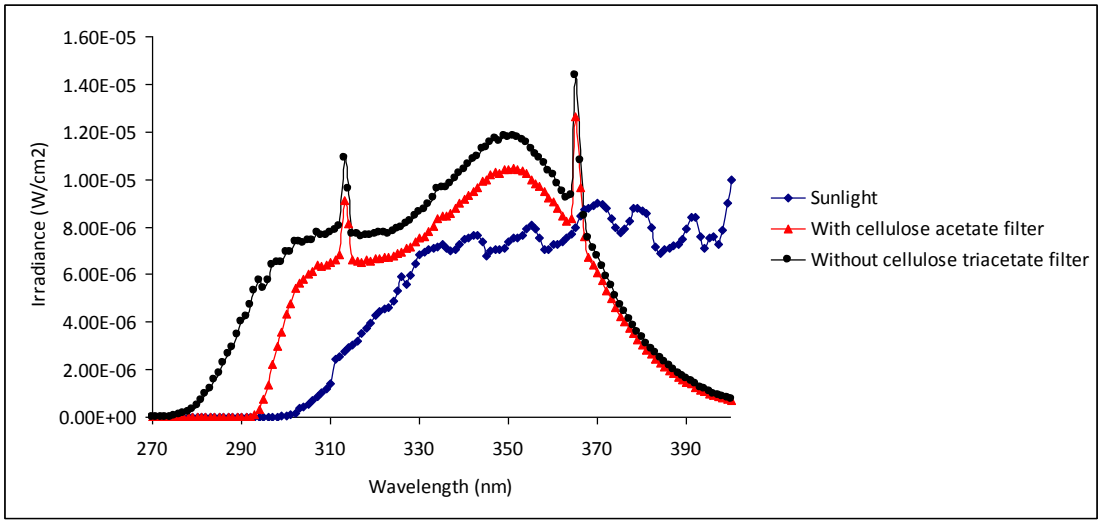

Figure 2.3 Output of the UV lamps. UV irradiances as measure by a calibrated OL754 spectroradiometer. The black line demonstrates output without a triacetate filter. The red line represents experimental radiation with a cellulose triacetate filter, to mimic the filtering effect of the ozone, which is seen on the blue line taken at midday in March in Sydney, Australia

2.2.10 Application of treatments and inhibitors

For all experiments, cells were treated post-UVR with vehicle, 1,25$(OH)_2$D, 20(OH)D, THC, inhibitors or a combination of the vitamin D compounds and an inhibitor. As stated in 2.1.5, inhibitors used were DIDS and IWR-1-endo. Inhibitors need a longer time to exert their inhibitory effects on cells, thus they were applied with Martinez buffer solution immediately before UVR and were present throughout the procedure. For keratinocytes, treatment media was KGM with 5% FBS.

2.2.11 Immunocytochemistry for the detection of thymine dimers and 8oxodG

Cells were incubated at 37°C for 1 or 3 hours post-UVR and with treatment before fixation. Cells were rinsed with 100µl DPBS/well and then fixed with ice-cold 100%

methanol at -20°C for 7-10 minutes. Subsequently cells were washed 3 times with MilliQ H_2O and dried overnight. Endogenous peroxidases were blocked with the addition of 1% hydrogen peroxide (H_2O_2) (v/v) in MilliQ H_2O for 5 minutes. Antigen retrieval was achieved by application of 70 mM NaOH in 100% ethanol to cells for 2 minutes to denature DNA before proteolytic digestion using 1μg/ml proteinase K for 5 minutes at room temperature for thymine dimer detection and 10 minutes at 37°C for 8-oxoguanine detection. The cells were then submerged in 50% horse serum (w/v) in PBS for 1 hour at room temperature on the plate shaker to block non-specific antibody binding. After application of H_2O_2, proteinase K and horse serum the cells were washed twice for 2 minutes with MilliQ H_2O.

The primary antibody for thymine dimer detection was mouse monoclonal IgG_1 anti-thymine dimer antibody H_3 and for 8-oxoguanine detection was mouse monoclonal IgG_1 anti-8-oxoguanine antibody 2E2. Anti-thymine dimer (5 μg/ml) antibody or 8-oxoguanine (0.5 mg/ml) were diluted in 0.1% Tween-20 (v/v) in Tris-buffered saline (TBST) and added to cells for 1 hour with continuous agitation on the plate shaker. The high sensitivity LSAB kit was utilised to visualise primary antibody binding. The LSAB yellow biotinylated secondary antibody was applied to the cells for 15 minutes (1 drop/well). Subsequently, streptavidin-linked HRP was added to the cells for 15 minutes at 1 drop per well. After exposure to the primary antibody and each reagent following, cells were washed twice for 2 minutes each with TBST. 3'3'-diaminobenzidine (DAB) chromagen solution (DAKO) was applied 5 minutes to visualise and localise thymine dimer or 8-oxodG nuclear staining in the cells. Cells were then washed in MilliQ H_2O and coverslips were mounted on

Ultracruz, Santa Cruz Biotechnology (CA, USA) aqueous mountant that contains 4',6-diamidino-2-phenylindole (DAPI) counterstain. DAPI stained all nuclei blue specifically, with very little cytoplasmic labelling when observed with the UV filter in the Nikon epifluourescence microscopy, whilst DAB staining was visualised by bright field microscopy.

2.2.12 Image analysis

Coverslips were examined with 20x objective using the Nikon Eclipse E800 Macro-Imaging Microscope. For bright field images, the light intensity remained constant throughout analysis of each experiment. A Leica DFC500 colour camera was used to capture brightfield image for the DAB stained DNA lesions DAPI fluorescence image of the same area was taken for counting the total nuclei in the same field. Three brightfield images and their corresponding DAPI images were taken of each sham coverslip, and four brightfield images and their corresponding DAPI images were taken of each UV coverslip for analysis.

Using the MetaMorph Imaging System, images were analysed for the occurrence of thymine dimer or 8-oxodG staining. Using greyscale and intensity transformation, saturation threshold values for positive staining were obtained from sham images and applied to the UV images for analysis. When DNA damaged nuclei take up the DAB stain, the DAPI staining becomes masked by the chromagen precipitate in the nuclei, the total number of nuclei in the image was calculated by combining the area of DAB staining with the total area of DAPI staining. Positively stained nuclei

with DNA damage were expressed as a percentage of the total nuclei in each region of interest (ROI).

2.3 *IN VIVO* METHODS

2.3.1 Maintenance and treatment of animals

Female and male Skh:hr1, albino, hairless mice and female C57 estrogen receptor β knockout (ERβKO) and wildtype C57/B16 mice were used for *in vivo* experimentation. Hairless mice were age matched and randomly separated into 14 groups of 3 mice per group for immunohistochemistry studies and 8 groups of 5 mice per group for immunosuppression studies. Sexes were kept separate. Mice were housed in wire topped plastic boxes lined with compressed corn cob bedding, with a constant supply of rodent pellets and fresh H_2O. Since male mice are typically more aggressive than females, males remained in the same smaller boxes from birth with no more than 4 littermates in one box. Temperature was maintained at 23-25°C throughout experimentation.

2.3.2 Genotyping

Mice with a completely disrupted estrogen receptor β (ERβ) gene in both sexes appear to develop normally to adulthood and are phenotypically identical to their wild-type counterparts. However, female mice have reduced fertility, resulting in breeding difficulties. Thus breeding pairs must be heterozygous.

DNA extraction solution was prepared on ice by mixing 50 μl extraction and 12.5 μl tissue preparation solutions from the REDExtract-N-Amp tissue polymerase chain reaction (PCR) kit in a 600 μl microcentrifuge tube. After combining the two solutions, the mixture is viable for a maximum of two hours. A 1-1.5 cm tail sample

was cut from each mouse. In a Petri dish, the bony core was mechanically separated from the tail skin and both were surgically cut into smaller pieces. The pieces were placed into the tube containing DNA extraction solution and shaken to ensure all pieces were thoroughly exposed. The samples were vortexed and incubated at room temperature for 10 minutes, then heat shocked at 95˚C for 3 minutes. One hundred μl of neutralisation solution was added to the tube, which was vortexed and spun down at room temperature. In two 200 μl microcentrifuge tubes 2 μl of DNA extraction solution supernatant, 7 μl of distilled MilliQ H_2O, 10 μl of REDExtract -N-Amp PCR ReadyMIX, 2 μl of each of the forward and reverse primers (Table 2.2) were mixed.

Table 2-2 The forward and reverse primers used in PCR analysis of knockout mice

Area of DNA	**Primer**
Forward	5'-GTGATGAGCTGAGGTGGTGCTT-3'
Reverse (normal ERβ gene)	5'-CATCCTTCACAGGACCAGACAC-3'
Reverse (mutant ERβ gene)	5'-GCAGCCTCTGTTCCACATACAC-3'

One tube contained wildtype primers and the other contained primers for the knockout genes. The tubes were vortexed and centrifuged briefly before DNA amplification in the PCR thermal cycler. Thermal cycling included initial denaturation for 3 mins at 94˚C, denaturation for 1 minute at 94˚C, annealing at 45-68˚C for 1 minute, extension at 72˚C for 1-2 minutes and final extension for 10 minutes at 72˚C before reducing the temperature to 4˚C.

Amplified DNA was identified using agarose gel electrophoresis. Twenty μl of the PCR solution from the both the wildtype and knockout gene samples were added to the agarose gel, in corresponding wells. The gel was run at a constant voltage of 100 V for 60 mins. Bands were visualised using the UVP agarose gel digital imaging system (fig. 2.3). Samples from homozygous knockout mice show a 1479-base pair (bp) band, whilst homozygous wild-type mice show a 1435-bp band. Samples from heterozygous mice show both bands.

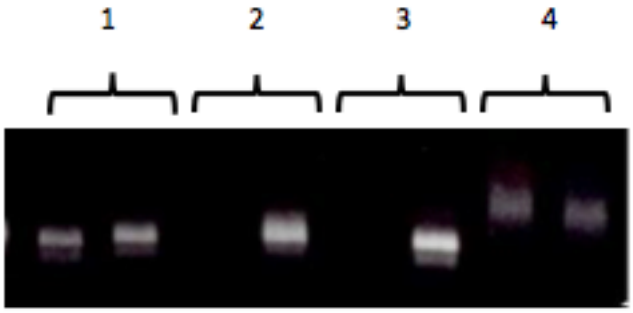

Figure 2.4 Confirmation of ERβ knockout mice, born from heterozygous parents. Samples 1 and 4 are heterozygous since the blot shows the presence of two bands. Samples 2 and 3 are homozygous for the knockout gene since they have no bands in the first lane of their pair.

2.3.3 Topical treatments

Stock solutions of 1,25$(OH)_2$D, 20(OH)D and THC were diluted in spectroscopic grade ethanol and then into polypropylene glycol and MilliQ H_2O so that the ratio of treatment in ethanol:polypropylene glycol:MilliQ H_2O was 2:1:1. Concentrations of the active agent were expressed as ρmol/cm^2 where 100μl of solution covered 7cm^2 of back skin.

2.3.4 UV irradiation

The solar simulator was switched on at least 30 minutes prior to irradiation of the mice so as to ensure the bulbs had warmed up and emitting the correct wavelengths. Wavelength activity was checked by radiometer and the time calculated for a 2.5 MED dose of UV radiation for each experiment. Mice receiving UVR were irradiated in open topped boxes covered with cellulose tri-acetate (0.125 mm) to eliminate wavelengths below 290nm. As UV fluence is affected by temperature, a steady temperature was maintained via a direct fan. Since ERβ-KO mice and ERβ-WT mice are hairy, it was necessary to shave the dorsum of their backs to ensure their skin received the UVR. For immunosuppression studies, skin fold thickness in all groups was measured and recorded immediately before UV irradiation, described in more detail in section 2.3.5.

Immediately following UV irradiation, mice were treated with either vehicle, 1,25 $(OH)_2$D or 20(OH)D for immunosuppression studies, and either vehicle, 1,25$(OH)_2$D, 20(OH)D or THC for immunohistochemistry studies. One hundred μl of the treatment was painted dorsally on the mouse using a pipette.

2.3.5 Measurement of erythema and skin oedema

The inflammatory response to UV irradiation was observed by measurement of dorsal skinfold thickness using a spring micrometer (Fig. 2.4). Measurements were taken immediately prior to UV irradiation and at 24, 48 and 72 hours post UVR. Change in skinfold thickness was expressed as the difference between measurements taken at specified time points post UV irradiation and the pre measurements.

Figure 2.5 Measurement of dorsal skinfold thickness on a hairless Skh:Hr1 mouse using a spring micrometer

2.3.6 Contact hypersensitivity reaction

This laboratory has previously reported a protective effect of 1,25$(OH)_2$D and vitamin D-like compounds against UVR-induced systemic immunosuppression. This is measured using the contact hypersensitivity (CHS) reaction, as described in Reeve (2002). One week after UV irradiation all mice were sensitised with 100 μl of 2%

oxazolone (w/v) in 100% ethanol applied to abdominal skin (Fig. 2.5). Sensitisation was repeated the following day to ensure there was sufficient exposure to the skin irritant to induce an immune response.

Figure 2.6 Abdominal application of 2% oxazolone using a pipette to sensitise the mice

Two weeks following UV irradiation, 5 μl of 2% oxazolone was applied to each side of the pinnae of each ear of all mice. The degree to which the ears of the mice swelled is an indication of the secondary immune response to the re-exposure of the contact antigen. A spring micrometer was utilised to objectively measure the ear thickness prior to, and 16 hours following antigen challenge. Mice were subject to a gaseous anaesthetic for a short period of time so as to gain accurate measurements of ear thickness, shown in figure 2.6.

Figure 2.7 Measurement of ear swelling on a hairless Skh:Hr1 mouse using a spring micrometer

The degree of immunosuppression for UVR exposed mice was calculated as the difference between pre- and post-challenge ear thickness measurements of non-irradiated mice as a proportion of the difference between pre- and post-challenge ear thickness measurements of irradiated mice for each treatment. Percentage of immunosuppression was calculated by subtracting the previous value from 100% (Dixon et al., 2007).

2.3.7 Harvesting of skin biopsies for immunohistochemical staining

Three hours post UV irradiation and treatment, mice were sacrificed by inhalation of CO_2 within an enclosed chamber. Dorsal skin biopsies were dissected from the area between the shoulders known as the "hotspot" using surgical scissors, shown in figure 2.7. Skins were immediately preserved in HistoChoice (Amresco) for 6 hours at 4°C, before being washed with ethanol. Skins were taken to Blackburn

Pathology Facility where they were embedded on paraffin blocks, cut into 5 μm sections and mounted onto glass slides for immunohistochemical staining.

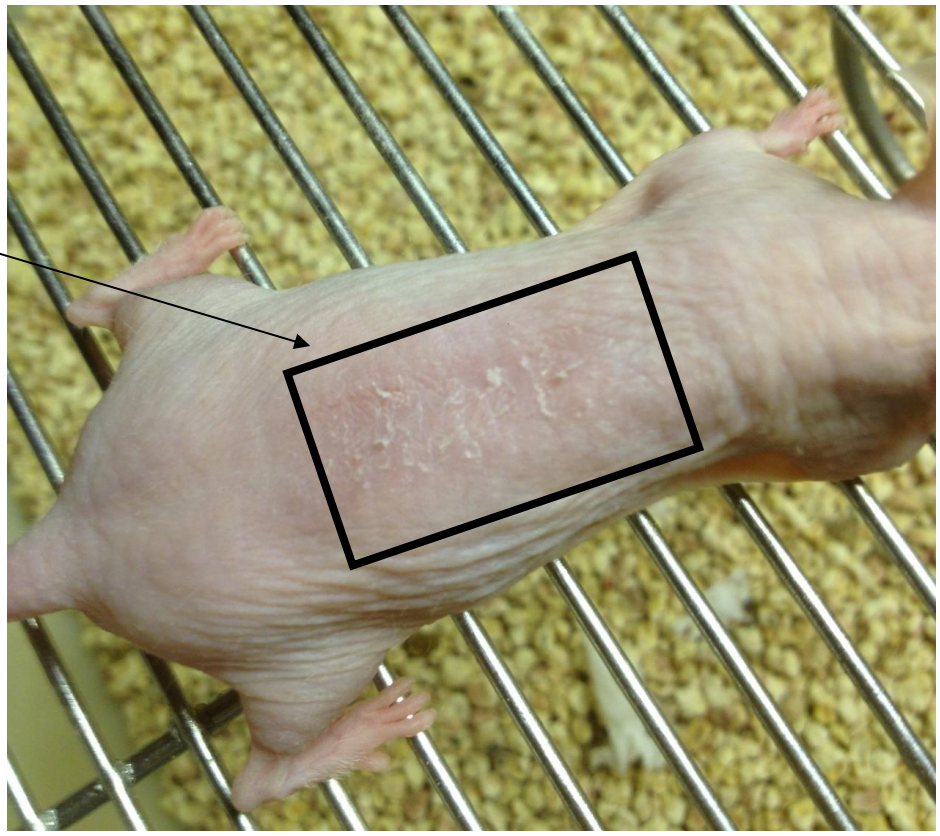

Figure 2.8 Example of a dorsal "hotspot" after exposure to UVR from which biopsies were taken for immunohistochemical staining

2.3.8 Immunohistochemistry for detection of thymine dimers in fixed mouse skin

Slides were prewarmed at 37°C for 10 minutes before de-paraffinisation through 2 washes of xylol for 10 minutes each. Sections were then rehydrated through graded alcohol solutions. This was achieved by exposure to two washes of absolute ethanol, two of 95%, one in 70% and then H_2O for 2 minutes in each. Antigen retrieval was achieved by submerging slides in heated 0.01 M citrate buffer for 10

minutes at 95°C, before two consecutive washes in TBS for 3 minutes each. Sections were then subject to 1% H_2O_2 for 5 minutes to block endogenous peroxidases with three subsequent washes in TBST for 2 minutes each. To block non-specific antibody binding, sections were allowed to sit in 10% horse serum in TBST for 30 minutes at room temperature with constant agitation.

The DAKO Animal Research Kit was used for immunohistochemistry. The primary antibody (2 μg/ml), mouse monoclonal antibody IgG_1 to the thymine dimer clone H_3 was diluted in antibody diluent (DAKO) together with the biotinylation reagent containing biotinylated anti-mouse immunoglobulin in Tris-HCl with stabilising protein and 0.015 M sodium azide from the ARK kit for 15 minutes followed by the kit blocking reagent containing normal mouse serum and incubated for 5 minutes. The sections were then incubated in the solution for a further hour at room temperature. Streptavidin conjugated to the reporter molecule HRP was added to the sections for 15 minutes following which diaminobenzidene (DAB) chromagen was applied to the sections for 5 minutes to visualise direct localisation of thymine dimers in the skins. After exposure to the primary antibody and streptavidin-HRP, sections were rinsed in three two minute washes of TBST, whilst after DAB application, sections were washed in MilliQ H_2O for 2 minutes.

For the dehydration process, sections were exposed to one wash of MilliQ H_2O, one wash in 70% ethanol, two washes in 95% ethanol, and two washes in absolute ethanol for 2 minutes each. Subsequently, slides were subjected to two washes of

xylol for 10 minutes each before coverslips were mounted with Entellin mounting medium for visualisation under the microscope.

2.3.9 Image analysis

Image analysis for the sections of mouse skin were carried out as detailed in 2.2.12, except that images were captured at 200x the original magnification and positive staining was expressed as percentage of total area of the epidermis. The amount of DNA damage was calculated as the proportion of DAB positive-stained nuclei in the epidermis

2.4 Statistical analysis

For *in vitro* studies of CPDs and oxidative stress in 96 well plates, results were from quadruplicates of each treatment. For ELISAs, results were derived from triplicates of each treatment. Except where indicated, each experiment was performed a minimum of two times. For *in vivo* studies of CPD formation, results are based on 3 mice per treatment group and expressed as mean +/- 1 standard deviation. For immunosuppression, results are from a single experiment of 5 mice per treatment group and expressed as mean +/- 1 standard error of the mean (SEM). For all studies, treatment groups were compared by one way analysis of variance (ANOVA) followed by Tukey-Kramer post-test using the GraphPad Instat statistical program. A P value of less than 0.05 was considered significant.

3 PHOTOPROTECTION AGAINST UVR INDUCED DNA DAMAGE BY NOVEL VITAMIN D COMPOUNDS

3.1 RESULTS

3.1.1 Effect of 1,25(OH)$_2$D, 20(OH)D and THC on the presence of thymine dimers in cultured keratinocytes following UVR

Previous work in this laboratory has established that the application of 1nM 1,25(OH)$_2$D exerts a photoprotective effect against DNA damage, in particular thymine dimers, a subset of cyclobutane pyrimidine dimer (CPD) in keratinocytes and fibroblasts following UVR (Dixon et al., 2005, Dixon et al., 2011, Sequeira et al., 2012b, Song et al., 2012, Wong et al., 2004). Additionally, several studies have demonstrated that the non-genomic 1,25(OH)2D analogues (JN, QW) and vitamin D-like compounds such as curcumin at this concentration reduce the presence of UVR-induced thymine dimers, to the same extent as 1,25(OH)$_2$D itself (Poliakov, 2009; (Gordon-Thomson et al., 2012, Sequeira, 2011). Protective effects of 1,25(OH)$_2$D were confirmed in the study, and protection was also shown for the first time by 20(OH)D (1nM and 10nM) and THC (1nM). Figure 3.1 is a representation of images used for the analysis off thymine dimer positive staining in sham and UVR exposed cells. The image of vehicle-treated unirradiated cells (sham) (Fig. 3.1a) represents all the sham treated groups, as unirradiated skin treated with 1,25(OH)$_2$D, 20(OH)D or THC, also showed no positive staining (not shown). There is increased staining in nuclei in vehicle treated cells (Fig. 3.1 b) following UVR compared to its sham counterpart (Fig.3.1a). As expected the number of positively stained nuclei in 1,25(OH)$_2$D-treated cells (Fig.3.1c) was markedly reduced in comparison to vehicle-

treated cells, following UVR. Similarly, addition of 1nM 20(OH)D following UVR reduced positive staining compared to vehicle-treated UVR-exposed cells (Fig. 3.1d), indicating that 20(OH)D is photoprotective. This was also seen with treatment of 10 nM 20(OH)D and 1nM THC with UVR (Fig.3.1e,f, respectively). Figure 3.2 quantitatively shows a significant reduction in thymine dimers following UVR by 1,25$(OH)_2$D and various doses of 20(OH)D when compared to vehicle-treated cells. One nM THC was also effective in reducing thymine dimers following UVR.

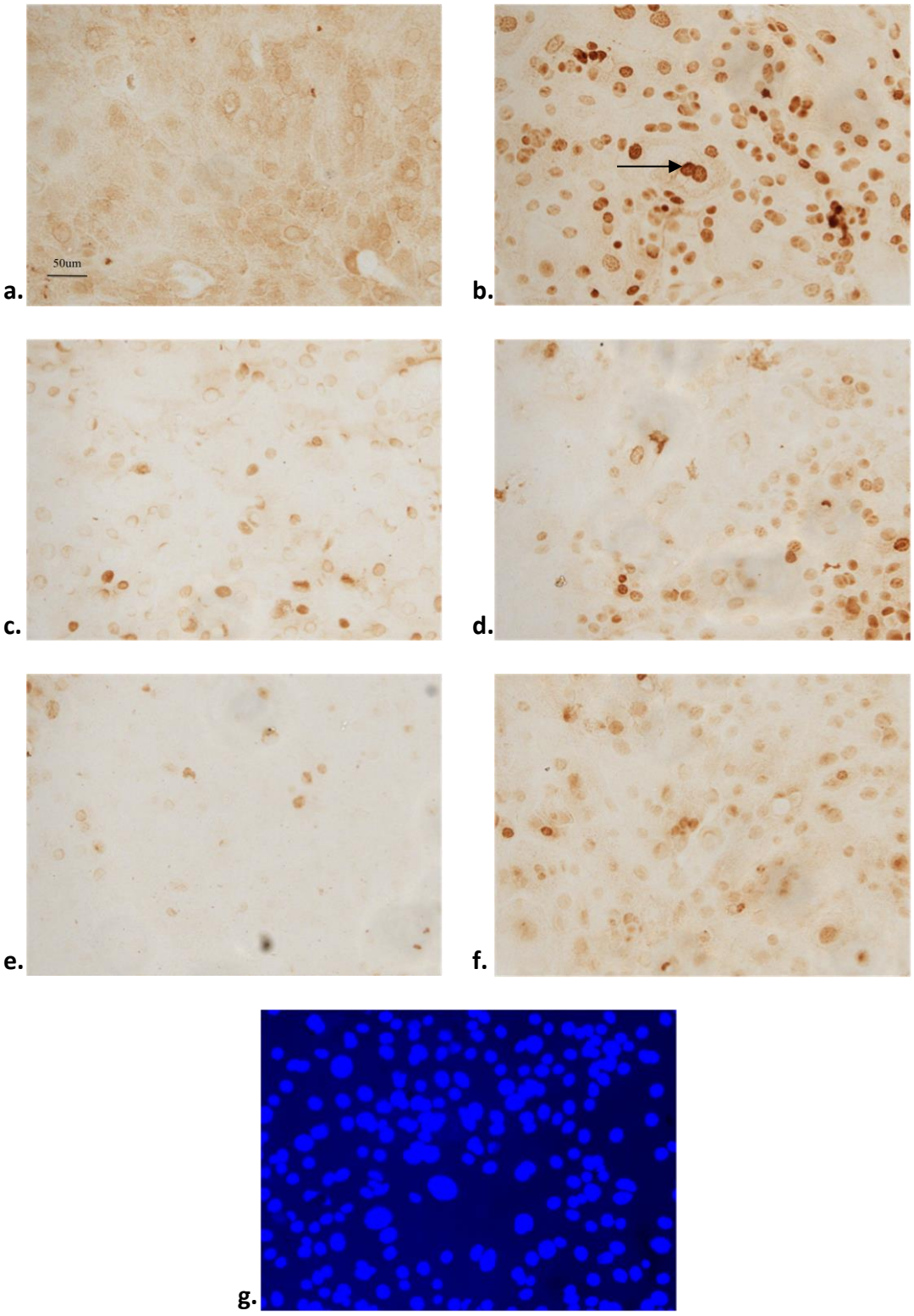

Figure 3-1 Photomicrographs showing a reduction in UV-induced thymine dimers in keratinocytes after treatment with 1,25(OH)$_2$D, 20(OH)D and THC

Keratinocytes were treated with vehicle (0.1% EtOH) in (a) unirradiated (sham) and after UV irradiation (b), and irradiated cells were treated with (c) 1nM $1,25(OH)_2D$, (d, e) 1nM or 10 nM 20(OH)D, or (f) 1nM THC immediately following UVR. Cells were fixed at 3 hours post-UVR, and subjected to immunohistochemical staining using an antibody directed against thymine dimers. Dark brown staining in nuclei indicate the presence of thymine dimers (dark arrow). Positive staining was absent in sham-irradiated cells, with all sham groups represented by the single micrograph. (g) shows an example of DAPI stained nuclei, used to calculate total nuclei. Scale bar represents 50μm for all images.

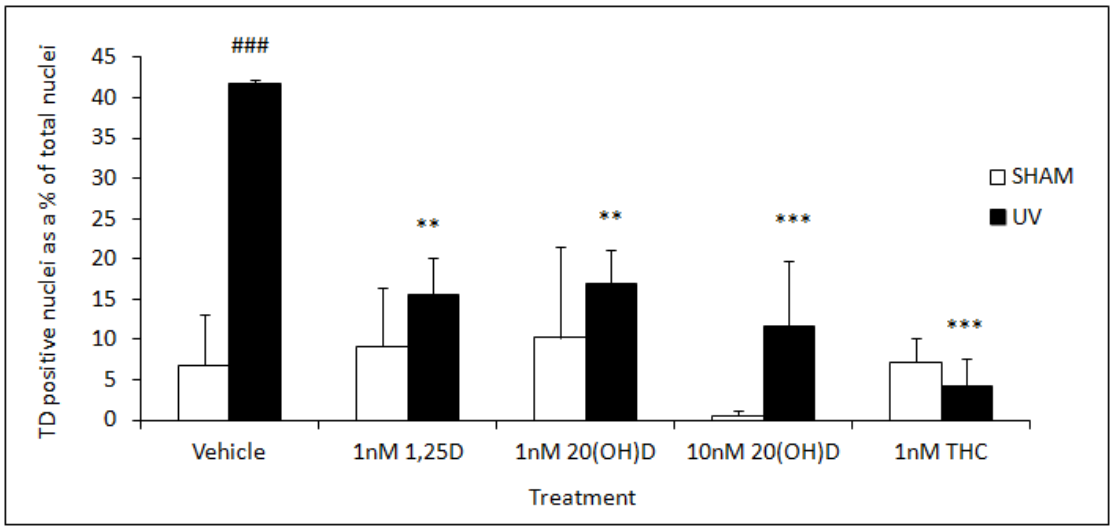

Figure 3.2 1,25(OH)$_2$D, 20(OH)D and THC reduce the number of thymine dimers in human keratinocytes following UVR. Keratinocytes were treated with vehicle (0.1% EtOH), 1nM 1,25(OH)$_2$D, 1nM 20(OH)D, 10nM 20(OH)D, or 1nM THC immediately following UVR. Cells were fixed 3 hours post-UVR, and subjected to immunohistochemical staining using an antibody directed against thymine dimers. Image analysis was used to quantify stained nuclei as a proportion of total nuclei. Results are from a single experiment performed in quadruplicate, mean ± SD. Similar results were observed in a two further independent experiments. ***, ** represents significantly different to UV vehicle $p<0.001$, $p<0.01$ respectively; ### represents significantly different to sham groups, $p<0.001$.

3.1.2 Effect of 1,25(OH)$_2$D, 20(OH)D and THC on 8oxodG formation in cultured keratinocytes following UVR

It has previously been shown in our lab that 1,25(OH)$_2$D and THC reduce the formation of oxidative DNA damage after UVR, indicated by a reduction in nuclear presence of 8oxoguanine (Dixon et al., 2011). This finding, along with the antioxidant capacity of 20(OH)D was confirmed in the current study. Like thymine dimers, 8oxodG positive cells were indicated by a dark stain in the nuclei. Since oxidative damage occurs naturally in all cells in culture, heavy background staining was commonly observed in sham treated cells. Figure 3.3 shows representative micrographs of sham and UVR exposed keratinocytes, used to analyse 8oxodG staining. The image of sham irradiated cells treated with vehicle is representative of 1,25(OH)$_2$D, 20(OH)D and THC treated cells, as staining was similar between groups (Fig3.3a). Cells irradiated with UV and treated with vehicle show a marked increase of 8-oxoguanine positive staining (Fig.3.3b) in comparison to sham cells (Fig.3.3a). The number of positively stained cells in both 1,25(OH)$_2$D-, 20(OH)D- and THC-treated cells following UVR was decreased (Figs 3.3 c,d,e respectively) compared to their UVR vehicle treated counterparts. A quantitative representation of 8-oxoguanine staining is shown in Figure 3.4.

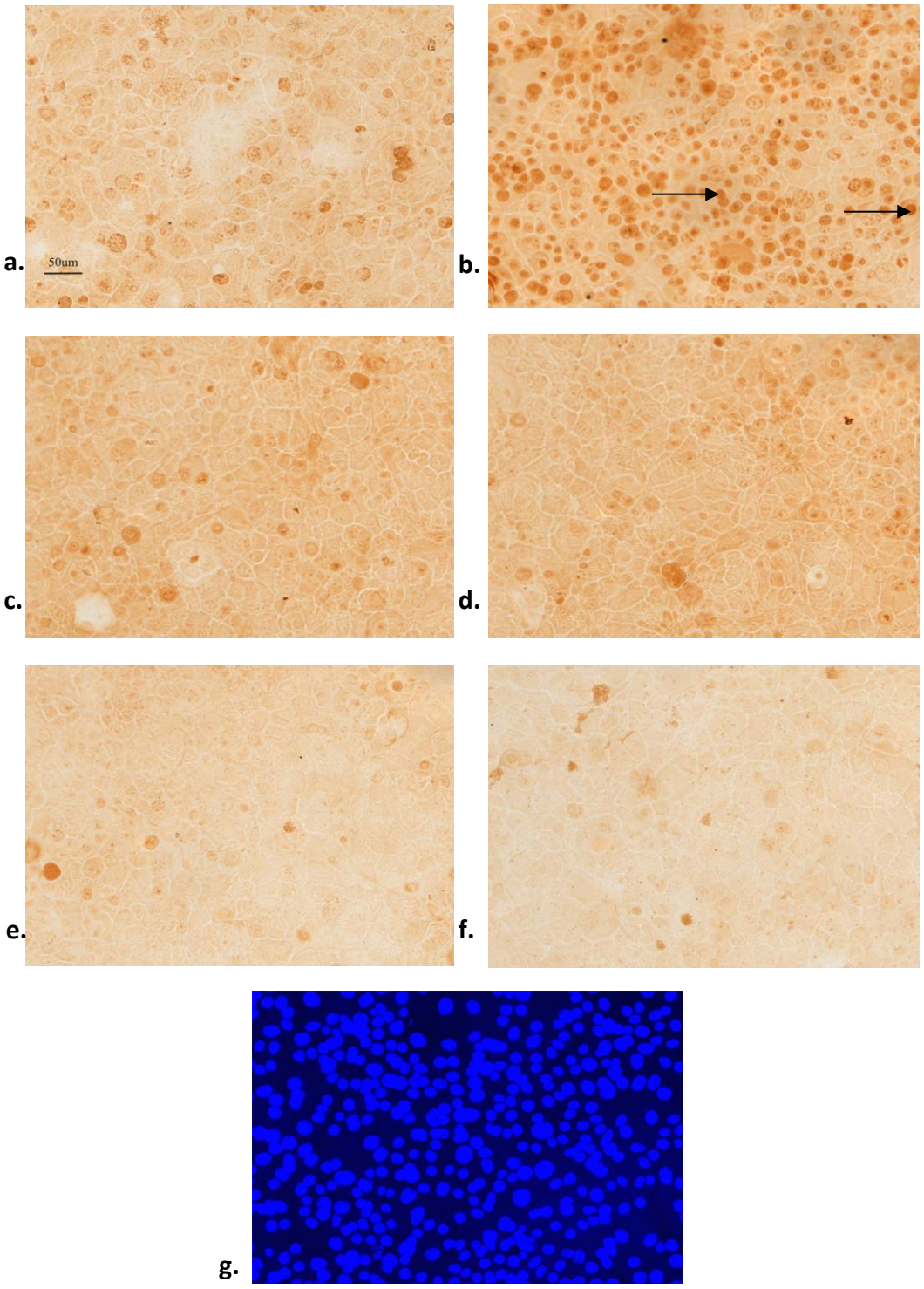

Figure 3-3 Photomicrographs showing a reduction in UV-induced 8-oxoguanine in human keratinocytes after treatment with 1,25(OH)$_2$D, 20(OH)D and THC

Keratinocytes were treated with vehicle (0.1% EtOH) in (a) unirradiated (sham) and after UV irradiation (b), and irradiated cells were treated with (c) 1nM1,25$(OH)_2$D, (d, e) 1nM or 10 nM 20(OH)D, or (f) 1nM THC immediately following UVR. Cells were fixed at 3 hours post-UVR, and subjected to immunohistochemical staining using an antibody directed against 8-oxoguanine. Dark brown staining in nuclei indicate the presence of 8-oxoguanine (dark arrow). Positive staining was low in sham-irradiated cells, with all sham groups represented by the single micrograph. (g) shows an example of DAPI stained nuclei, used to calculate total nuclei. Scale bar represents 50μm for all images.

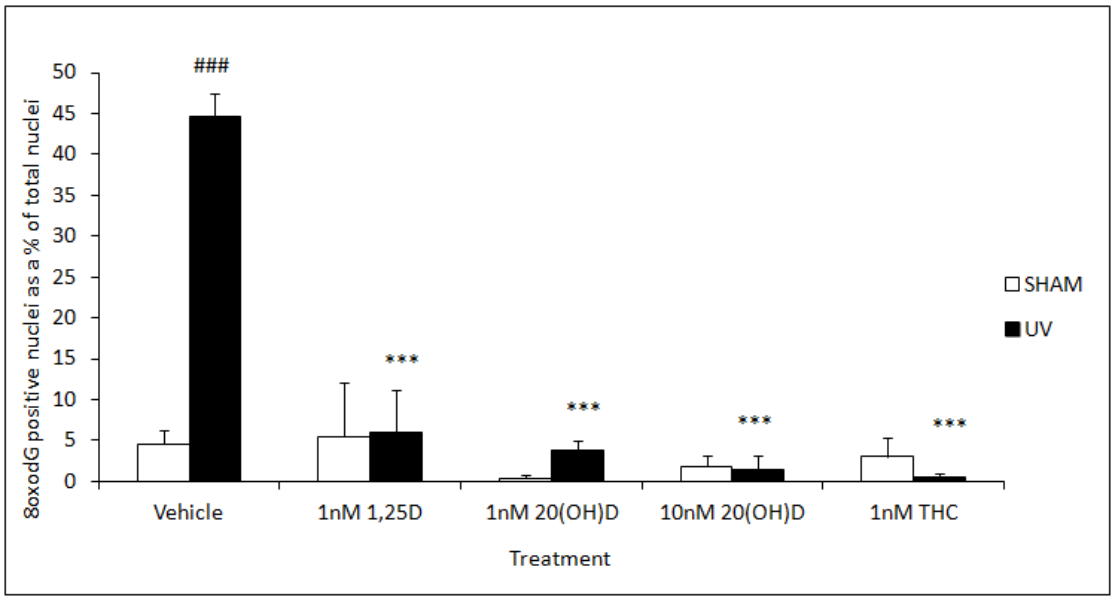

Figure 3.4 1,25(OH)$_2$D, 20(OH)D and THC reduce 8-oxoguanine formation present in keratinocytes following UVR. Keratinocytes were treated with vehicle (0.1% EtOH), 1nM 1,25(OH)$_2$D, 1nM 20(OH)D, 10nM 20(OH)D, or 1nM THC immediately following UVR. Cells were fixed 3 hours post-UVR, and subjected to immunohistochemical staining using an antibody directed against 8 oxoguanine. Image analysis was used to quantify stained nuclei as a proportion of total nuclei. Results are from a single experiment performed in quadruplicate, mean ± SD. Similar results were observed in a 1 further experiment. *** represents significantly different to UV vehicle $p<0.001$; ### represents significantly different to sham groups, $p<0.001$.

3.1.3 Effect of 1,25(OH)2D, 20(OH)D and THC on the presence of thymine dimers in male and female hairless Skh:Hr1 mice following UVR

Previous reports from this laboratory have also shown that 1,25$(OH)_2$D and vitamin D-like compounds and analogues reduce the presence of UVR-induced thymine dimers in hairless Skh:Hr1 mice (Gordon-Thomson et al., 2012, Ryan, 2010, Song et al., 2012). Additionally, recent research has exposed a significant gender bias in both mice and humans, with males generally more susceptible to UVR-induced DNA damage and subsequent photocarcinogenesis than females. Therefore the protective effect of 1,25$(OH)_2$D, 20(OH)D and THC against the formation of thymine dimers following exposure to UVR was tested *in vivo* in the present study in both sexes using the hairless Skh:Hr1 mouse model. The current study confirmed the protective effects of 1,25$(OH)_2$D, and demonstrated for the first time those of 20(OH)D and THC against UVR-induced thymine dimers, and also confirmed that males are more susceptible to DNA damage following UVR. Additionally, preliminary results of the current study suggest that lower concentrations of 1,25$(OH)_2$D are not as effective in reducing UVR-induced thymine dimers in male mice, compared to their female counterparts.

Figure 3.5 is a representation of images used for the analysis of thymine dimer positive staining in sham and UVR exposed murine skin. The image of vehicle-treated unirradiated skin (Fig. 3.5a) represents all sham treated groups, as unirradiated skin treated with 1,25$(OH)_2$D, 20(OH)D or THC, also showed no positive staining (not shown).The presence of thymine dimers was highest in UVR-exposed

epidermis of mice in the vehicle group (Fig. 3.5b), reflected in the darkly stained nuclei. The number of positively stained cells in male skins treated with 4.6pmol/cm^2 1,25(OH)$_2$D was reduced (Fig. 3.5c) in comparison to vehicle-treated cells following UVR (Fig. 3.5b, however this reduction was more striking in female skins (Fig. 3.5d). Similarly, groups of both sexes who received treatment with 23 and 46pmol/cm^2 1,25(OH)$_2$D following UVR had little to no thymine dimer positive staining, equivalent to sham groups. A similar reduction in positive staining following UVR seen with 23 and 46pmol/cm^2 20(OH)D and 115pmol/cm^2 THC treatments in both sexes. Figure 3.6(a,b) is the quantitative representation of positively stained cells as a percentage of total epidermal area in sham and UVR-exposed female and male mice. It can be seen that sham-irradiated mice in all treatment groups, regardless of sex, showed insignificant presence of thymine dimers. On the other hand, in mice of both sexes exposed to UVR, thymine dimer formation was highest in vehicle treatment, with males evidently expressing more compared to females. Additionally, UVR-exposed mice showed a significant reduction in thymine dimers following treatment with all doses of 1,25(OH)$_2$D, 20(OH)D and THC, compared to their vehicle treatment.

Figure 3.7 (a and b) is a quantitative depiction of photoprotection by the different compounds, expressed as a percentage of vehicle. In both sexes 1,25(OH)$_2$D appears to be concentration dependent, however, it can be seen that in males, topical application of 4.6pmol/cm^2 1,25(OH)$_2$D was not as effective in reducing thymine dimers as it was in female mice. Effectiveness of 20(OH)D was comparable to 46pmol/cm^2 1,25(OH)$_2$D in both sexes. As seen in UVR exposed keratinocytes,

treatment with THC was highly effective in reducing thymine dimers in murine epidermis.

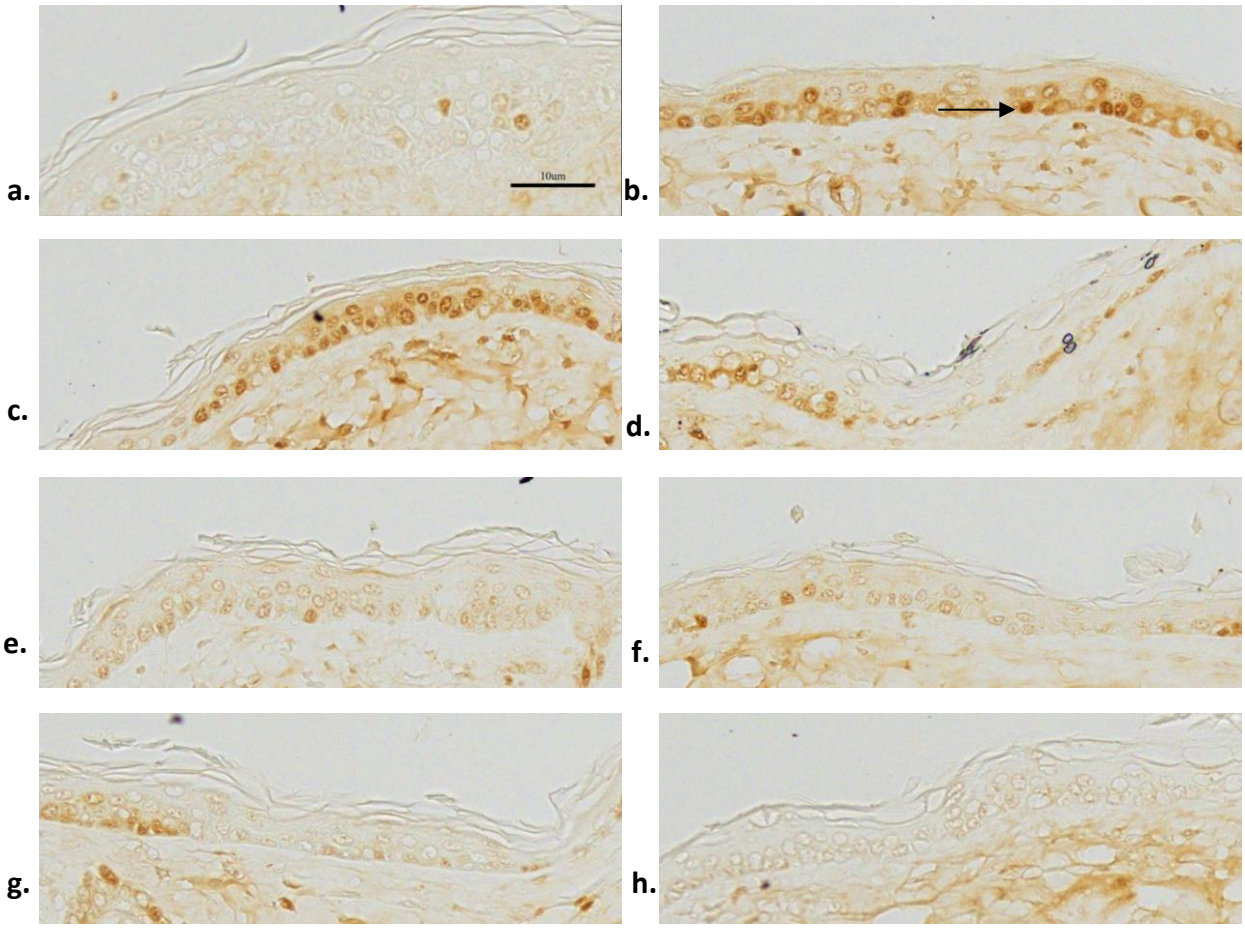

Figure 3-5 Photomicrographs showing $1,25(OH)_2D$, 20(OH)D and THC reduce the presence of thymine dimers in female and male murine epidermis following UVR

Groups of 3 mice were treated immediately after 2.5MED UVR with vehicle (0.1%(v/v) EtOH) (b), 4.6pmol/cm^2 1,25$(OH)_2$D (c), 23pmol/cm^2 1,25$(OH)_2$D (d), 46pmol/cm^2 1,25$(OH)_2$D (e), 23pmol/cm^2 20D (f), 46pmol/cm^2 20D (g) or 115pmol/cm^2 THC (h). Mice in sham groups were treated with the same solutions as their UV-irradiated counterparts, (a) is a representation of the staining seen in the sham groups. Dorsal skin biopsies were dissected from the "hotspot" 3 hours post-UVR, fixed in HistoChoice, and subjected to immunohistochemical staining using an antibody directed against thymine dimers. Shown are representative images of staining in each treatment group in female mice, which also qualitatively reflect those of the male mice treatment groups. Darkly stained nuclei indicate the presence of thymine dimers, highlighted by the dark arrow. CPD staining was absent in sham-irradiated mice, with all sham groups represented by the single micrograph, whilst there is a clear increase in positively stained nuclei in vehicle-treated cells following UVR. Scale bar represents 10μm for all images.

a.

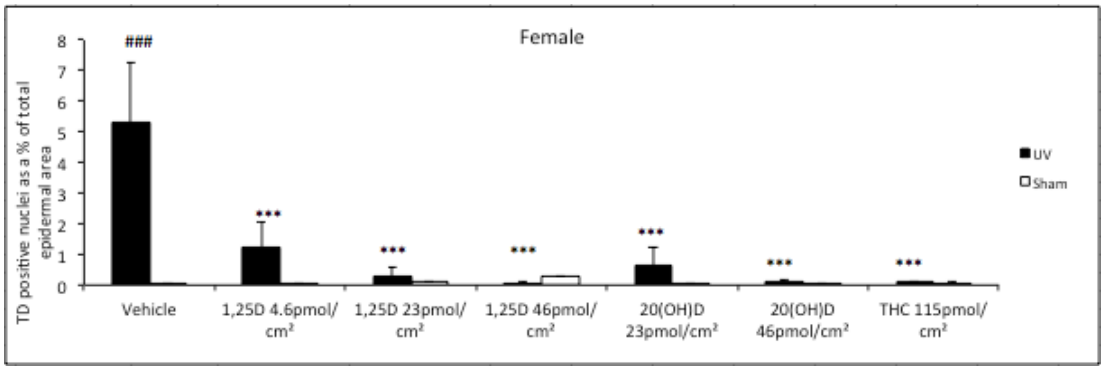

b.

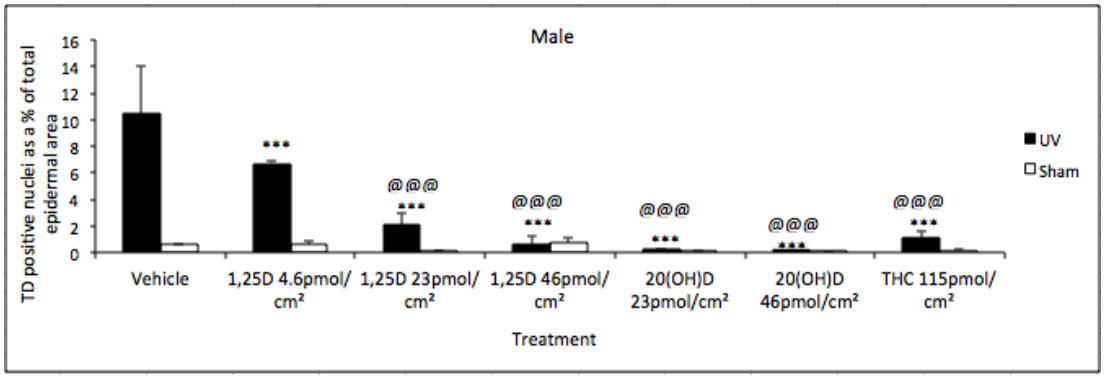

Figure 3.6 $1,25(OH)_2D$, 20(OH)D and THC reduced the presence of thymine dimers 3 hours following UVR in male and female Skh:Hr1 hairless, albino mice. a. Thymine dimers in female mice; b. Thymine dimers in male mice. Groups of 3 mice were treated immediately after 2.5MED UVR with vehicle (0.1%(v/v) EtOH), 4.6pmol/cm^2 $1,25(OH)_2D$, 23pmol/cm^2 $1,25(OH)_2D$, 46pmol/cm^2 $1,25(OH)_2D$, 23pmol/cm^2 20D, 46pmol/cm^2 20D or 115pmol/cm^2 THC. Dorsal skin biopsies were dissected from the "hotspot" 3 hours post-UVR, fixed in Histochoice, and subjected to immunohistochemical staining using an antibody directed against thymine dimers. Image analysis was used to quantify stained cells as a proportion of total epidermal area. Results are from a single experiment, mean ± SD. ***, ** represents significantly different to UV vehicle $p<0.001$, $p<0.01$ respectively; @@@

represents significantly different to UV 4.6pmol/cm^2 1,25$(OH)_2$D $p<0.001$. Sham groups were not significantly different to each other ($p>0.05$, not shown).

a.

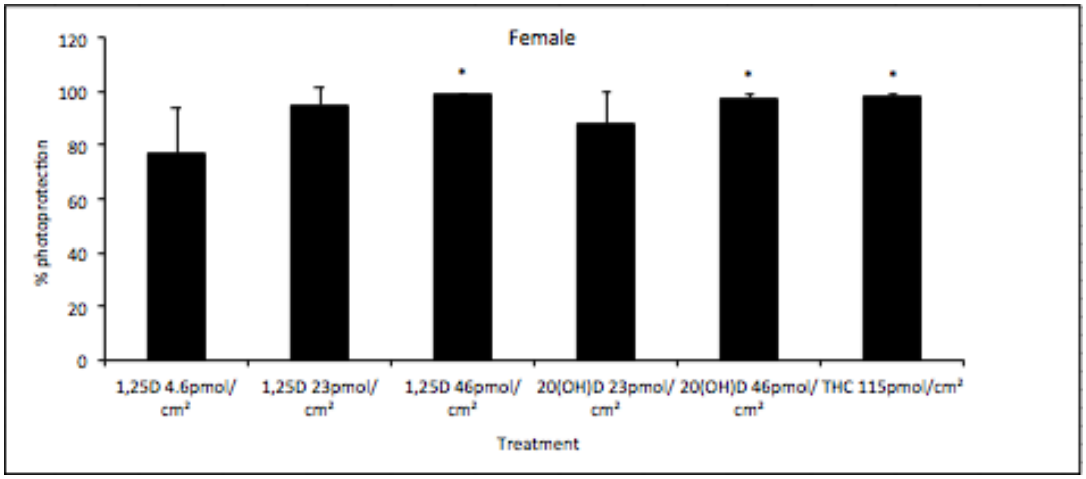

b.

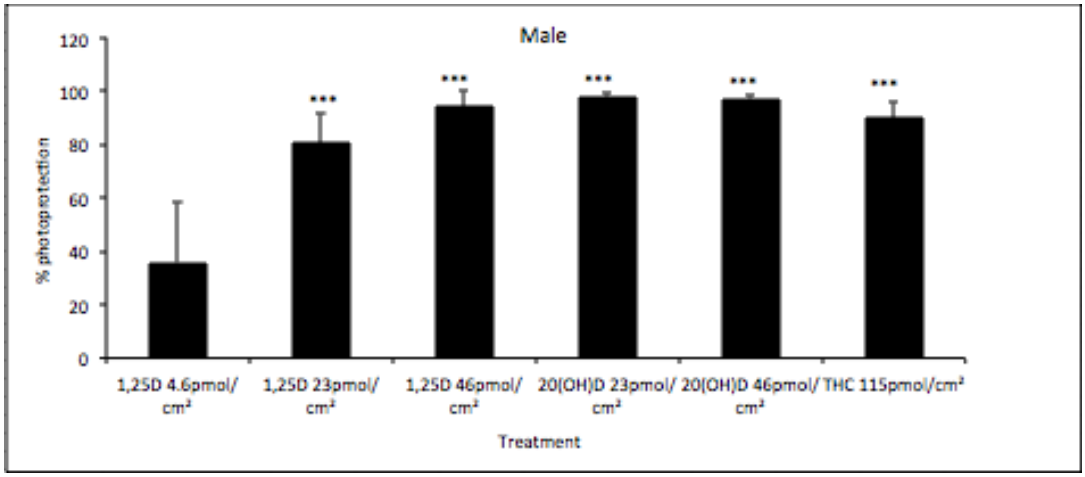

Figure 3.7 Effect of $1,25(OH)_2D$, 20(OH)D and THC on protection against DNA damage expressed as a percentage of vehicle in a) female and b) male Skh:Hr1 hairless albino mice. *, *** represents significantly different to 4.6pmol/cm^2 $1,25(OH)_2D$, at 3 hours post UVR, $p<0.05$, 0.001, respectively. Results are from a single experiment, with 3 mice per group.

3.1.4 Effect of DIDS on 1,25(OH)$_2$D and 20(OH)D reduction of thymine dimers following UVR

It has been established in this lab that DIDS, a chloride channel antagonist, completely reverses the protective effect of 1,25(OH)$_2$D and in thymine dimer formation (Dixon et al., 2007, Dixon et al., 2011). The current study not only confirmed this finding but also suggests that the protective effect of 20(OH)D is also inhibited by DIDS. According to previous work in this lab, DIDS was used at 50µM to block outwardly rectifying chloride channels (Sequeira et al., 2012a). Figure 3.8 shows a significant reduction in thymine dimers when keratinocytes were treated with 1nM1,25(OH)$_2$D or 20(OH)D compared to vehicle-treated cells. As expected DIDS on its own at 50µM had no protective effect. The combination of 50µM DIDS and 1nM 125D was not significantly different to vehicle or 50µM DIDS treated cells, which shows that DIDS completely reverses the protective effect of 125D. The same phenomena was seen in the combination of 50µM DIDS and 1nM 20(OH)D.

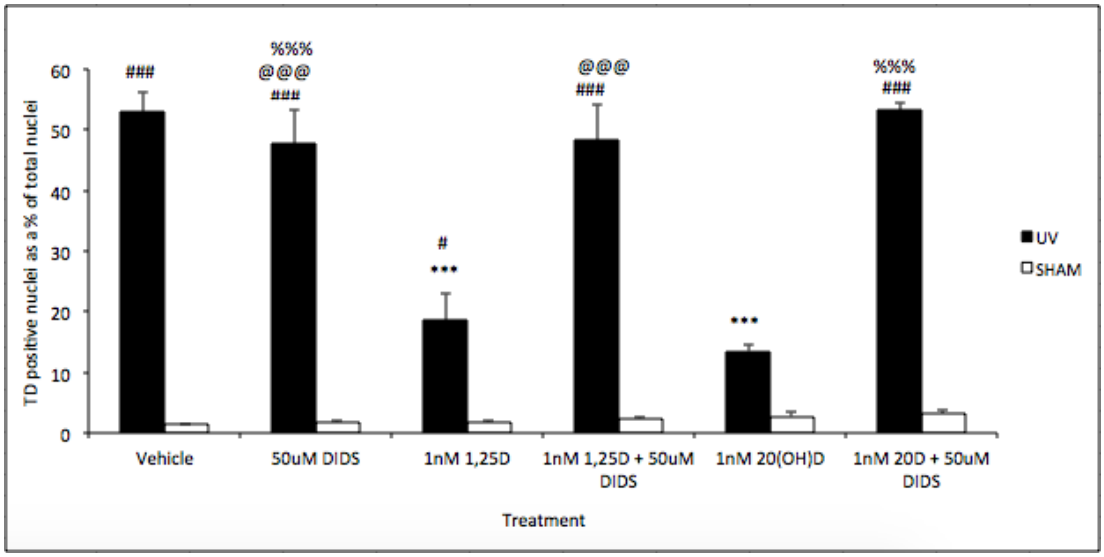

Figure 3.8 DIDS completely reverses 1,25(OH)$_2$D- and 20(OH)D-induced reduction of thymine dimers in human keratinocytes following UVR.

Keratinocytes were treated immediately before UVR with vehicle (0.1% DMSO) or 50µM DIDS. Immediately following UVR, cells were incubated with vehicle (1% EtOH and 1% DMSO), 1nM 1,25(OH)$_2$D, 50µM DIDS, the combination of 1,25(OH)$_2$D and 50µM DIDS, 1nM 20(OH)D, and the combination of 1nM 20(OH)D and 50µM DIDS. Cells were fixed 3 hours post-UVR, and subjected to immunohistochemical staining using an antibody directed against thymine dimers. Image analysis was used to quantify stained nuclei as a proportion of total nuclei. Results express the mean of quadruplicate wells ± SEM pooled from a total of two independently tested experiments. *** represents significantly different from vehicle, $p<0.001$; ###, # represent significantly different from the corresponding sham group, $p<0.001$, $p<0.05$ respectively; @@@ represents significantly different to 1nM 1,25(OH)$_2$D, $p<0.001$; %%% represent significantly different to 1nM 20(OH)D, $p<0.001$.

3.1.5 Effect of the Wnt pathway inhibitor IWR-1 on the photoprotective effects of 1,25(OH)$_2$D- and 20(OH)D-induced reduction of thymine dimers following UVR.

In the current study, IWR-1, a Wnt inhibitor was used to determine whether Wnt signalling is involved in vitamin D compound-mediated protection against DNA damage, namely thymine dimers. As expected, at 3 hours post-UVR exposure, 1,25(OH)$_2$D and 20(OH)D were significantly photoprotective at 1nM, compared to vehicle treatment (fig 3.9). IWR-1 at 12 μM was also photoprotective, although not to the same extent as 1,25(OH)$_2$D and 20(OH)D. Additionally, protection against thymine dimers remained when 1nM 1,25(OH)$_2$D and 12 mM IWR-1 were combined or 1nM 20(OH)D and 12 mM IWR-1 were combined.

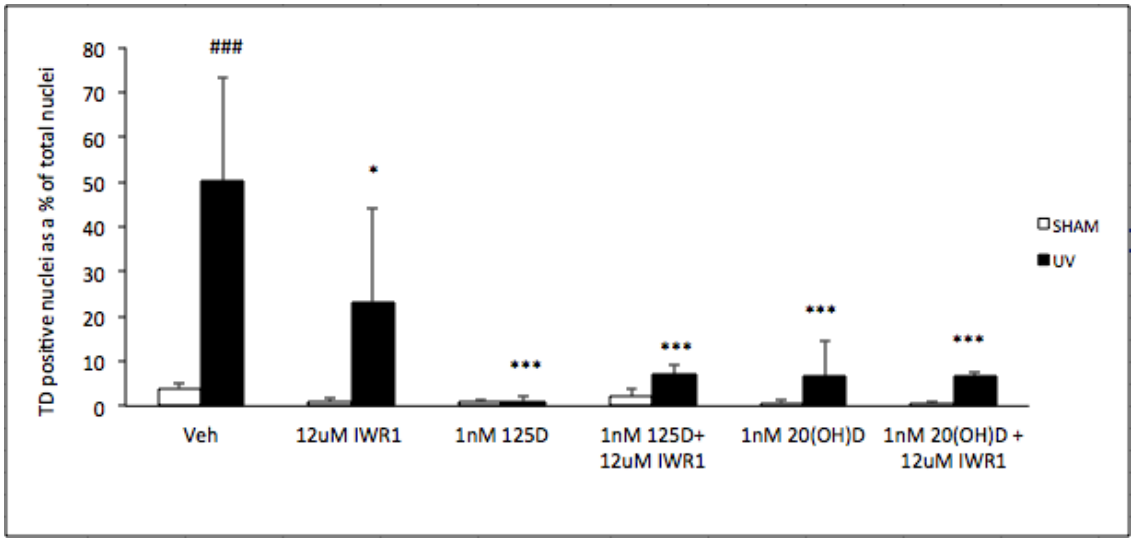

Figure 3.9 The Wnt pathway inhibitor IWR-1 reduced thymine dimers and had no effect on 1,25(OH)$_2$D- and 20(OH)D-induced reduction of thymine dimers following UVR. Keratinocytes were treated immediately before UVR with vehicle (0.1% DMSO) or 12µM IWR-1. Immediately following UVR, cells were incubated with vehicle (1% EtOH and 1% DMSO), 1nM 1,25(OH)$_2$D, 12µM IWR-1, the combination of 1,25(OH)$_2$D and 12µM IWR-1, 1nM 20(OH)D, or the combination of 1nM 20(OH)D and 12µM IWR-1 immediately following UVR. Cells were fixed 3 hours post-UVR, and subjected to immunohistochemical staining using an antibody directed against thymine dimers. Image analysis was used to quantify stained nuclei as a proportion of total nuclei. Results express the mean of quadruplicate wells ± SD. Similar results were seen in one further experiment. *** represents significantly different from vehicle, $p<0.001$; ###, # represent significantly different from the corresponding sham group, $p<0.001$, $p<0.05$ respectively; @@@ represents significantly different to 1nM 1,25(OH)$_2$D, $p<0.001$; %%% represent significantly different to 1nM 20(OH)D, $p<0.001$.

3.2 DISCUSSION

3.2.1 Photoprotection by 1,25(OH)$_2$D, 20(OH)D and THC

Reports from this laboratory have shown the photoprotective abilities of 1,25(OH)$_2$D and 1,25(OH)$_2$D analogues against the formation of UVR-induced thymine dimers. The current study confirmed this finding in both *in vitro* and *in vivo* experiments. While thymine dimers are not mutagenic, they accurately represent the proportion of mutagenic pyrimidine dimers such as cytosine-thymine dimers that form following UVR exposure (Mouret et al., 2006, Matsumura and Ananthaswamy, 2004). In this study thymine dimer formation was detected via immunohistochemistry with a monoclonal antibody and image analysis. Various reports have previously shown that 1,25(OH)$_2$D is photoprotective against the formation of DNA damage thus this was used as the positive control for the experiments (Bikle et al., 2013, Dixon et al., 2007, Dixon et al., 2005, Dixon et al., 2011, Gordon-Thomson et al., 2012, Sequeira et al., 2012a, Sequeira et al., 2012b). The current study confirmed this finding. Application of 20(OH)D or THC following exposure to UVR caused a reduction in thymine dimers in both cultured keratinocytes and Skh:Hr1 mouse epithelium, indicating protection against UVR-induced DNA damage.

20(OH)D, along with other metabolites, is formed via the hydroxylation of the side chain of vitamin D3 by the CYP11A1 enzyme present in the skin (Slominski et al., 2012b, Tuckey et al., 2011, Slominski et al., 2005b, Guryev et al., 2003a, Tuckey et al., 2008b). 20(OH)D has already been shown to have 1,25(OH)$_2$D-like activity by

inducing the differentiation of keratinocytes and monocytes, as well as anti-proliferative and anti-inflammatory effects in human keratinocytes and melanoma cells (Zbytek et al., 2008a, Janjetovic et al., 2011a, Slominski et al., 2013), making it an excellent anticancer candidate.

As a newly discovered molecule, there is no data on the photoprotective capabilities of 20(OH)D. Despite the evidence for photoprotection by 1,25$(OH)_2$D, its use as a topical photoprotective agent is not viable since it causes toxic hypercalcaemia. 20(OH)D is far more chemically stable than 1,25$(OH)_2$D and does not cause hypercalcaemia, even at high doses (Wang et al., 2012a) and thus shows promise as a novel pharmacological agent to enhance photoprotection. VDR knockout (VDRKO) mice, which do not express the genes for encoding the VDR, are more prone to the development of photocarcinogenesis. It has been reported that 1α-hydroxylase knockout mice, which cannot 1α-hydroxylate vitamin D compounds to produce 1,25$(OH)_2$D or presumably 1,25-dihydroxylumisterol (JN), are not more susceptible to photocarcinogenesis (Bikle et al., 2012).. This strongly suggests that other vitamin D derivatives, such as 20(OH)D, could potentially contribute to protection from UV damage, by binding to the VDR.

Prior studies on the effects of 20(OH)D have shown that it binds to the VDR, though at a lower affinity than 1,25$(OH)_2$D to exert its effects (Zbytek et al., 2008b, Janjetovic et al., 2011b). However, results from the Mason group have also shown that whilst photoprotection by 1,25$(OH)_2$D requires the VDR, the VDR does not necessarily need to be intact. Fibroblasts from donors with hereditary vitamin D-

resistant rickets (HDVRR) with a defective DNA binding domain, or a mutation in helix H1 of the ligand binding domain, were still protected from UVR-induced DNA damage with 1,25$(OH)_2$D application compared to non-treated fibroblasts. Mutations in these areas of the receptor mean that genomic effects of ligand binding are abolished. Fibroblasts which did not express the VDR at all were not protected from UV induced DNA damage by 1,25$(OH)_2$D (Sequeira et al., 2012b). \ Treatment of normal fibroblasts with an antiserum to the membrane bound putative vitamin D receptor (siRNA to ERp57) reversed 1,25$(OH)_2$D-mediated protection (Zbytek et al., 2008b, Janjetovic et al., 2011b). This suggests ligand binding to both the VDR and ERp57 to initiate non-genomic effects as one of the essential steps photoprotection. The membrane bound receptor ERp57, preferentially binds the planar 6-s-cis locked non-genomic agonists of vitamin D sterols, such as JN (Mizwicki et al., 2004, Mizwicki et al., 2010, Mizwicki and Norman, 2009). The biologically active form of 20(OH)D, is in the s-enantiomer form (Zbytek et al., 2008b) also mediates non-genomic effects following binding to the VDR, without generating genomic effects (Slominski et al., 2010). This makes 20(OH)D a viable option as an ERp57 or alternate VDR pocket agonist, through which could mediate photoprotection against UVR. However, further molecular modelling studies on its confirmation and VDR-binding would be required to fully determine this theory.

It has recently been observed in this laboratory that 1,25$(OH)_2$D reduces DNA damage resulting from the potent oxidative stress caused by UVR (Gordon-Thomson et al., 2012, Gupta et al., 2007, Sequeira et al., 2012b). Previous results

from this group have shown by immunohistochemical staining of mouse skin that $1,25(OH)_2D$ at a concentration of $23\rho mol/cm^2$ reduced formation of 8-oxo-7,8-dihydro-2'-deoxyguanosine (8oxodG), the predominant UVR-induced oxidative lesion, following UVR when compared to untreated mice at 3 hours post treatment. Furthermore, using a newly developed comet assay, human 8-oxoguanine glycosylase (hOGG) repair enzyme sites were shown to be reduced as early as 30 minutes following UVR with $1,25(OH)_2D$ compared to vehicle (Gordon-Thomson et al., 2012). Thus, use of $1,25(OH)_2D$ was used as a positive control and results presented in this chapter indicate that in cultured keratinocytes, $1,25(OH)_2D$ reduced 8oxodG lesions compared to vehicle treated cells. 8oxodG is formed by oxidative radical-mediated oxidation of guanine on DNA strands, by UVR induced ROS, such as super oxide and hydroxyl radicals (Cadet et al., 2003, Cadet et al., 2005). Reduction in 8oxodG when tissue is treated with $1,25(OH)_2D$ suggests that $1,25(OH)_2D$ has antioxidant capacity or enhances repair of these lesions.

THC as an antioxidant has mixed reviews. THC has been shown to have stronger antioxidant activity than its parent molecule curcumin (Okada et al., 2001, Osawa et al., 1995, Sugiyama et al., 1996), in several types of cells whilst in others it is not as effective (Murakami et al., 2008, Hong et al., 2004). Curcumin is a known suppressor of the expression of iNOS, JNK, nuclear factor kappa B (NF-κb) and COX-2, all mediators of cellular inflammation and oxidation (Hong et al., 2004, Menon and Sudheer, 2007). THC reduced the oxidation of low density lipoproteins (LDLs) both in *in vivo* and *in vitro* models, suggesting that it might be a good candidate for the prevention of atherosclerosis (Naito et al., 2002). The oxidative mechanism of

THC is thought to be attributed to scavenging of oxidative free radicals such as tertbutoxyls and peroxyls (Sugiyama et al., 1996). Similarly, hydrogenation of the central carbon bonds of curcumin to get THC make it a better scavenger of radicals in red blood cell haemolysis models, even in comparison to a known anti-oxidant, trolox (Somparn et al., 2007). It should be noted however that in the previously mentioned studies on the antioxidant abilities of THC, the THC was used was at micromolar concentrations, whereas the current study saw functional antioxidant effects at nanomolar concentrations.

Considering the current results showing that THC reduced UVR-induced oxidative damage, and that oxidative damage may also contribute to CPD formation (Gordon-Thomson et al., 2012), it is possible to propose that THC prevents both CPD formation and oxidative mutations in DNA via scavenging free radicals caused by UVR. Additionally it is known that curcumin is an analogue of $1,25(OH)_2D$ and can bind to the alternative pocket of the VDR, to induce non-genomic effects, as seen with $1,25(OH)_2D$ (Jurutka et al., 2007). Given that THC and curcumin have similar chemical structure and THC displays almost identical effects to curcumin (Pari and Amali, 2005), it is therefore possible that THC at nanomolar concentrations may be exerting photoprotection from UVR via binding to the alternate pocket of the VDR. The data in this chapter however are preliminary results so further inquiries into anti-oxidant capabilities of the two compounds must be sought.

3.2.2 Mechanisms of photoprotection by $1,25(OH)_2D$ and 20(OH)D

The mechanism of photoprotection from DNA damage through the non-genomic actions of $1,25(OH)_2D$ is not yet well understood. It has previously been demonstrated via whole-cell patch clamping that $1,25(OH)_2D$ and related compounds cause upregulation of chloride channels in osteoblastic ROS cell lines resulting rapid non-genomic changes within the cell (Zanello and Norman, 2006, Zanello and Norman, 1996, Zanello and Norman, 1997, Zanello and Norman, 2003). Using DIDS, a specific chloride channel inhibitor, the non-genomic effects of the $1,25(OH)_2D$ were abolished in this cell line. Recent findings from this laboratory have shown the involvement of these outwardly rectifying chloride channels in photoprotection against formation of UVR-induced thymine dimer-type CPDs by $1,25(OH)_2D$ (Sequeira et al., 2012a).

Since 20(OH)D binds to the VDR (Zbytek et al., 2008b) and has been shown to produce the non-genomic effects of $1,25(OH)_2D$ almost exclusively (Slominski et al., 2010), it was of interest to investigate whether chloride channel blockade by DIDS reversed its effect on DNA damage following UVR. UVR- induced thymine dimer formation was reduced in the current study following treatment with $1,25(OH)_2D$ and 20(OH)D at a low dosage titration compared to controls. As a positive control, I showed that photoprotection by $1,25(OH)_2D$ following UVR was reversed with the addition of DIDS, as was discovered in the study by Sequiera et al (2012). The photoprotective effect of 20(OH)D was completely reversed in the presence of DIDS. It is evident that 20(OH)D-mediated protection against UVR-induced CPD

formation occurs via induction and upregulation of chloride channels following binding to the VDR. This supports the hypothesis that the photoprotective abilities of 20(OH)D occur in a similar manner to the non-genomic effects of 1,25$(OH)_2$D binding to the VDR.

An additional mechanism of photoprotection by 1,25$(OH)_2$D is thought to be via the induction or inhibition of several molecular and intracellular signalling pathways pertaining to altered apoptosis activation (De Haes et al., 2003). 1,25$(OH)_2$D caused an increase in phosphorylation of ERK and Akt compared to untreated cells (De Haes et al., 2004a). Treatment of keratinocytes with MEK/ERK or PI3K/Akt inhibitors, PD98059 or LY294002 following UVR, reversed the anti-apoptotic effect of 1,25$(OH)_2$D, suggesting that 1,25$(OH)_2$D promotes cellular survival after UV exposure via these pathways. However, it is difficult to know whether this effect is due to 1,25$(OH)_2$D alone, since UVR itself promotes activation of ERK and Akt also (Peus et al., 1999, Wang et al., 2004).

As for DNA damage, previous studies from this group have shown that inhibition of the PI3K/Akt or ERK pathway by wortmannin or ERK peptide inhibitor significantly reduce the formation of CPDs 3 hours following exposure to UVR, in comparison to untreated cells (Sequeira, 2011).. This is similar to the previous reports which show that use of ERK and PI3K/Akt inhibitors reduce apoptosis following UVR (Peus et al., 1999, Wang et al., 2003). On a methodological note, results from De Haes et al (2004a) required pharmacological concentrations (10^{-6}M) of 1,25$(OH)_2$D to achieve

an anti-apoptotic effect, whilst our group, have shown that 1,25$(OH)_2$D is effective at physiological concentrations (10^{-9}M).

It has been shown in osteoblasts that phosphorylation of Akt in turn phosphorylates β-catenin, allowing it to move to the nucleus to begin gene transcription for cell survival (Rybchyn et al., 2011). Phosphatidylinositol 3'-OH kinase (PI3K) is known to be activated in keratinocytes exposed to UVR (Wang et al., 2003) and its activation is known to cause recruitment of Akt to the plasma membrane (Stein and Waterfield, 2000). Induction of the PI3K/Akt pathway in skin cells exposed to low dose UVR is associated with a decrease in the presence of apoptotic proteins such as cytochrome c and caspases 3, 8 and 9 (Peus et al., 1999, Wang et al., 2003).

At present the link between the ability of 1,25$(OH)_2$D to reduce both apoptosis and DNA damage is not totally understood. The current study showed that inhibition of Wnt caused a slight but significant reduction in thymine dimers following UVR compared to vehicle treated keratinocytes, but not to the same significance as 1,25$(OH)_2$D or 20(OH)D. This is perhaps indicative that downstream targets of Wnt may have been activated via other pathways such as PI3K/Akt, that were affected by 1,25$(OH)_2$D and 20(OH)D in order to reduce the presence of UVR-induced thymine dimers.

The difficulty of interpreting the present results lies in the fact that the Wnt inhibitor IWR-1-endo alone caused a moderate reduction in the number of thymine dimers present following UVR-exposure in keratinocytes. Additionally,

photoprotection against UVR-induced DNA damage by 1,25$(OH)_2$D or 20(OH)D remained in the presence of the IWR-1-endo. Interestingly although the Wnt-inhibitor was effective at UVR photoprotection on its own, the combination of 1,25$(OH)_2$D or 20(OH)D plus IWR-1 did not produce compounded effectiveness of photoprotection, when compared to 1,25$(OH)_2$D or 20(OH)D alone. The maintenance of photoprotection with 1,25$(OH)_2$D and 20(OH)D in the presence of the Wnt inhibitor suggests that there are other intracellular mechanisms occurring which are facilitating their photoprotective abilities.

A study by Haussler et al (2010) found that in keratinocytes the VDR upregulates the transcriptional activity of β-catenin, independently of a bound ligand. Thus the photoprotective abilities of the VDR ligands, such as 1,25$(OH)_2$D or 20(OH)D which are both produced endogenously, may occur via the ligand binding to the VDR which make it unavailable for β-catenin interaction, decreasing proto-oncogenic gene transcription. Since unregulated growth activity is one of the six hallmarks of cancer (Hanahan and Weinberg, 2011, Hanahan and Weinberg, 2000) ligand binding to the VDR by naturally occurring hormones such as 1,25$(OH)_2$D or 20(OH)D, causing inhibition of β-catenin signalling may play a role in the multifaceted mechanism of 1,25$(OH)_2$D and 1,25$(OH)_2$D -like compound prevention of photocarcinogenesis. In addition, basal cell carcinomas (BCCs) of keratinocytes were demonstrated to have abnormally high nuclear β-catenin levels with low VDR expression (Aszterbaum et al., 1999), which suggests that the protective effects of ligand binding to the VDR are lost with a complete gain of function in the β-catenin pathway, allowing

unregulated growth (Chen et al., 2009, Ordonez-Moran et al., 2008, Palmer et al., 2008, Pendas-Franco et al., 2008). Moreover, that the protective abilities of $1,25(OH)_2D$ and other VDR ligands, may be most protective at the early stages of photocarcinogenesis.

Upregulation of Wnt activity is a common occurrence in several types of cancers (Polakis, 2000, Segditsas and Tomlinson, 2006). Blockade of Wnt activity by IWR-1-endo increases intracellular proteosomal degradation of β-catenin, ultimately downregulating the transcription of proto-oncogenes (Chen et al., 2009). Downregulation of the Wnt signalling pathway has also been reported to reduce UV-induced skin carcinogenesis (Chaudhary et al., 2013).

The protective abilities of $1,25(OH)_2D$ and its analogues may not be limited to prevention of the formation of DNA damage, but also in the repair of UV-induced DNA damage. Studies from the Mason lab have shown that $1,25(OH)_2D$ and 1α-25-dihydroxylumisterol (JN), a vitamin D-like compound, reduce the formation of nitrotyrosine and nitrates in human keratinocytes (Dixon et al., 2011, Gupta et al., 2007, Sequeira et al., 2012a). Presence of nitric oxide products inhibits the efficacy of DNA repair (Bau et al., 2001) and induces DNA damage (Gordon-Thomson et al., 2012), thus their reduction may allow for enhanced DNA repair and diminish the formation of thymine dimers and nitrosative DNA lesions. Furthermore, the Mason lab has shown that p53 is upregulated in primary human keratinocytes following treatment with UVR, and this was further heightened in cells treated with both UVR and $1,25(OH)_2D$ (Sequeira et al., 2012b). p53 is the major cell cycle checkpoint

regulator, increasing time for DNA damage repair or apoptosis if the damage is unrepairable (Matsumura and Ananthaswamy, 2002). Since 20(OH)D and THC are equally as photoprotective as 1,25$(OH)_2$D against the formation of UV-induced DNA damage, further studies into their effects on nitric oxide products and p53, and would be advantageous.

3.2.3 Gender bias in photoprotection

It is currently well established that prevalence of skin cancer is higher in males than females, and that prognosis for most cancers is generally better for females than for males (Molife et al., 2001, Thomas-Ahner et al., 2007, Leiter and Garbe, 2008, Staples et al., 1998, Staples et al., 2006). In the present studies, development of thymine dimers was greater in male mice in comparison to female mice following the same time of exposure to the same dose of UVR, which suggests that the disparity in photocarcinogenesis between the sexes may occur even as early as the first DNA damage.

Moreover, in agreement with previous findings, 1,25$(OH)_2$D decreased the formation of CPDs in mice skin 3 hours following UVR exposure. However, whilst treatment with 1,25$(OH)_2$D following UVR was effective at reducing thymine dimer formation in both sexes, the reduction was more pronounced in females than males at the lowest dosage (4.6ρmol/cm^2).

Application of 20(OH)D also significantly reduced the appearance of thymine dimers following UVR, to an equal extent as 1,25$(OH)_2$D at the same concentration.

However, 20(OH)D was not applied at 4.6ρmol/cm^2, thus it cannot be concluded that 20(OH)D would be more effective in males than females at this concentration. Similarly, THC was used only at 115ρmol/cm^2, a concentration known to effectively reduce DNA damage (Ryan, 2010).

At present there is limited data on the difference in effectiveness of photoprotection by 1,25$(OH)_2$D between male and female mice. However, results from this study suggest that female skin requires a smaller concentration of 1,25$(OH)_2$D than does male skin to achieve protection from UVR-induced DNA damage, indicating the existence of another factor mediating protection in females.

In general, males are more susceptible to UVR-induced immunosuppression, sunburn, and photocarcinogenesis than females (Broekmans et al., 2003, Damian et al., 2008, Foote et al., 2001, Preston and Stern, 1992). Furthermore, following menopause, women with drastically reduced oestrogen production, have decreased skin elasticity, increased dryness and dermal thickness, all of which are improved with oestrogen therapy (Bottai et al., 2013). Taken together, this suggests that oestrogen or a female sex hormone receptor is vital in the maintenance of skin health and protection from UVR.

Skin cells, both keratinocytes and fibroblasts, treated with exogenous 17β-estradiol show a reduction in peroxide-induced oxidative damage in comparison to their vehicle treated counterparts (Bottai et al., 2013). Since UVR causes oxidative damage (Matsumura and Ananthaswamy, 2004) and oxidative damage may lead to

the formation of CPDs (Gordon-Thomson et al., 2012, Gupta et al., 2007), this indicates that in females, endogenous 17β-estradiol may attenuate both direct and indirect forms of UVR-induced damage. In contrast, pre-treatment of HaCaT cells with 17β-estradiol slowed removal of UVB-induced thymine dimers 4 hours following UV irradiation (Evans et al., 2003). As a result, it was concluded that since nucleotide excision repair (NER) is responsible for the elimination of CPDs, treatment with exogenous oestrogen inhibited NER, and thus oestrogens may also play a role in the progression of DNA damage to pathologic mutations in photocarcinogenesis (Evans et al., 2003).

Recently, it has been proposed that the gender bias seen in carcinogenesis may be mediated by oestrogen receptor (ER)-β signalling (Catley et al., 2008, Chaudhary et al., 2013, Cho et al., 2010, Reeve et al., 2009, Thornton et al., 2003b). Male and female human skin contains mostly ER-β with no significant difference in distribution between the sexes (Thornton et al., 2003b). ER-β has been shown to mediate tumour suppression in colon, kidney and hepatic tumours, and had been shown to reduce immunosuppression induced by UVR (Cho et al., 2010).

Furthermore, a recent study by Chaudhary et al. (2013) showed that topical treatment with an ER-β agonist, Erb-041, on UVB-exposed Skh:Hr1 hairless mice caused a reduction in UVB-induced tumour growth compared to vehicle treated cells. Furthermore, the study showed that Erb-041 attenuated growth and proliferation of a squamous cell carcinoma cell line, and also prevented invasiveness

and migration of tumours via downregulation of Wnt signalling, which hindered β-catenin mediated cell growth and angiogenesis (Chaudhary et al., 2013). These findings, in conjunction with the results from the current study provide evidence for a role in inhibition of Wnt and ER-β agonists in the prevention of photocarcinogenesis, from its beginnings with DNA damage to tumour metastasis. In other studies from the Mason group, use of an ER-β inhibitor in female Skh:Hr1 mice reduced the ability of 1,25$(OH)_2$D to decrease DNA damage induced by UVR (Tongkao-on, 2014).

4 PHOTOPROTECTION AGAINST UVR-INDUCED INFLAMMATION AND IMMUNOSUPPRESSION USING NOVEL VITAMIN D COMPOUNDS IN MICE

4.1 RESULTS

4.1.1 Effect of 1,25$(OH)_2$D and 20(OH)D on the acute inflammatory effects of UVR in hairless Skh:Hr1 mice

Several preliminary reports from this laboratory have shown that 1,25$(OH)_2$D and various compounds reduce inflammation and oedema produced in mouse skin following UVR (Dixon et al., 2011, Poliakov, 2009, Ryan, 2010). This finding was confirmed in the current study. Hairless Skh:Hr1 female mice were exposed to 2.5MED UVR or sham-UVR and immediately treated with vehicle, 23 ρmol/cm^2 1,25$(OH)_2$D, 23 ρmol/cm^2 20(OH)D, or 46 ρmol/cm^2 20(OH)D. The inflammatory erythema reaction to UVR exposure was quantified by measuring the increase in dorsal skinfold thickness (Fig 4.1). UVR-exposed mice in all groups displayed inflamed and oedematous dorsal skin for approximately 3 days following UVR, whilst their sham-irradiated counterparts showed no signs of skin changes between pre- and post-treatment. Groups of mice exposed to UVR and treated with vehicle were more susceptible to the acute inflammatory effects of UVR, generally displaying the greatest increase in skinfold thickness, when compared to other treatment groups. On the other hand, 20(OH)D at both concentrations significantly reduced inflammation, whilst 1,25$(OH)_2$D had no significant effect. Erythema and oedema became less prevalent at approximately 72 hours and treatment and UVR-

exposed mice showed signs of desquamation, or “peeling” with tough, thickened skin.

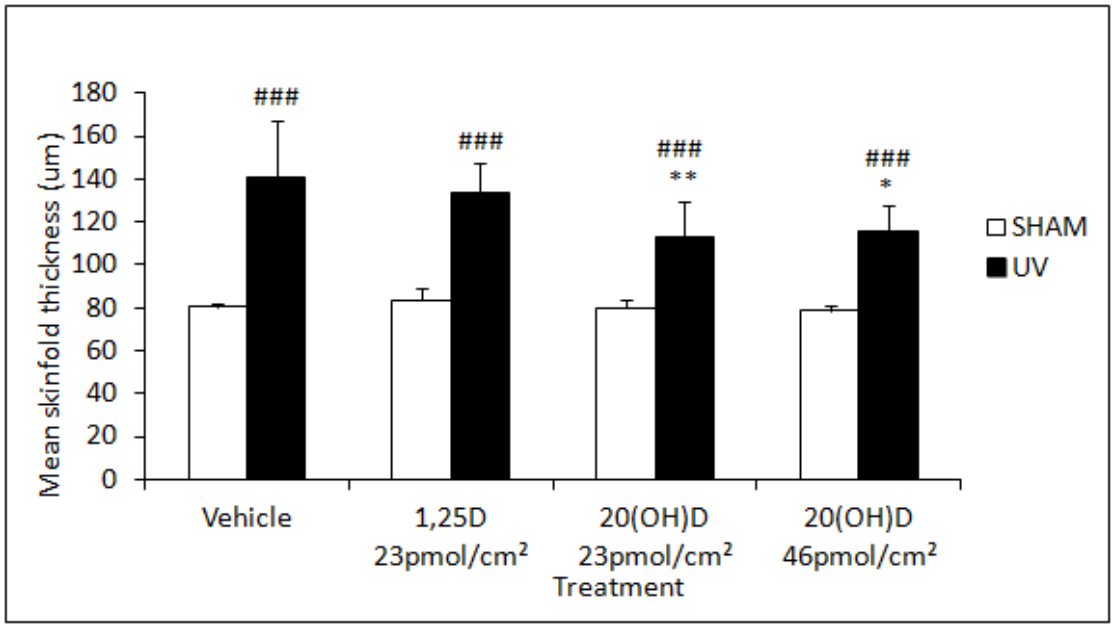

Figure 4.1 Two concentrations of 20(OH)D reduce the acute inflammatory effects of UVR in female Skh:Hr1 hairless mice. Groups of 5 mice were exposed to 2.5MED UVR or sham-UVR and immediately treated with vehicle, 23 pmol/cm^2 1,25(OH)$_2$D, 23 pmol/cm^2 20(OH)D, or 46 pmol/cm^2 20(OH)D. Mid dorsal skin-fold thickness was measured at 24 hours post UVR to give a quantification of inflammation and oedema. *, ** represents significantly different to UV vehicle $p<0.05$, $p<0.01$ respectively; ### represents significantly different to sham groups, $p<0.001$. Sham groups were not significantly different from each other, $p>0.05$.

In addition to the initial experiment, the effect of treatment with 1,25$(OH)_2$D and 20(OH)D on UVR-induced skin inflammation was studied in male and female Skh:Hr1 mice to determine any variation between sexes. A higher dose of 1,25$(OH)_2$D (46 ρmol/cm^2) was used in the successive experiment as the lower dose (23 ρmol/cm^2) had previously shown no protection against UVR-induced inflammation in females.

In this experiment, mice in all treatment groups exposed to 2.5MED UVR showed a significant increase in skin inflammation, compared to their sham-UVR counterparts, as seen in Figure 4.2 (a and b). In general, the extent of UVR-induced inflammation was greater in female groups (fig 4.2a), compared to males (fig 4.2b), however treatment with 1,25$(OH)_2$D and both concentrations of 20(OH)D was more effective in reducing inflammation in females than males.

a.

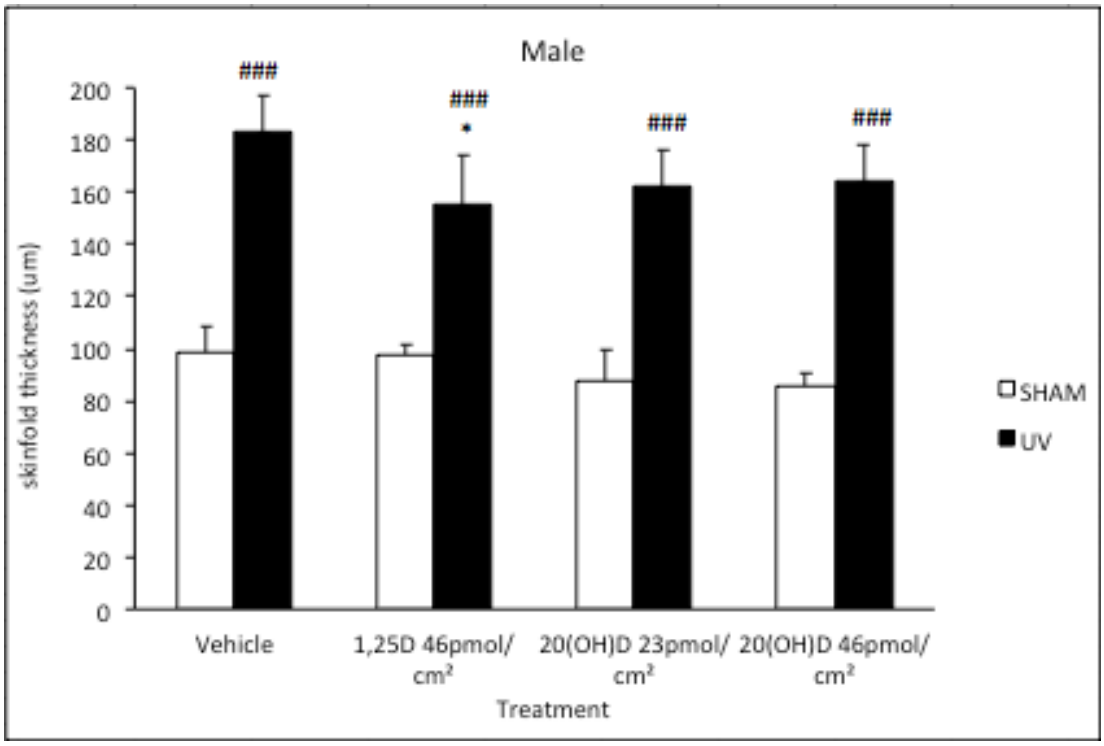

b.

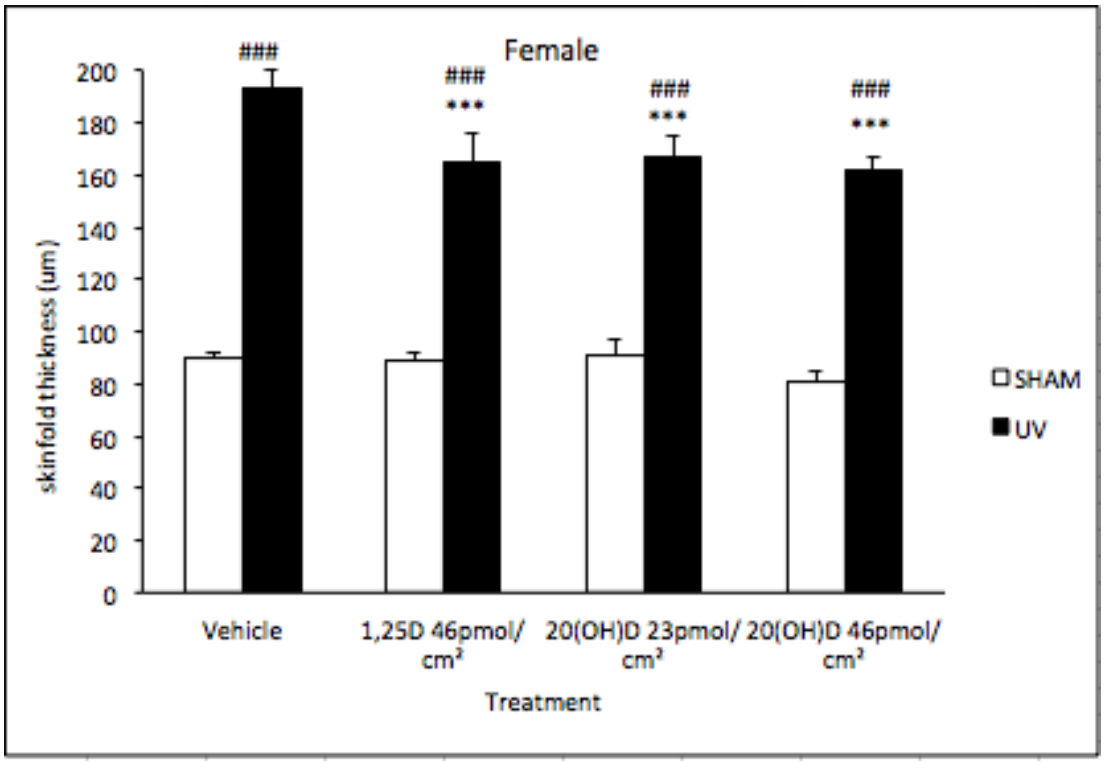

Figure 4.2 Effect of 1,25(OH)$_2$D and 20(OH)D on UVR-induced skin inflammation in a. male and b. female Skh:Hr1 hairless mice.

Groups of 5 mice were exposed to 2.5MED UVR or sham-UVR and immediately treated with vehicle, 46 ρmol/cm^2 1,25$(OH)_2$D, 23 ρmol/cm^2 20(OH)D, or 46 ρmol/cm^2 20(OH)D. Mid dorsal skin-fold thickness was measured at 48 hours post UVR to give a quantification of inflammation and oedema. *, *** represents significantly different to UV vehicle $p<0.05$, $p<0.001$ respectively; ### represents significantly different to sham groups, $p<0.001$. Sham groups were not significantly different from each other, $p>0.05$.

4.1.2 Effect of 1,25(OH)$_2$D and 20(OH)D on UVR-induced immunosuppression in female Skh:Hr1 mice

Previous data from this lab has shown evidence for defence from UVR-induced immunosuppression by 1,25(OH)$_2$D and its analogues in Skh:Hr1 mice (Dixon et al, 2005, Dixon et al 2011). In order to determine whether 20(OH)D may be protective against UVR-induced immunosuppression, using the contact hypersensitivity (CHS) test, mice from 4 out of the 8 groups were irradiated with 2.5MED of UVR and immediately following UVR all mice were treated with vehicle, 23 pmol/cm^2 1,25(OH)$_2$D, 23 pmol/cm^2 20(OH)D, or 46 pmol/cm^2 20(OH)D. One week following UVR all mice were sensitised with 2% oxazolone ventrally, and a further 7 days later, mice were challenged with the same antigen, away from the initial site of sensitisation on the each side of the pinnae of the ears.

The effect of 1,25(OH)$_2$D and 20(OH)D on UVR-induced systemic immunosuppression was assessed by using difference in ear thickness measurements taken from both UV-irradiated and sham mice pre- and post-challenge. Generally, elicitation of the local reaction is seen most notably 16 to 20 hours post-challenge. Immunosuppression is manifest in a lack of, or sub-normal ear swelling following challenge, compared to sham-UVR vehicle treated mice.

Figure 4.3a shows the CHS response at 16 hours following challenge was seen most notably in sham-UVR groups. Application of 1,25D(OH)$_2$D or 20(OH)D at both doses had no effect on ear swelling following challenge in mice exposed to sham-UVR,

compared to the sham-UVR vehicle-treated control group. UVR caused suppression of the systemic CHS response to oxazolone and as expected, mice treated with vehicle following irradiation exhibited significantly less ear swelling compared to mice in the vehicle treated sham-UVR group. Suppression was reversed in mice treated with $1,25(OH)_2D$ or 20(OH)D at both doses.

Figure 4.3b is a quantitative representation of immunosuppression in UVR-exposed mice expressed as a percentage of their sham counterparts in each treatment group. Immunosuppression in mice treated with vehicle was 37.5±5.7%, which was reduced to 7.8±4.4% with 23 pmol/cm^2 $1,25(OH)_2D$. Treatment with 23 pmol/cm^2 or 46 pmol/cm^2 20(OH)D significantly reversed immunosuppression to 3.6±0.5% and 4.8±0.6%, respectively. There was no significant difference in protection from UVR-induced immunosuppression between $1,25(OH)_2D$ and 20(OH)D at both doses.

a.

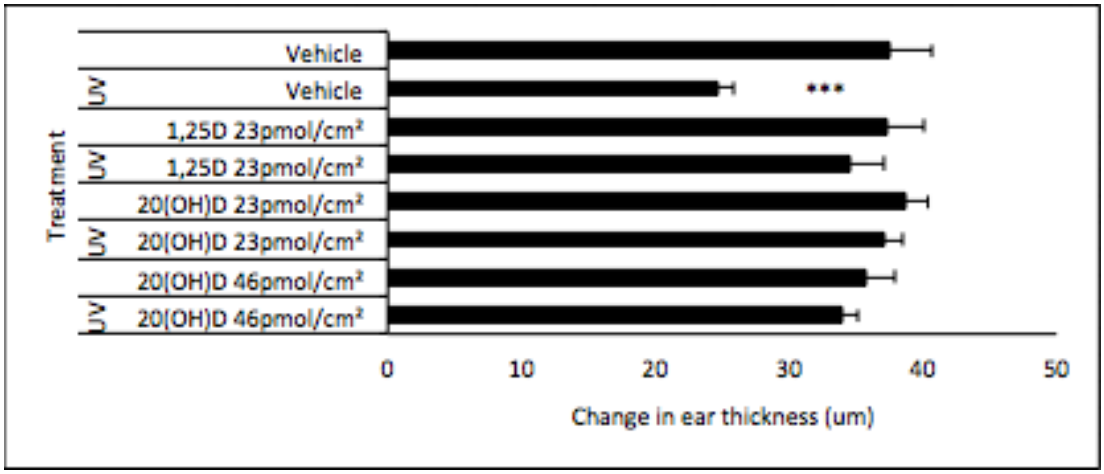

b.

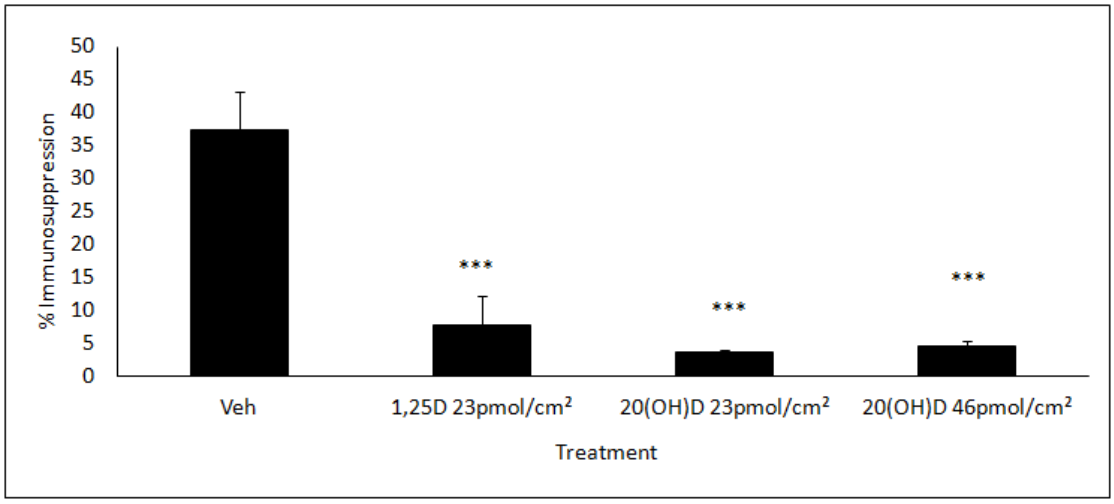

Figure 4.3 1,25(OH)$_2$D and 20D reduce UVR-induced immunosuppression in female Skh:Hr1 hairless albino mice. Groups of 5 mice were irradiated with 2.5MED UVR and treated immediately with 23 pmol/cm^2 1,25(OH)$_2$D, 23 pmol/cm^2 20D or 46 pmol/cm^2. Ear thickness measurements were recorded pre-oxazolone challenge and 16 hours following challenge. a) Difference in change in ear thickness between pre- and 16 hours post-challenge b) Percent immunosuppression, calculated as described in 2.3.6. *** represents significantly different to vehicle at 16 hours post UVR (***p<0.001). Results are from a single experiment.

4.1.3 Effect of a high dose of 1,25(OH)$_2$D and 20(OH)D on UVR-induced immunosuppression in both male and female Skh:Hr1 mice.

In contrast to the findings of Dixon et al (2007) that vitamin D compounds protect against UVR-induced immunosuppression and have no basal immunosuppressive effects in mice, the Mason group and others previously reported in humans that at high physiological concentrations 1,25(OH)$_2$D was immunosuppressive (Damien et al, 2010, Zuo et al, 1992). Additionally, Gorman et al (2009) found that in BALBc hairy mice topical application of 1,25(OH)$_2$D alone was slightly immunosuppressive, and when used in combination with UVR-exposure had an additive effect on UVR-induced immunosuppression. In addition, it has been shown that male mice with normal serum 25(OH)D levels have a reduced CHS response compared with females under the same conditions. Since the initial immunosuppression experiment showed that a low dose of 1,25(OH)$_2$D (23 pmol/cm^2) did not cause basal immunosuppression, and a higher dose of 1,25(OH)$_2$D (46 pmol/cm^2) was required to reduced oedema following UVR exposure, it was of interest to test whether the higher dose caused basal immunosuppression and further, whether 20(OH)D at the same concentration was comparable. In the current study male and female Skh:Hr1 mice were exposed to either 2.5 MED UVR or sham-UVR, and were treated immediately treated with vehicle, 46 pmol/cm^2 1,25(OH)$_2$D, 23 pmol/cm^2 20(OH)D, or 46 pmol/cm^2 20(OH)D. Sensitisation and challenge was undertaken as in section 4.1.2.

In this experiment, peak ear swelling was seen within 16-18 hours post-oxazolone challenge, and for both males and females, the sham-UVR vehicle treated mice elicited the greatest swelling or the ears (fig 4.4). In males, application of 46 pmol/cm^2 1,25(OH)$_2$D and 23 pmol/cm^{2}or 46 pmol/cm^2 20(OH)D caused basal reduction in ear swelling compared to sham-UVR vehicle, with no additional exposure to UVR (fig 4.4a) for 20(OH)D. Treatment with 46pmol/cm^2 1,25(OH)$_2$D and UVR caused the greatest reduction in CHS response compared to both concentrations of 20(OH)D under sham and UVR conditions. In females, UVR caused significant suppression of the CHS response (fig 4.4b). Treatment with 23 pmol/cm^2 20(OH)D had no effect on the basal CHS response, and also protected against UVR-induced CHS suppression. Application of 46 pmol/cm^2 1,25(OH)$_2$D and 46 pmol/cm^2 20(OH)D caused reduction in ear swelling, however this was slightly reversed in the UVR-exposed 46 pmol/cm^2 20(OH)D treated mice.

Figure 4.5 shows percent immunosuppression in UVR-exposed mice expressed by comparison with their sham counterparts in each treatment group (see 2.3.6). In the male vehicle group, the percentage immunosuppression was 41.5±5.2% whilst in females it was 28.7±2.1%, showing that males were more susceptible to UVR-induced immunosuppression. It could be argued that it is not possible to interpret results in the face of immune suppression by test agent alone. Nevertheless data analysis showed that there was slightly less reduction in ear swelling caused by UV in male mice treated with 46 pmol/cm^2 1,25(OH)$_2$D, while in female mice treatment with 46 pmol/cm^2 1,25(OH)$_2$D caused no further reduction in ear swelling. In both sexes, despite basal suppression of the CHS response, treatment with 46 pmol/cm^2

$1,25(OH)_2D$ significantly reduced UVR-induced immunosuppression, 30.57±3.11% in males and 3.0±0.4% in females. Males treated with 20(OH)D at 23 pmol/cm^2 showed 4.6±0.6% , and 46pmol/cm^2 were 0.9±0.1% immunosuppressed, which was more effective than 46 pmol/cm^2 $1,25(OH)_2D$ (fig 4.5a). At 23 pmol/cm^2 20(OH)D female mice had significantly lower UVR-induced immunosuppression, 4.0±0.4%, and a greater change in ear swelling compared with no UV in mice treated with 46 pmol/cm^2 and UV (fig 4.5b).

a.

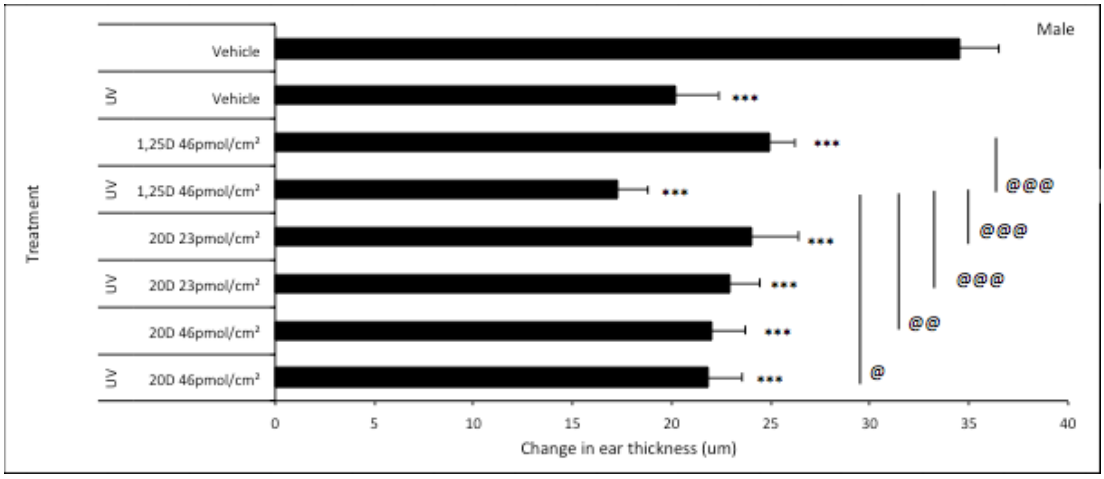

b.

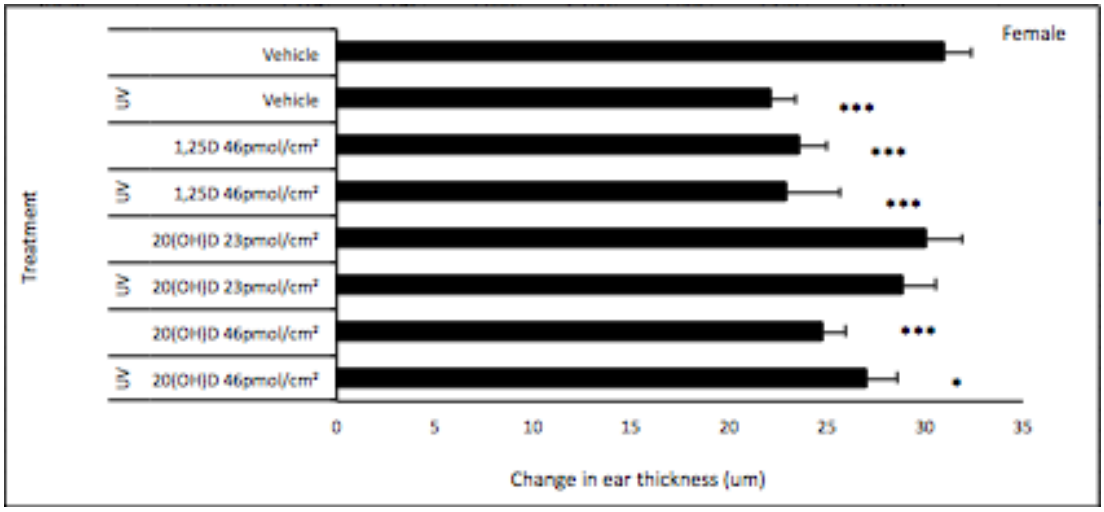

Figure 4.4 Change in ear thickness between pre- and 16-18 hours post-challenge in a) male and b) female Skh:Hr1 mice. Groups of 5 mice were irradiated with 2.5MED UVR and treated immediately with 23 pmol/cm^2 1,25(OH)$_2$D, 23 pmol/cm^2 20(OH)D or 46 pmol/cm^2 20(OH)D. Ear thickness measurements were recorded pre-oxazolone challenge and 16 hours following challenge.*,*** represents significantly different to sham vehicle, $p<0.05$, 0.001 respectively. @, @@, @@@ represents significantly different to UV 1,25(OH)$_2$D, $p<0.05$, 0.01, 0.001 respectively.

a.

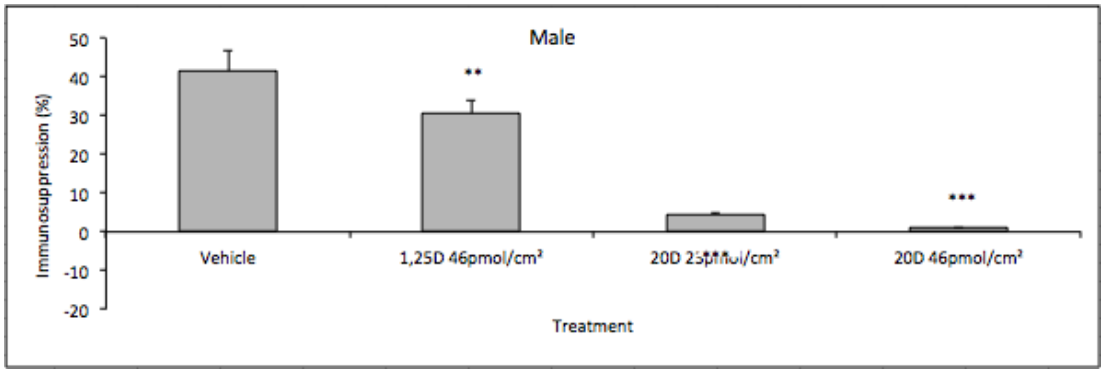

b.

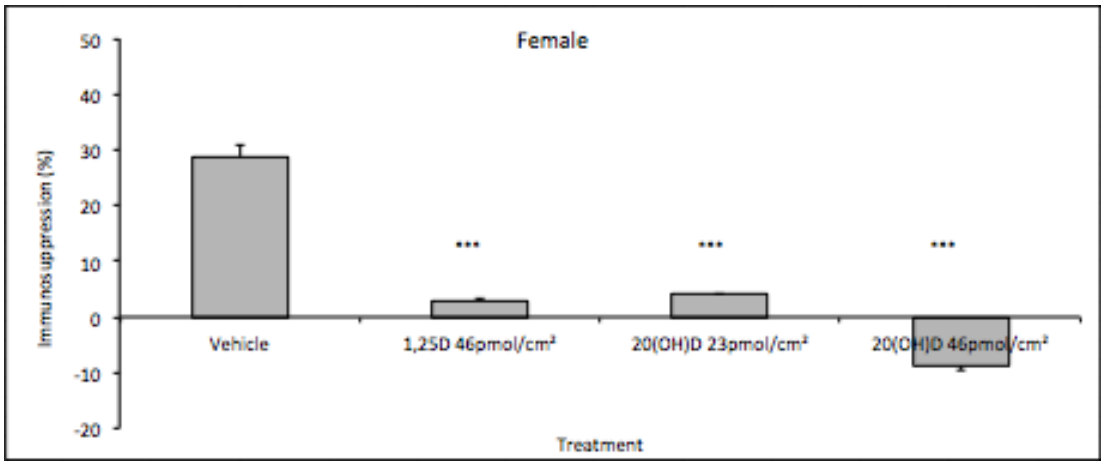

Figure 4.5 1,25(OH)$_2$D and 20(OH)D reduce UVR-induced immunosuppression compared to 1,25(OH)$_2$D and 20(OH)D sham treated mice in a) male and b) female Skh:Hr1 hairless albino mice. **, *** represents significantly different to vehicle at 16 hours post UVR, $p<0.01$, 0.001 respectively. Results are from a single experiment, with 5 mice per group.

4.1.4 Effect of 20(OH)D on UVR-induced immunosuppression in female estrogen receptor β-knockout (ERβ-KO) and wildtype mice

It has previously been reported that female mice with an ablated estrogen receptor-β (ER-β) show a significant decreased protection against UVR-induced immunosuppression and enhanced tumour growth (Cho et al, 2010). In addition to this preliminary reports from the Mason lab have shown that female ER-β knockout mice are more susceptible to CPD formation following UVR, and that $1,25(OH)_2D$-mediated protection against UVR-induced immunosuppression is reversed with topical application of ICI 182780, an ER-β antagonist, in female Skh:Hr1 mice (Tongkao-on, 2014). Since, I also found that male Skh:Hr1 mice were more susceptible to immunosuppression and that 20(OH)D-mediated protection was better than $1,25(OH)_2D$-mediated protection, yet female Skh:Hr1 mice treated with $1,25(OH)_2D$ or 20(OH)D were equally protected (4.4), I tested the effect of 20(OH)D on UVR-induced immunosuppression on ER-β knockout mice in comparison to wildtype.

Under the same conditions as 4.3 and 4.4, mice were either exposed or not exposed to 2.5 MED UVR and immediately treated with vehicle (0.1% v/v ethanol), 23 $pmol/cm^2$ 20(OH)D or 46 $pmol/cm^2$ 20(OH)D. Since these mice were hairy, they were shaved dorsally prior to irradiation to ensure skin exposure to UVR and treatment. Additionally, seven days following UVR, mice were shaved and painted with 2% oxazolone on their ventral side. In this experiment, ear thickness measurements were taken 16-18 hours post-oxazolone challenge, two weeks after

UVR, since this was when peak swelling occurred. As expected, the thickest ear swelling in response to challenge were those of sham-UVR vehicle treated mice in both ER-β and wildtype groups (fig 4.6). UVR caused suppression of the CHS response in both groups. Application of 23 pmol/cm^2 20(OH)D had no basal immunosuppressive effects in mice from either group, and in wildtype mice it reversed UVR-induced suppression of CHS but had no protective effect in ER-β knockout mice (fig 4.6b). In wildtype mice, 46 pmol/cm^2 20(OH)D was suppressive on its own, but did inhibit UVR-induced suppression of CHS (fig 4.6a). In the ER-β knockout mice, 46 pmol/cm^2 20(OH)D alone suppressed CHS though not significantly. Ear swelling was similar with or without UV in mice treated with 46 pmol/cm^2 20(OH)D (fig 4.6b).

Calculated protection against UVR-induced immunosuppression for wildtype and ER-β knockout mice is depicted in Figure 4.7a and Figure 4.7b, respectively. ER- β knockouts were 17% more immunosuppressed than their wildtype equivalents with vehicle treatment. Wildtype mice were completely protected at both concentrations of 20(OH)D. On the other hand, at 23pmol/cm^2 20(OH)D had no protective effects in ER-β knockout mice, whilst 46 pmol/cm^2 was protective, at least compared with sham mice treated with the same concentration 20(OH)D.

a.

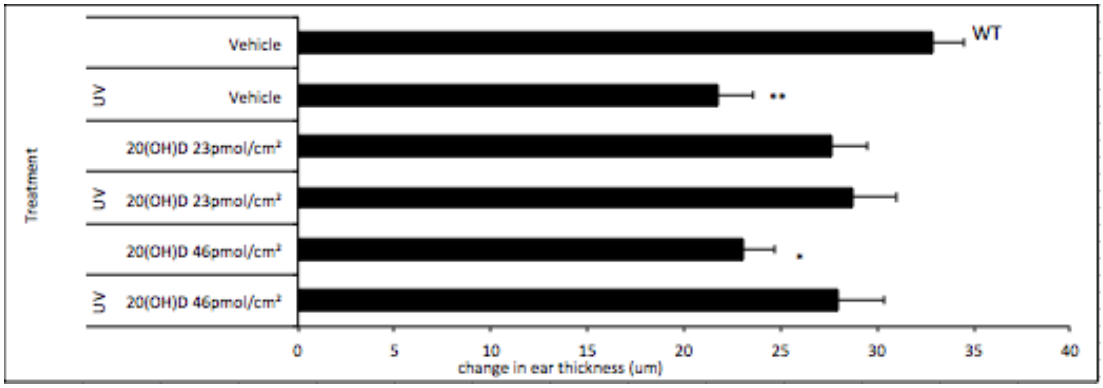

b.

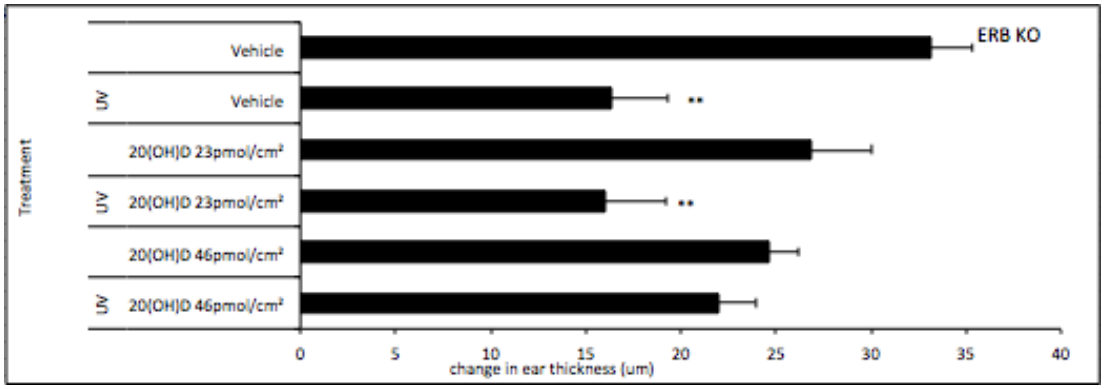

Figure 4.6 Difference in change in ear thickness between pre- and 16-18 hours post-challenge in female a) wildtype and b) ERβ-KO mice. Groups of 5 mice were irradiated with 2.5MED UVR and treated immediately with vehicle, 23 pmol/cm^2 20(OH)D or 46 pmol/cm^2 20(OH)D. Ear thickness measurements were recorded pre-oxazolone challenge and 16-18 hours following challenge.*,** represents significantly different to vehicle, $p<0.05$ and $p<0.01$, respectively.

a.

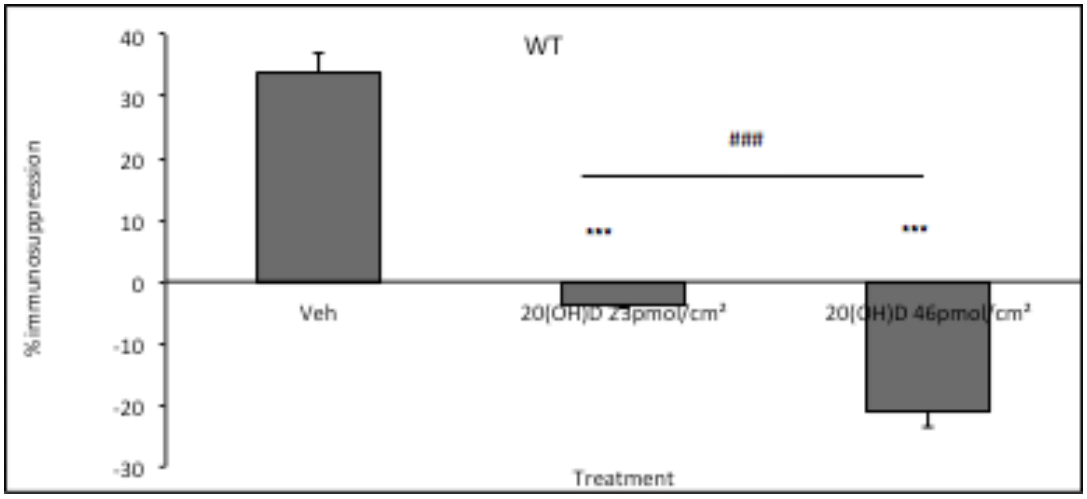

b.

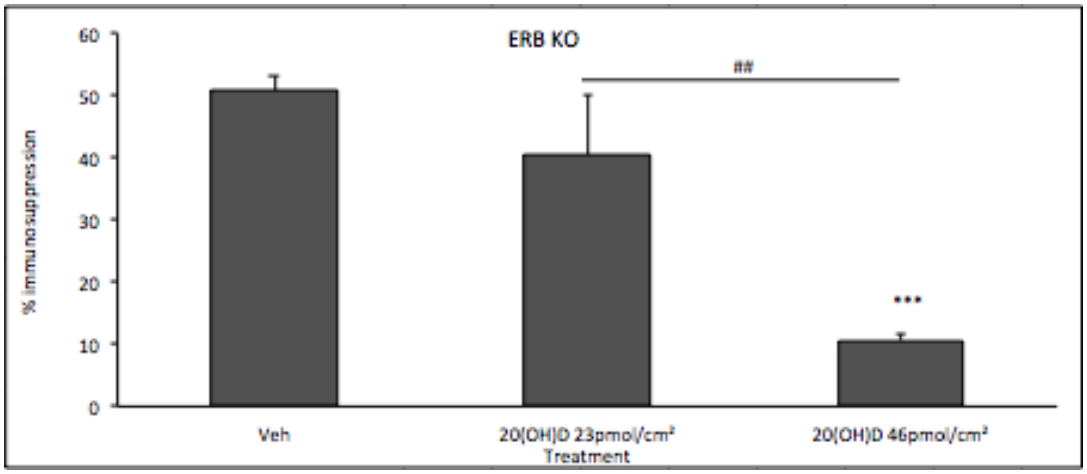

Figure 4.7 1,25(OH)$_2$D and 20(OH)D reduce UVR-induced immunosuppression in female a) wildtype and b) ERβ-KO mice. *** represents significantly different to vehicle at 16-18 hours post UVR, $p<0.001$. ### represents significantly different from each other, $p<0.001$. Results are from a single experiment, with 5 mice per group.

4.2 Discussion

4.2.1 1,25(OH)$_2$D and 20(OH)D and UVR-induced inflammation

Acute exposure to UV irradiation is characterised initially by erythema and oedema (Matsumura and Ananthaswamy, 2002) and then cornification of keratinocytes within several days of the exposure (Lippens et al., 2005). Currently there is limited data on the effect of 1,25(OH)$_2$D on UVR-induced inflammation, however preliminary results from this group have shown that 1,25(OH)$_2$D (Dixon et al., 2011), and analogues such as curcumin and THC, significantly reduce inflammation in mice exposed to UVR, in comparison to littermates treated with vehicle. The effect of 1,25(OH)$_2$D on UVR-induced inflammation was used as a positive control, to test whether 20(OH)D acts as an anti-inflammatory agent following UVR in female and male albino Skh:Hr1 mice. In vehicle treated mice exposed to 2.5MED UVR, inflammation in the form of erythema and oedema was seen within 24 hours, whilst unirradiated mice showed no manifestations. As expected, 1,25(OH)$_2$D caused a reduction in inflammation, as measured by skin thickness, following UVR in all experiments, with the most pronounced effect seen in males at the higher dosage (46ρmol/cm^2). The decrease in skinfold thickness following UVR radiation by application of 1,25(OH)$_2$D to female mice in section 4.1.1 was not significant which is contradictory to previous findings from this laboratory. Since this finding arose from a single initial experiment, without further testing it is not explicitly clear whether this is a true inconsistency or due to experimentation bias, such as human error in skinfold measurements. Time constraints prevented repetition of this investigation.

Female mice tended to respond better to applications of 20(OH)D compared to males, with maximal protection at 23ρmol/cm^2. However, 20(OH)D at both concentrations reduced UVR-induced inflammation in males also. Furthermore, topical application of 20(OH)D did not cause inflammation in unirraditated mice, which was expected since it has been shown that 1,25$(OH)_2$D does not cause any basal inflammation.

Cyclooxygenase-2 (COX-2) is an enzyme induced by proinflammatory reagents in most tissues of the body (Horton et al., 1999, Williams et al., 1999). Its induction breaks down arachidonic acid to the inflammatory prostaglandin PG-E2 from (Williams et al., 1999), which is known to be a mediator of the vascular permeability causing erythema and oedema associated with UVR exposure (Warin, 1978b, Clydesdale et al., 2001). COX-2 induction and chronic inflammation has been implicated in the development and formation of carcinogenesis in many systems and because of this has been the target of development of non-steroidal anti-inflammatory drugs (NSAIDS) as chemopreventative agents (Williams et al., 1999, Speed and Blair, 2011).

It has previously been described that use of topical application of anti-inflammatory agents reduces the formation of tumours in UVR-exposed skin (Burns et al., 2013, Wilgus et al., 2004). Furthermore, a retrospective study in Denmark identified that incidences of malignant melanoma and SCC were lower in a population of people who were taking the commonly prescribed COX-2 inhibitors diclofenac, etodolac, and meloxicam (Johannesdottir et al., 2012). Similarly, topical application of the specific COX-2 inhibitor celecoxib in combination with ibuprofen, a non-specific

COX-2 inhibitor, to UVB irradiated mice decreased oedema and PG-E2 levels associated with UVR-induced inflammation (Johannesdottir et al., 2012). Furthermore, diclofenac, a topical COX-2 inhibitor reduced formation of tumour burden in mice exposed to 10 days of 1MED UVB, compared to untreated mice (Wilgus et al., 2000). These findings highlight the role of COX-2 in inflammation and photocarcinogenesis.

Both $1,25(OH)_2D$ and a low-calcaemic analogue, $1\alpha,25(OH)_2$-16-ene-23-yne-D3 caused inhibition of COX-2 in the RAW 264.7 lipopolysaccharide (LPS) stimulated mouse macrophage cells (Aparna et al., 2008). Furthermore the analogue inhibited proliferation of LPS activated mouse macrophages through reduction in iNOS and interleukin (IL)-2, both mediators of the inflammatory response (Aparna et al., 2008). This suggests that $1,25(OH)_2D$ may be mediating its anti-inflammatory effects via COX-2 inhibition. Since an analogue with low genomic effects has proven to be as effective as $1,25(OH)_2D$ at reducing inflammation via inhibition of COX-2, and 20(OH)D significantly reduced skinfold thickness following UVR, this shows promise that 20(OH)D may be an efficient anti-inflammatory agent working via a similar pathway.

$1,25(OH)_2D$ is a known inhibitor of nuclear factor kappa-B (NF-κB) by upregulating the NF-κB-inhibitor IκB-α (Cohen-Lahav et al., 2007, Cohen-Lahav et al., 2006, Riis et al., 2004). NF-κB is an intracellular a transcription factor involved in activating inflammatory mediators, such as increasing expression of COX-2 (Du et al., 2007). As a newly discovered molecule, there is limited evidence for the role of 20(OH)D as an anti-inflammatory agent. However, one paper has provided strong evidence that

20(OH)D inhibited NF-κB by simultaneously upregulated IκB-α in human transformed and normal keratinocytes to the same extent as active 1,25$(OH)_2$D, and that this effect was mediated via binding to the VDR (Janjetovic et al., 2009). Such evidence suggests that the decrease in skinfold thickness with topical application of 1,25$(OH)_2$D and 20(OH)D seen in the current experiment may be due their direct modulation of inflammatory mediators such as COX-2, or indirectly via pro-inflammatory transcription factors such as NF-κB.

Another mechanism for the reduction in inflammation by 1,25$(OH)_2$D is through suppression of pro-inflammatory IL-6, previously shown to be decreased in UV irradiated keratinocytes by concentration dependent application of 1,25$(OH)_2$D (De Haes et al., 2003). Preliminary *in vivo* studies in this laboratory have also shown reduced IL-6 expression following UVR in mice treated with 1,25$(OH)_2$D (Mason *et al.,* 2010).

In agreement with previous research (Thomas-Ahner et al., 2007, Reeve et al., 2012), the present study found that female mice exhibited a greater increase in skin fold thickness compared to males following UVR, suggestive that their inflammatory response to UVR was greater. Moreover, mice skin displayed different responses to 1,25$(OH)_2$D and 20(OH)D depending on their gender, and the concentration of the utilised. It is well established that there are several differences between male and female skin, which has been attributed to factors such as hormones, protein expression and biochemical properties (Tur, 1997). Men generally have thicker epidermal layers than women (Seidenari et al., 1994), however women display greater amounts subcutaneous adipose tissue (Sjostrom et al., 1972). It was noted

in the current study that male mice had rough, thicker skin compared with female mice who had softer, pink skin.

In terms of hormones, oestrogen is said to be a major determining factor in the difference between male and female skin. Female skin contains the enzyme aromatase, which converts excess testosterone to estradiol, the active form of oestrogen. As discussed in section 3.2.3, application of 17β-estradiol to peroxide treated keratinocytes reduced oxidative damage (Widyarini et al., 2006), which shows a protective role for estradiol in pro-oxidative insults to the skin, such as UV. Further evidence for the protective role of oestrogen in skin lies in the fact that during the time following menopause, women's skin thins substantially with a loss of barrier function, hypothesised to be due to the loss of circulating oestrogen (Shuster et al., 1975). Transepidermal water loss is greatest at the time during the menstrual cycle, when serum levels of oestrogen are at their lowest, just prior to menses, suggestive that oestrogen also helps maintain the barrier function of the skin. Validation of this comes from hormone replacement therapy studies that show skin thickness in post-menopausal women was increased by topical application of an oestrogen (Maheux et al., 1994).

A recent study by collaborators of this group, observed via immunohistochemical staining, a smaller increase in the pro-inflammatory cytokine IL-6 in male mice following UVR, compared with the large increase seen in UVR-irradiated female mice (Reeve et al., 2012). Oestrogen generally stimulates the immune system, and it has been observed that women of reproductive age express higher amounts of pro-inflammatory cytokines mediated through a heightened T_1-helper cell response to

an antigen (Whitacre et al., 1999). Furthermore, results from a study in the female immune reaction showed that post-menopausal females spontaneously produce cytokines IL-4, IL-6, IL-10, IFN-γ and TNF-α. Presence of high amounts of these cytokines caused antagonism of each other making there net effect immunosuppressive (Dao and Kazin, 2007). It is likely that the loss of oestrogen reduces stimulation of the pro-inflammatory response. It should also be noted that the greater proportion of autoimmune diseases occur in women compared to men (Dao and Kazin, 2007). Influences of oestrogen may explain the greater skinfold thickness measured in females compared to males following UVR in this study and the results from Reeve et al., (2012).

A recent paper by Chaudhary et al., (2013) found that use of Erb-041, an ER-β1 agonist in a Skh:Hr1 photocarcinogenesis model, reduced UVB-induced inflammation via reduction in IL-6, IL-10, iNOS, COX-2 and NF-κB, amongst several others. The reduction in these cytokines was mediated via reduced phosphorylation of the MAPK/ERK signalling pathway, associated with cell inflammation and stress signalling. Furthermore, myeloperoxidase activity an indicator of neutrophil infiltration was reduced in Erb-041 treated mice (Chaudhary et al., 2013).

The role of naturally occurring hormones 1,25$(OH)_2$D and 20(OH)D in the skin in terms of anti-inflammation in humans is still not certain, and whether their effect is mediated by other naturally occurring hormones or gender-specific factors is certainly an area that needs further validation through experimentation.

4.2.2 1,25(OH)$_2$D and 20(OH)D and immunosuppression

The current study confirmed previous findings that mice treated with vehicle alone after UVR showed an impaired response to the second application of the antigen, indicating immunosuppression. As expected (Dixon et al., 2007, Dixon et al., 2005), 1,25(OH)$_2$D at 23ρmol/cm^2 reversed UVR-induced immunosuppression in female Skh:Hr1 mice, measured by the contact hypersensitivity reaction. Additionally, at this concentration (23ρmol/cm^2), 1,25(OH)$_2$D did not cause any basal immunosuppression in unirradiated mice. Treatment with 1,25(OH)$_2$D, at the higher concentration of 46ρmol/cm^2 was basally immunosuppressive in both females and males, an outcome of topical 1,25(OH)$_2$D treatment also seen in humans (Damian et al., 2008). This dose of 1,25(OH)$_2$D prevented further UVR-induced immunosuppression in females and reduced further UV-immunosuppression in males compared to vehicle.

It was also shown, for the first time, that at a concentration of 23ρmol/cm^2 20(OH)D caused no basal immunosuppression and was as effective as 1,25(OH)$_2$D at reducing immunosuppression following UVR in female mice. Like 1,25(OH)$_2$D, 20(OH)D at 46ρmol/cm^2 did cause some basal immunosuppression in both sexes, and at 23ρmol/cm^2, despite the basal reduction in the immune response, further immune suppression by UVR was not observed in either male and female mice. The difficulty in interpreting the current results is that the vitamin D compounds were immunosuppressive on their own, which makes statements like “they reversed immunosuppression caused by UVR” somewhat problematic. Interestingly, the preliminary investigation (section 4.1.2, figure 4.3b) showed that 20(OH)D at

46ρmol/cm^2 caused no basal immunosuppression in female mice, whilst further experimentation (section 4.1.3, figure 4.4b) demonstrated that there was basal immunosuppression. Determining the source of this inconsistency is challenging and since this is the first time 20(OH)D has been tested in UVR-immunosuppressive mice studies, further experimentation and repetition that was not possible due to time constraints, is necessary to clarify these findings.

As described in section 4.2.1, studies on the action of 20(OH)D on keratinocytes showed that it blocks activation of NF-κB, via inhibition of IL-1 and lipopolysaccharide, known stimulators of the inflammatory response (Janjetovic et al., 2009). Whilst this is advantageous following acute inflammation, inhibition of NF-κB transcription is immunosuppressive, which suggests that 20(OH)D is likely to be immunosuppressive. Given that NF-κB has been implicated in the skin photoresponse to UVR, and 20(OH)D is produced by CYP11A1 action on vitamin D, this may be one endogenous pathway through which UVR-induced immunosuppression is mediated. On the other hand, studies by Gorman and colleagues have shown that UVR-induced immunosuppression still occurs both locally and globally in animal models of vitamin-D deficiency and repletion (Gorman et al., 2007).

In contrast to being basally immunosuppressive, the current study also shows that both 1,25(OH)$_2$D and 20(OH)D prevented additional immune suppression following UVR, with the caveat expressed above, which suggests that there are other mechanisms of action through which these agents confer partial protection. It has

been observed that removal of UVR-induced DNA damage results in a reduced immunosuppression in mice (Applegate et al., 1989). Since 20(OH)D and 1,25$(OH)_2$D at the same concentrations used in the CHS experiments reduced formation of both thymine dimers and 8oxodG, this is likely to be a mechanism through which they are protective against UVR-induced immunosuppression also.

The presence of Metallothionein I and II isoforms have been implicated in the prevention of tissue damage in the epidermis, via their ROS scavenging abilities as potent antioxidants. Cells with high expression of metallothionein appear to be resistant to sunburn cells, apoptotic keratinocytes, caused by UVR (Hanada et al., 1998, Reeve et al., 2000, Wang et al., 2004). The relevance of this to the current results comes from Reeve and colleagues (2012) that metallothionein KO mice, unable to express metallothionein, are more prone to immunosuppression following UVR exposure. Additionally, since 1,25$(OH)_2$D upregulates mRNA expression of metallothionein mRNA (De Haes et al., 2004b), this may be a mechanism through which it prevents UVR-induced immunosuppression. While the upregulation of MT by 1,25$(OH)_2$D us likely, further studies to test whether 20(OH)D affects metallothionein expression would be helpful.

As seen in both inflammation and DNA damage, there also appeared to be a gender bias present in the immunosuppression results. In agreement with previous reports (Reeve et al., 2012, Thomas-Ahner et al., 2007), male Skh:Hr1 mice were more immunosuppressed than females following UVR. This has also been noted in experiments with humans by our collaborators (Damian et al., 2008).

IL-10 is an immunosuppressive cytokine known to be released in keratinocytes following UVR exposure. IL-10 induction causes a reduction in the CHS response in mice, and this was shown to be greater in males following UVR compared to their female counterparts (Reeve et al., 2012). In addition, topical oestrogens inhibited UVR-induced immunosuppression during a CHS test in mice. In male mice injected with 17β-estradiol following UVR, photo-immunosuppression was reversed, along with a reduction in serum IL-10, a major anti-inflammatory, immunosuppressive cytokine (Cho et al., 2010). Moreover, when females were exposed to UVR and treated with anti-estradiol agents or tamoxifen, IL-10 serum levels increased significantly, which ultimately reduced the CHS response (Hiramoto et al., 2004).

Use of ICI 182,780 an estrogen receptor antagonist, caused exacerbation of UVR-induced immunological suppression (Widyarini et al., 2006). The expression of the ER-β1 receptor female skin is not significantly different to that of male skin (Thornton et al., 2003b). However, since females produce the natural oestrogen ligand for the receptor at greater concentrations than males, the presence of the natural ligand may explain the difference in photoprotection between the sexes.

In relation to gender bias and immunosuppression with 1,25$(OH)_2$D, preliminary experimentation from our group has shown that found that 1,25$(OH)_2$D reduction of UVR-induced CHS suppression in female Skh:Hr1 mice was reversed following treatment with ICI 182780 (Tongkao-on et al., 2012). Since there is evidence for the 1,25$(OH)_2$D reducing pro-inflammatory cytokines IL-6 (De Haes et al., 2003, Mason et al., 2010) and IL-12 (Bikle, 2009), and increasing IL-10 receptor gene expression (Michel et al., 1997) in keratinocytes, an immunosuppressive cytokine, and these

cytokines have been shown to be decreased by an ER-β agonist (Chaudhary et al., 2013) it is possible that 1,25$(OH)_2$D and other photoprotective analogues may interact with oestrogen signalling to produce greater protection against UVR-induced immune response suppression in female mice.

Given that the current studies showed that there was higher UVR-induced immunosuppression in males compared to females, and there is evidence for the role of ER-β in mediation of photoprotection (Cho et al., 2010, Reeve et al., 2009, Widyarini et al., 2006), it seemed valid to use ER-β KO mouse model for further immunosuppression studies. The results showed that application of 20(OH)D at 23ρmol/cm^2 did not produce any basal immunosuppressive results, in either WT and ER-β null mice, however KO mice were not protected from UVR-induced immunosuppression at this concentration of 20(OH)D, where their WT counterparts were. Such findings suggest that the mechanisms through which the lowest dose of 20(OH)D that reduces immunosuppression following UVR, requires ER-β signalling. Inhibition of further UVR-induced immunosuppression in ER-β KO mice, was seen at the higher concentration of 46ρmol/cm^2 20(OH)D. At this dose of 20(OH)D WT mice showed significantly reduced ear swelling, indicating immunosuppression. These results are consistent with the proposal that the presence of ER-β in skin potentiates the actions of 20(OH)D. Further studies might benefit from the use of ICI 182780 the ER-β1 antagonist in conjunction with 20(OH)D in WT mice, to complement the current findings.

5 CONCLUSIONS AND FUTURE DIRECTIONS

This study has shown for the first time that use of 20(OH)D in both *in vitro* and *in vitro* models following UVR exposure is photoprotective to a similar extent as $1,25(OH)_2D$. 20(OH)D reduced direct UV-induced DNA damage, thymine dimers, 3 hours after UVR in both cultured human keratinocytes and Skh:Hr1 hairless mouse skin. Furthermore, 20(OH)D reduced formation of indirect UV-induced DNA damage, 8oxodG, in cultured human keratinocytes, within the same timeframe. Use of the curcuminoid THC produced analogous results under the same settings, which is in line with previous data. Photoprotection by 20(OH)D was greater in females than males.

Previous studies from the Mason group showed evidence for chloride currents an essential mechanism for $1,25(OH)_2D$ protection against UVR-induced DNA damage (Sequeira et al., 2012a). Results from this study showed that chloride channel permeability is also vital for 20(OH)D mediated reduction in thymine dimer formation in cultured human keratinocytes. Since 20(OH)D and THC do not cause some of the genomic effects of $1,25(OH)_2D$ such as hypercalcaemia, but have been shown to bind to the VDR, there is reason to consider that 20(OH)D exerts its photoprotective effects via the non-genomic ERp57/MARRS binding protein like $1,25(OH)_2D$ (Sequeira et al., 2012b). But this remains to be directly tested.

Downregulation of Wnt has been shown to reduce UVR-induced skin carcinogenesis in mice (Chaudhary et al., 2013), and the present study showed that inhibition of

Wnt was photoprotective on its own and had no effect on photoprotection by $1,25(OH)_2D$ and 20(OH)D on the formation of thymine dimers in cultured human keratinocytes as early as 3 hours following UVR. Experimentation into the downstream targets of Wnt, such as β-catenin, and whether $1,25(OH)_2D$ and 20(OH)D or other ligand binding to the VDR interacts with them to mediate their photoprotective effects against UVR-induced DNA damage would be a reasonable proposal. Furthermore, since $1,25(OH)_2D$ has been shown to reduce UVR-induced skin carcinogenesis, and preliminary studies from the Mason group show that $1,25(OH)_2D$ increases nucleotide excision repair proteins (Song, 2014), further study with 20(OH)D on this is necessary. Similarly, recent results from Halliday and colleagues on HaCaT cells and melanocytes showed that use of nicotinamide, a precursor in the formation of ATP, reduces 8oxodG and thymine dimers following exposure to UVR (Surjana et al., 2013, Thompson et al., 2014). Since both $1,25(OH)_2D$ and 20(OH)D reduce these forms of DNA damage additional experimentation is necessary to determine whether they have an effect on energy production and DNA repair.

The results also indicate that 20(OH)D was as efficacious as $1,25(OH)_2D$ at preventing UVR-induced inflammation and inhibits further immunosuppression caused by UVR, however at high doses caused some basal immunosuppression as is seen with $1,25(OH)_2D$, and immunosuppression was in general greater in male mice. In experiments with ER-β KO mice reversal of the UVR-induced immunosuppression required high doses of 20(OH)D which also caused basal immunosuppression, suggesting photoprotection at the lower dose may be mediated by an interaction

between 20(OH)D and ER-β signalling. More study into the interactions between inflammatory cytokines influenced by 1,25$(OH)_2$D and 20(OH)D and ER-β are necessary for elucidation of their immunosuppressive and anti-inflammatory effects following UVR exposure, and may explain some of the gender bias in the results of this study.

REFERENCES

APARNA, R., SUBHASHINI, J., ROY, K. R., REDDY, G. S., ROBINSON, M., USKOKOVIC, M. R., VENKATESWARA REDDY, G. & REDDANNA, P. 2008. Selective inhibition of cyclooxygenase-2 (COX-2) by 1alpha,25-dihydroxy-16-ene-23-yne-vitamin D3, a less calcemic vitamin D analog. *J Cell Biochem,* 104**,** 1832-42.

APPLEGATE, L. A., LEY, R. D., ALCALAY, J. & KRIPKE, M. L. 1989. Identification of the molecular target for the suppression of contact hypersensitivity by ultraviolet radiation. *J Exp Med,* 170**,** 1117-31.

ASSEFA, Z., VAN LAETHEM, A., GARMYN, M. & AGOSTINIS, P. 2005. Ultraviolet radiation-induced apoptosis in keratinocytes: on the role of cytosolic factors. *Biochim Biophys Acta,* 1755**,** 90-106.

ASZTERBAUM, M., EPSTEIN, J., ORO, A., DOUGLAS, V., LEBOIT, P. E., SCOTT, M. P. & EPSTEIN, E. H., JR. 1999. Ultraviolet and ionizing radiation enhance the growth of BCCs and trichoblastomas in patched heterozygous knockout mice. *Nat Med,* 5**,** 1285-91.

AUBIN, F. 2003. Mechanisms involved in ultraviolet light-induced immunosuppression. *Eur J Dermatol,* 13**,** 515-23.

BARONI, A., BUOMMINO, E., DE GREGORIO, V., RUOCCO, E., RUOCCO, V. & WOLF, R. 2012. Structure and function of the epidermis related to barrier properties. *Clin Dermatol,* 30**,** 257-62.

BARTIK, L., WHITFIELD, G. K., KACZMARSKA, M., LOWMILLER, C. L., MOFFET, E. W., FURMICK, J. K., HERNANDEZ, Z., HAUSSLER, C. A., HAUSSLER, M. R. & JURUTKA, P. W. 2010. Curcumin: a novel nutritionally derived ligand of the vitamin D receptor with implications for colon cancer chemoprevention. *J Nutr Biochem,* 21**,** 1153-61.

BAU, D. T., GURR, J. R. & JAN, K. Y. 2001. Nitric oxide is involved in arsenite inhibition of pyrimidine dimer excision. *Carcinogenesis,* 22**,** 709-16.

BEISSERT, S. & LOSER, K. 2008. Molecular and cellular mechanisms of photocarcinogenesis. *Photochem Photobiol,* 84**,** 29-34.

BENASSI, L., OTTANI, D., FANTINI, F., MARCONI, A., CHIODINO, C., GIANNETTI, A. & PINCELLI, C. 1997. 1,25-dihydroxyvitamin D3, transforming growth factor beta1, calcium, and ultraviolet B radiation induce apoptosis in cultured human keratinocytes. *J Invest Dermatol,* 109**,** 276-82.

BESARATINIA, A., YOON, J. I., SCHROEDER, C., BRADFORTH, S. E., COCKBURN, M. & PFEIFER, G. P. 2011. Wavelength dependence of ultraviolet radiation-induced DNA damage as determined by laser irradiation suggests that cyclobutane pyrimidine dimers are the principal DNA lesions produced by terrestrial sunlight. *FASEB J,* 25**,** 3079-91.

BIKLE, D. D. 2009. Vitamin D and immune function: understanding common pathways. *Curr Osteoporos Rep,* 7**,** 58-63.

BIKLE, D. D. 2011a. Vitamin D metabolism and function in the skin. *Mol Cell Endocrinol,* 347**,** 80-9.

BIKLE, D. D. 2011b. Vitamin D regulation of immune function. *Vitamins and Hormones,* 86**,** 1-21.

BIKLE, D. D. 2012. Vitamin D and bone. *Curr Osteoporos Rep,* 10**,** 151-9.

BIKLE, D. D., CHANG, S., CRUMRINE, D., ELALIEH, H., MAN, M. Q., CHOI, E. H., DARDENNE, O., XIE, Z., ARNAUD, R. S., FEINGOLD, K. & ELIAS, P. M. 2004. 25 Hydroxyvitamin D 1 alpha-hydroxylase is required for optimal epidermal differentiation and permeability barrier homeostasis. *J Invest Dermatol,* 122**,** 984-92.

BIKLE, D. D., ELALIEH, H., WELSH, J., OH, D., CLEAVER, J. & TEICHERT, A. 2012. Protective role of vitamin D signaling in skin cancer formation. *J Steroid Biochem Mol Biol*.

BIKLE, D. D., ELALIEH, H., WELSH, J., OH, D., CLEAVER, J. & TEICHERT, A. 2013. Protective role of vitamin D signaling in skin cancer formation. *J Steroid Biochem Mol Biol,* 136**,** 271-9.

BIKLE, D. D., NEMANIC, M. K., GEE, E. & ELIAS, P. 1986. 1,25-Dihydroxyvitamin D3 production by human keratinocytes. Kinetics and regulation. *J Clin Invest,* 78**,** 557-66.

BODE, A. M. & DONG, Z. 2003. Mitogen-activated protein kinase activation in UV-induced signal transduction. *Sci STKE,* 2003**,** RE2.

BOTTAI, G., MANCINA, R., MURATORI, M., DI GENNARO, P. & LOTTI, T. 2013. 17beta-estradiol protects human skin fibroblasts and keratinocytes against oxidative damage. *J Eur Acad Dermatol Venereol,* 27**,** 1236-43.

BRASH, D. E. 1997. Sunlight and the onset of skin cancer. *Trends Genet,* 13**,** 410-4.

BROEKMANS, W. M., VINK, A. A., BOELSMA, E., KLOPPING-KETELAARS, W. A., TIJBURG, L. B., VAN'T VEER, P., VAN POPPEL, G. & KARDINAAL, A. F. 2003. Determinants of skin sensitivity to solar irradiation. *Eur J Clin Nutr,* 57**,** 1222-9.

BURNS, E. M., TOBER, K. L., RIGGENBACH, J. A., SCHICK, J. S., LAMPING, K. N., KUSEWITT, D. F., YOUNG, G. S. & OBERYSZYN, T. M. 2013. Preventative topical diclofenac treatment differentially decreases tumor burden in male and female Skh-1 mice in a model of UVB-induced cutaneous squamous cell carcinoma. *Carcinogenesis,* 34**,** 370-7.

CADET, J., DOUKI, T., GASPARUTTO, D. & RAVANAT, J. L. 2003. Oxidative damage to DNA: formation, measurement and biochemical features. *Mutat Res,* 531**,** 5-23.

CADET, J., SAGE, E. & DOUKI, T. 2005. Ultraviolet radiation-mediated damage to cellular DNA. *Mutat Res,* 571**,** 3-17.

CATLEY, M. C., BIRRELL, M. A., HARDAKER, E. L., DE ALBA, J., FARROW, S., HAJ-YAHIA, S. & BELVISI, M. G. 2008. Estrogen receptor beta: expression profile and possible anti-inflammatory role in disease. *J Pharmacol Exp Ther,* 326**,** 83-8.

CHAUDHARY, S. C., SINGH, T., TALWELKAR, S. S., SRIVASTAVA, R. K., ARUMUGAM, A., WENG, Z., ELMETS, C. A., AFAQ, F., KOPELOVICH, L. & ATHAR, M. 2013. Erb-041, an estrogen receptor beta agonist inhibits skin photocarcinogenesis in SKH-1 hairless mice by down-regulating WNT signaling pathway. *Cancer Prev Res (Phila)*.

CHEN, B., DODGE, M. E., TANG, W., LU, J., MA, Z., FAN, C. W., WEI, S., HAO, W., KILGORE, J., WILLIAMS, N. S., ROTH, M. G., AMATRUDA, J. F., CHEN, C. & LUM, L. 2009. Small molecule-mediated disruption of Wnt-dependent signaling in tissue regeneration and cancer. *Nat Chem Biol,* 5**,** 100-7.

CHEN, S., SIMS, G. P., CHEN, X. X., GU, Y. Y., CHEN, S. & LIPSKY, P. E. 2007. Modulatory effects of 1,25-dihydroxyvitamin D3 on human B cell differentiation. *J Immunol,* 179**,** 1634-47.

CHO, J. L., ALLANSON, M. & REEVE, V. E. 2010. Oestrogen receptor-beta signalling protects against transplanted skin tumour growth in the mouse. *Photochem Photobiol Sci,* 9**,** 608-14.

CHRISTENSEN, A. D. & HAASE, C. 2012. Immunological mechanisms of contact hypersensitivity in mice. *APMIS,* 120**,** 1-27.

CLYDESDALE, G. J., DANDIE, G. W. & MULLER, H. K. 2001. Ultraviolet light induced injury: immunological and inflammatory effects. *Immunol Cell Biol,* 79**,** 547-68.

COHEN-LAHAV, M., DOUVDEVANI, A., CHAIMOVITZ, C. & SHANY, S. 2007. The anti-inflammatory activity of 1,25-dihydroxyvitamin D3 in macrophages. *J Steroid Biochem Mol Biol,* 103**,** 558-62.

COHEN-LAHAV, M., SHANY, S., TOBVIN, D., CHAIMOVITZ, C. & DOUVDEVANI, A. 2006. Vitamin D decreases NFkappaB activity by increasing IkappaBalpha levels. *Nephrol Dial Transplant,* 21**,** 889-97.

CORSINI, E. & GALLI, C. L. 2000. Epidermal cytokines in experimental contact dermatitis. *Toxicology,* 142**,** 203-11.

COTRIM, C. Z., FABRIS, V., DORIA, M. L., LINDBERG, K., GUSTAFSSON, J. A., AMADO, F., LANARI, C. & HELGUERO, L. A. 2013. Estrogen receptor beta growth-inhibitory effects are repressed through activation of MAPK and PI3K signalling in mammary epithelial and breast cancer cells. *Oncogene,* 32**,** 2390-402.

CROSS, D. A., ALESSI, D. R., COHEN, P., ANDJELKOVICH, M. & HEMMINGS, B. A. 1995. Inhibition of glycogen synthase kinase-3 by insulin mediated by protein kinase B. *Nature,* 378**,** 785-9.

D'ORAZIO, J. A., JARRETT, S., MARSCH, A., LAGREW, J. & CLEARY, L. 2013. *Melanoma — Epidemiology, Genetics and Risk Factors, Recent Advances in the Biology, Therapy and Management of Melanoma*, InTech.

DAMIAN, D. L., KIM, Y. J., DIXON, K. M., HALLIDAY, G. M., JAVERI, A. & MASON, R. S. 2010. Topical calcitriol protects from UV-induced genetic damage but suppresses cutaneous immunity in humans. *Exp Dermatol,* 19**,** e23-30.

DAMIAN, D. L., PATTERSON, C. R., STAPELBERG, M., PARK, J., BARNETSON, R. S. & HALLIDAY, G. M. 2008. UV radiation-induced immunosuppression is greater in men and prevented by topical nicotinamide. *J Invest Dermatol,* 128**,** 447-54.

DAO, H., JR. & KAZIN, R. A. 2007. Gender differences in skin: a review of the literature. *Gend Med,* 4**,** 308-28.

DE GRUIJL, F. R. 2008. UV-induced immunosuppression in the balance. *Photochem Photobiol,* 84**,** 2-9.

DE HAES, P., GARMYN, M., CARMELIET, G., DEGREEF, H., VANTIEGHEM, K., BOUILLON, R. & SEGAERT, S. 2004a. Molecular pathways involved in the anti-apoptotic effect of 1,25-dihydroxyvitamin D3 in primary human keratinocytes. *J Cell Biochem,* 93**,** 951-67.

DE HAES, P., GARMYN, M., DEGREEF, H., VANTIEGHEM, K., BOUILLON, R. & SEGAERT, S. 2003. 1,25-Dihydroxyvitamin D3 inhibits ultraviolet B-induced

apoptosis, Jun kinase activation, and interleukin-6 production in primary human keratinocytes. *J Cell Biochem,* 89**,** 663-73.

DE HAES, P., GARMYN, M., VERSTUYF, A., DE CLERCQ, P., VANDEWALLE, M., DEGREEF, H., VANTIEGHEM, K., BOUILLON, R. & SEGAERT, S. 2005. 1,25-Dihydroxyvitamin D3 and analogues protect primary human keratinocytes against UVB-induced DNA damage. *J Photochem Photobiol B,* 78**,** 141-8.

DE HAES, P., GARMYN, M., VERSTUYF, A., DE CLERCQ, P., VANDEWALLE, M., VANTIEGHEM, K., DEGREEF, H., BOUILLON, R. & SEGAERT, S. 2004b. Two 14-epi analogues of 1,25-dihydroxyvitamin D3 protect human keratinocytes against the effects of UVB. *Arch Dermatol Res,* 295**,** 527-34.

DE LAAT, W. L., JASPERS, N. G. & HOEIJMAKERS, J. H. 1999. Molecular mechanism of nucleotide excision repair. *Genes Dev,* 13**,** 768-85.

DE WINTER, S., VINK, A. A., ROZA, L. & PAVEL, S. 2001. Solar-simulated skin adaptation and its effect on subsequent UV-induced epidermal DNA damage. *J Invest Dermatol,* 117**,** 678-82.

DIFFEY, B. L. 2002. Sources and measurement of ultraviolet radiation. *Methods,* 28**,** 4-13.

DIKER-COHEN, T., KOREN, R. & RAVID, A. 2006. Programmed cell death of stressed keratinocytes and its inhibition by vitamin D: the role of death and survival signaling pathways. *Apoptosis,* 11**,** 519-34.

DIXON, K. M., DEO, S. S., NORMAN, A. W., BISHOP, J. E., HALLIDAY, G. M., REEVE, V. E. & MASON, R. S. 2007. In vivo relevance for photoprotection by the vitamin D rapid response pathway. *J Steroid Biochem Mol Biol,* 103**,** 451-6.

DIXON, K. M., DEO, S. S., WONG, G., SLATER, M., NORMAN, A. W., BISHOP, J. E., POSNER, G. H., ISHIZUKA, S., HALLIDAY, G. M., REEVE, V. E. & MASON, R. S. 2005. Skin cancer prevention: a possible role of 1,25dihydroxyvitamin D3 and its analogs. *J Steroid Biochem Mol Biol,* 97**,** 137-43.

DIXON, K. M., NORMAN, A. W., SEQUEIRA, V. B., MOHAN, R., RYBCHYN, M. S., REEVE, V. E., HALLIDAY, G. M. & MASON, R. S. 2011. 1alpha,25(OH)(2)-vitamin D and a nongenomic vitamin D analogue inhibit ultraviolet radiation-induced skin carcinogenesis. *Cancer Prev Res (Phila),* 4**,** 1485-94.

DU, Z., WEI, L., MURTI, A., PFEFFER, S. R., FAN, M., YANG, C. H. & PFEFFER, L. M. 2007. Non-conventional signal transduction by type 1 interferons: the NF-kappaB pathway. *J Cell Biochem,* 102**,** 1087-94.

ELLISON, T. I., SMITH, M. K., GILLIAM, A. C. & MACDONALD, P. N. 2008. Inactivation of the vitamin D receptor enhances susceptibility of murine skin to UV-induced tumorigenesis. *J Invest Dermatol,* 128**,** 2508-17.

EVANS, M. D., BUTLER, J. M., NICOLL, K., COOKE, M. S. & LUNEC, J. 2003. 17 beta-Oestradiol attenuates nucleotide excision repair. *FEBS Lett,* 535**,** 153-8.

FOOTE, J. A., HARRIS, R. B., GIULIANO, A. R., ROE, D. J., MOON, T. E., CARTMEL, B. & ALBERTS, D. S. 2001. Predictors for cutaneous basal- and squamous-cell carcinoma among actinically damaged adults. *Int J Cancer,* 95**,** 7-11.

FRIEDBERG, E. C. 2001. How nucleotide excision repair protects against cancer. *Nat Rev Cancer,* 1**,** 22-33.

GORDON-THOMSON, C., GUPTA, R., TONGKAO-ON, W., RYAN, A., HALLIDAY, G. M. & MASON, R. S. 2012. 1alpha,25 dihydroxyvitamin D3 enhances cellular

defences against UV-induced oxidative and other forms of DNA damage in skin. *Photochem Photobiol Sci,* 11**,** 1837-47.

GORMAN, S., KURITZKY, L. A., JUDGE, M. A., DIXON, K. M., MCGLADE, J. P., MASON, R. S., FINLAY-JONES, J. J. & HART, P. H. 2007. Topically applied 1,25-dihydroxyvitamin D3 enhances the suppressive activity of CD4+CD25+ cells in the draining lymph nodes. *J Immunol,* 179**,** 6273-83.

GUPTA, R., DIXON, K. M., DEO, S. S., HOLLIDAY, C. J., SLATER, M., HALLIDAY, G. M., REEVE, V. E. & MASON, R. S. 2007. Photoprotection by 1,25 dihydroxyvitamin D3 is associated with an increase in p53 and a decrease in nitric oxide products. *J Invest Dermatol,* 127**,** 707-15.

GURYEV, O., CARVALHO, R. A., USANOV, S., GILEP, A. & ESTABROOK, R. W. 2003. A pathway for the metabolism of vitamin D3: unique hydroxylated metabolites formed during catalysis with cytochrome P450scc (CYP11A1). *Proc Natl Acad Sci U S A,* 100**,** 14754-9.

HALLIDAY, G. M. & CADET, J. 2012. It's all about position: the basal layer of human epidermis is particularly susceptible to different types of sunlight-induced DNA damage. *J Invest Dermatol,* 132**,** 265-7.

HANADA, K., SAWAMURA, D., HASHIMOTO, I., KIDA, K. & NAGANUMA, A. 1998. Epidermal proliferation of the skin in metallothionein-null mice. *J Invest Dermatol,* 110**,** 259-62.

HANAHAN, D. & WEINBERG, R. A. 2000. The hallmarks of cancer. *Cell,* 100**,** 57-70.

HANAHAN, D. & WEINBERG, R. A. 2011. Hallmarks of cancer: the next generation. *Cell,* 144**,** 646-74.

HANAWALT, P. C. 2002. Subpathways of nucleotide excision repair and their regulation. *Oncogene,* 21**,** 8949-56.

HART, P. H., GRIMBALDESTON, M. A. & FINLAY-JONES, J. J. 2001. Sunlight, immunosuppression and skin cancer: role of histamine and mast cells. *Clin Exp Pharmacol Physiol,* 28**,** 1-8.

HAUSSLER, M. R., JURUTKA, P. W., MIZWICKI, M. & NORMAN, A. W. 2011. Vitamin D receptor (VDR)-mediated actions of 1alpha,25(OH)(2)vitamin D(3): genomic and non-genomic mechanisms. *Best Pract Res Clin Endocrinol Metab,* 25**,** 543-59.

HIRAMOTO, K., TANAKA, H., YANAGIHARA, N., SATO, E. F. & INOUE, M. 2004. Effect of 17beta-estradiol on immunosuppression induced by ultraviolet B irradiation. *Arch Dermatol Res,* 295**,** 307-11.

HOLICK, M. F. 1981. The Cutaneous Photosynthesis of Previtamin D3: A Unique Photoendocrine System. *J Investig Dermatol,* 77**,** 8.

HOLICK, M. F. 2004. Vitamin D: importance in the prevention of cancers, type 1 diabetes, heart disease, and osteoporosis. *Am J Clin Nutr,* 79**,** 362-71.

HOLICK, M. F., USKOKOVIC, M., HENLEY, J. W., MACLAUGHLIN, J., HOLICK, S. A. & POTTS, J. T., JR. 1980. The photoproduction of 1 alpha,25-dihydroxyvitamin D3 in skin: an approach to the therapy of vitamin-D-resistant syndromes. *N Engl J Med,* 303**,** 349-54.

HONG, J., BOSE, M., JU, J., RYU, J. H., CHEN, X., SANG, S., LEE, M. J. & YANG, C. S. 2004. Modulation of arachidonic acid metabolism by curcumin and related beta-diketone derivatives: effects on cytosolic phospholipase A(2), cyclooxygenases and 5-lipoxygenase. *Carcinogenesis,* 25**,** 1671-9.

HORTON, J. K., WILLIAMS, A. S., SMITH-PHILLIPS, Z., MARTIN, R. C. & O'BEIRNE, G. 1999. Intracellular measurement of prostaglandin E2: effect of anti-inflammatory drugs on cyclooxygenase activity and prostanoid expression. *Anal Biochem,* 271**,** 18-28.

HUHTAKANGAS, J. A., OLIVERA, C. J., BISHOP, J. E., ZANELLO, L. P. & NORMAN, A. W. 2004. The vitamin D receptor is present in caveolae-enriched plasma membranes and binds 1 alpha,25(OH)2-vitamin D3 in vivo and in vitro. *Mol Endocrinol,* 18**,** 2660-71.

HUSSEIN, M. R. 2005. Ultraviolet radiation and skin cancer: molecular mechanisms. *J Cutan Pathol,* 32**,** 191-205.

JANE, S. M., TING, S. B. & CUNNINGHAM, J. M. 2005. Epidermal impermeable barriers in mouse and fly. *Curr Opin Genet Dev,* 15**,** 447-53.

JANJETOVIC, Z., BROZYNA, A. A., TUCKEY, R. C., KIM, T. K., NGUYEN, M. N., JOZWICKI, W., PFEFFER, S. R., PFEFFER, L. M. & SLOMINSKI, A. T. 2011a. High basal NF-[kappa]B activity in nonpigmented melanoma cells is associated with an enhanced sensitivity to vitamin D3 derivatives. *British Journal of Cancer,* 105**,** 1874-1884.

JANJETOVIC, Z., BROZYNA, A. A., TUCKEY, R. C., KIM, T. K., NGUYEN, M. N., JOZWICKI, W., PFEFFER, S. R., PFEFFER, L. M. & SLOMINSKI, A. T. 2011b. High basal NF-kappaB activity in nonpigmented melanoma cells is associated with an enhanced sensitivity to vitamin D3 derivatives. *Br J Cancer,* 105**,** 1874-84.

JANJETOVIC, Z., ZMIJEWSKI, M. A., TUCKEY, R. C., DELEON, D. A., NGUYEN, M. N., PFEFFER, L. M. & SLOMINSKI, A. T. 2009. 20-Hydroxycholecalciferol, product of vitamin D3 hydroxylation by P450scc, decreases NF-kappaB activity by increasing IkappaB alpha levels in human keratinocytes. *PLoS One,* 4**,** e5988.

JENA, N. R. 2012. DNA damage by reactive species: Mechanisms, mutation and repair. *J Biosci,* 37**,** 503-17.

JENA, N. R. & MISHRA, P. C. 2012. Formation of ring-opened and rearranged products of guanine: mechanisms and biological significance. *Free Radic Biol Med,* 53**,** 81-94.

JOHANNESDOTTIR, S. A., CHANG, E. T., MEHNERT, F., SCHMIDT, M., OLESEN, A. B. & SORENSEN, H. T. 2012. Nonsteroidal anti-inflammatory drugs and the risk of skin cancer: a population-based case-control study. *Cancer,* 118**,** 4768-76.

JURUTKA, P. W., BARTIK, L., WHITFIELD, G. K., MATHERN, D. R., BARTHEL, T. K., GUREVICH, M., HSIEH, J. C., KACZMARSKA, M., HAUSSLER, C. A. & HAUSSLER, M. R. 2007. Vitamin D receptor: key roles in bone mineral pathophysiology, molecular mechanism of action, and novel nutritional ligands. *J Bone Miner Res,* 22 Suppl 2**,** V2-10.

KADEKARO, A. L., KAVANAGH, R. J., WAKAMATSU, K., ITO, S., PIPITONE, M. A. & ABDEL-MALEK, Z. A. 2003. Cutaneous photobiology. The melanocyte vs. the sun: who will win the final round? *Pigment Cell Res,* 16**,** 434-47.

KANITAKIS, J. 2002. Anatomy, histology and immunohistochemistry of normal human skin. *Eur J Dermatol,* 12**,** 390-9; quiz 400-1.

KENSLER, T. W., DOLAN, P. M., GANGE, S. J., LEE, J. K., WANG, Q. & POSNER, G. H. 2000. Conceptually new deltanoids (vitamin D analogs) inhibit multistage skin tumorigenesis. *Carcinogenesis,* 21**,** 1341-5.

KHOPDE, S. M., PRIYADARSINI, K. I., GUHA, S. N., SATAV, J. G., VENKATESAN, P. & RAO, M. N. 2000. Inhibition of radiation-induced lipid peroxidation by tetrahydrocurcumin: possible mechanisms by pulse radiolysis. *Biosci Biotechnol Biochem,* 64**,** 503-9.

KREGE, J. H., HODGIN, J. B., COUSE, J. F., ENMARK, E., WARNER, M., MAHLER, J. F., SAR, M., KORACH, K. S., GUSTAFSSON, J. A. & SMITHIES, O. 1998. Generation and reproductive phenotypes of mice lacking estrogen receptor beta. *Proc Natl Acad Sci U S A,* 95**,** 15677-82.

KRIPKE, M. L., COX, P. A., ALAS, L. G. & YAROSH, D. B. 1992. Pyrimidine dimers in DNA initiate systemic immunosuppression in UV-irradiated mice. *Proc Natl Acad Sci U S A,* 89**,** 7516-20.

KULMS, D. & SCHWARZ, T. 2000. Molecular mechanisms of UV-induced apoptosis. *Photodermatol Photoimmunol Photomed,* 16**,** 195-201.

KULMS, D. & SCHWARZ, T. 2002. Independent contribution of three different pathways to ultraviolet-B-induced apoptosis. *Biochem Pharmacol,* 64**,** 837-41.

KUMAR, P. & CLARKE, M. (eds.) 2012. *Clinical Medicine,* Philedelphia, USA: Elsevier.

LEE, J. & YOUN, J. I. 1998. The photoprotective effect of 1,25-dihydroxyvitamin D3 on ultraviolet light B-induced damage in keratinocyte and its mechanism of action. *J Dermatol Sci,* 18**,** 11-8.

LEE, J. K., KIM, J. H., NAM, K. T. & LEE, S. H. 2003. Molecular events associated with apoptosis and proliferation induced by ultraviolet-B radiation in the skin of hairless mice. *J Dermatol Sci,* 32**,** 171-9.

LEHMANN, A. R. 2003. DNA repair-deficient diseases, xeroderma pigmentosum, Cockayne syndrome and trichothiodystrophy. *Biochimie,* 85**,** 1101-11.

LEHMANN, B. & MEURER, M. 2010. Vitamin D metabolism. *Dermatol Ther,* 23**,** 2-12.

LEITER, U. & GARBE, C. 2008. Epidemiology of melanoma and nonmelanoma skin cancer--the role of sunlight. *Adv Exp Med Biol,* 624**,** 89-103.

LIPPENS, S., DENECKER, G., OVAERE, P., VANDENABEELE, P. & DECLERCQ, W. 2005. Death penalty for keratinocytes: apoptosis versus cornification. *Cell Death Differ,* 12 Suppl 2**,** 1497-508.

LIPPENS, S., HOSTE, E., VANDENABEELE, P., AGOSTINIS, P. & DECLERCQ, W. 2009. Cell death in the skin. *Apoptosis,* 14**,** 549-69.

LOSER, K. & BEISSERT, S. 2009. Regulation of cutaneous immunity by the environment: an important role for UV irradiation and vitamin D. *Int Immunopharmacol,* 9**,** 587-9.

MAHEUX, R., NAUD, F., RIOUX, M., GRENIER, R., LEMAY, A., GUY, J. & LANGEVIN, M. 1994. A randomized, double-blind, placebo-controlled study on the effect of conjugated estrogens on skin thickness. *Am J Obstet Gynecol,* 170**,** 642-9.

MAKIN, J. 2011. Implications of climate change for skin cancer prevention in Australia. *Health Promot J Austr,* 22 Spec No**,** S39-41.

MALLOY, P. J., PIKE, J. W. & FELDMAN, D. 1999. The vitamin D receptor and the syndrome of hereditary 1,25-dihydroxyvitamin D-resistant rickets. *Endocr Rev,* 20**,** 156-88.

MANGGAU, M., KIM, D. S., RUWISCH, L., VOGLER, R., KORTING, H. C., SCHAFER-KORTING, M. & KLEUSER, B. 2001. 1Alpha,25-dihydroxyvitamin D3 protects

human keratinocytes from apoptosis by the formation of sphingosine-1-phosphate. *J Invest Dermatol,* 117**,** 1241-9.

MARIE, P. J. & KASSEM, M. 2011. Extrinsic mechanisms involved in age-related defective bone formation. *J Clin Endocrinol Metab,* 96**,** 600-9.

MARIEB, E. N. & HOEHN, K. N. 2012. *Human Anatomy and Physiology,* New Jersey, USA, Pearson Benjamin Cummings.

MASON, R. S., SEQUEIRA, V. B., DIXON, K. M., GORDON-THOMSON, C., POBRE, K., DILLEY, A., MIZWICKI, M. T., NORMAN, A. W., FELDMAN, D., HALLIDAY, G. M. & REEVE, V. E. 2010. Photoprotection by 1alpha,25-dihydroxyvitamin D and analogs: further studies on mechanisms and implications for UV-damage. *J Steroid Biochem Mol Biol,* 121**,** 164-8.

MATSUMURA, Y. & ANANTHASWAMY, H. N. 2002. Short-term and long-term cellular and molecular events following UV irradiation of skin: implications for molecular medicine. *Expert Rev Mol Med,* 4**,** 1-22.

MATSUMURA, Y. & ANANTHASWAMY, H. N. 2004. Toxic effects of ultraviolet radiation on the skin. *Toxicol Appl Pharmacol,* 195**,** 298-308.

MELNIKOVA, V. O. & ANANTHASWAMY, H. N. 2005. Cellular and molecular events leading to the development of skin cancer. *Mutat Res,* 571**,** 91-106.

MENON, V. P. & SUDHEER, A. R. 2007. Antioxidant and anti-inflammatory properties of curcumin. *Adv Exp Med Biol,* 595**,** 105-25.

MICHEL, G., GAILIS, A., JARZEBSKA-DEUSSEN, B., MUSCHEN, A., MIRMOHAMMADSADEGH, A. & RUZICKA, T. 1997. 1,25-(OH)2-vitamin D3 and calcipotriol induce IL-10 receptor gene expression in human epidermal cells. *Inflamm Res,* 46**,** 32-4.

MIZWICKI, M. T., KEIDEL, D., BULA, C. M., BISHOP, J. E., ZANELLO, L. P., WURTZ, J. M., MORAS, D. & NORMAN, A. W. 2004. Identification of an alternative ligand-binding pocket in the nuclear vitamin D receptor and its functional importance in 1alpha,25(OH)2-vitamin D3 signaling. *Proc Natl Acad Sci U S A,* 101**,** 12876-81.

MIZWICKI, M. T., MENEGAZ, D., YAGHMAEI, S., HENRY, H. L. & NORMAN, A. W. 2010. A molecular description of ligand binding to the two overlapping binding pockets of the nuclear vitamin D receptor (VDR): structure-function implications. *J Steroid Biochem Mol Biol,* 121**,** 98-105.

MIZWICKI, M. T. & NORMAN, A. W. 2009. The vitamin D sterol-vitamin D receptor ensemble model offers unique insights into both genomic and rapid-response signaling. *Sci Signal,* 2**,** re4.

MOLIFE, R., LORIGAN, P. & MACNEIL, S. 2001. Gender and survival in malignant tumours. *Cancer Treat Rev,* 27**,** 201-9.

MOURET, S., BAUDOUIN, C., CHARVERON, M., FAVIER, A., CADET, J. & DOUKI, T. 2006. Cyclobutane pyrimidine dimers are predominant DNA lesions in whole human skin exposed to UVA radiation. *Proc Natl Acad Sci U S A,* 103**,** 13765-70.

MURAKAMI, Y., ISHII, H., TAKADA, N., TANAKA, S., MACHINO, M., ITO, S. & FUJISAWA, S. 2008. Comparative anti-inflammatory activities of curcumin and tetrahydrocurcumin based on the phenolic O-H bond dissociation enthalpy, ionization potential and quantum chemical descriptor. *Anticancer Res,* 28**,** 699-707.

MURPHY, G. M. 2009. Ultraviolet radiation and immunosuppression. *Br J Dermatol,* 161 Suppl 3**,** 90-5.

MUTHUSAMY, V. & PIVA, T. J. 2010. The UV response of the skin: a review of the MAPK, NFkappaB and TNFalpha signal transduction pathways. *Arch Dermatol Res,* 302**,** 5-17.

NAITO, M., WU, X., NOMURA, H., KODAMA, M., KATO, Y., KATO, Y. & OSAWA, T. 2002. The protective effects of tetrahydrocurcumin on oxidative stress in cholesterol-fed rabbits. *J Atheroscler Thromb,* 9**,** 243-50.

NEMERE, I., DORMANEN, M. C., HAMMOND, M. W., OKAMURA, W. H. & NORMAN, A. W. 1994. Identification of a specific binding protein for 1 alpha,25-dihydroxyvitamin D3 in basal-lateral membranes of chick intestinal epithelium and relationship to transcaltachia. *J Biol Chem,* 269**,** 23750-6.

NEMERE, I., RAY, R. & MCMANUS, W. 2000. Immunochemical studies on the putative plasmalemmal receptor for 1, 25(OH)(2)D(3). I. Chick intestine. *Am J Physiol Endocrinol Metab,* 278**,** E1104-14.

NEMERE, I., YOSHIMOTO, Y. & NORMAN, A. W. 1984. Calcium transport in perfused duodena from normal chicks: enhancement within fourteen minutes of exposure to 1,25-dihydroxyvitamin D3. *Endocrinology,* 115**,** 1476-83.

NISHIGORI, C. 2006. Cellular aspects of photocarcinogenesis. *Photochem Photobiol Sci,* 5**,** 208-14.

NORMAN, A. W. 2008. From vitamin D to hormone D: fundamentals of the vitamin D endocrine system essential for good health. *Am J Clin Nutr,* 88**,** 491S-499S.

NORMAN, A. W., HENRY, H. L., BISHOP, J. E., SONG, X. D., BULA, C. & OKAMURA, W. H. 2001. Different shapes of the steroid hormone 1alpha,25(OH)(2)-vitamin D(3) act as agonists for two different receptors in the vitamin D endocrine system to mediate genomic and rapid responses. *Steroids,* 66**,** 147-58.

NORMAN, A. W., OLIVERA, C. J., BARRETO SILVA, F. R. & BISHOP, J. E. 2002. A specific binding protein/receptor for 1alpha,25-dihydroxyvitamin D(3) is present in an intestinal caveolae membrane fraction. *Biochem Biophys Res Commun,* 298**,** 414-9.

NORMAN, A. W., SONG, X., ZANELLO, L., BULA, C. & OKAMURA, W. H. 1999. Rapid and genomic biological responses are mediated by different shapes of the agonist steroid hormone, 1alpha,25(OH)2vitamin D3. *Steroids,* 64**,** 120-8.

OKADA, K., WANGPOENGTRAKUL, C., TANAKA, T., TOYOKUNI, S., UCHIDA, K. & OSAWA, T. 2001. Curcumin and especially tetrahydrocurcumin ameliorate oxidative stress-induced renal injury in mice. *J Nutr,* 131**,** 2090-5.

OKAMURA, W. H., MIDLAND, M. M., HAMMOND, M. W., ABD RAHMAN, N., DORMANEN, M. C., NEMERE, I. & NORMAN, A. W. 1995. Chemistry and conformation of vitamin D molecules. *J Steroid Biochem Mol Biol,* 53**,** 603-13.

ORDONEZ-MORAN, P., LARRIBA, M. J., PALMER, H. G., VALERO, R. A., BARBACHANO, A., DUNACH, M., DE HERREROS, A. G., VILLALOBOS, C., BERCIANO, M. T., LAFARGA, M. & MUNOZ, A. 2008. RhoA-ROCK and p38MAPK-MSK1 mediate vitamin D effects on gene expression, phenotype, and Wnt pathway in colon cancer cells. *J Cell Biol,* 183**,** 697-710.

OSAWA, T., SUGIYAMA, Y., INAYOSHI, M. & KAWAKISHI, S. 1995. Antioxidative activity of tetrahydrocurcuminoids. *Biosci Biotechnol Biochem,* 59**,** 1609-12.

PALMER, H. G., ANJOS-AFONSO, F., CARMELIET, G., TAKEDA, H. & WATT, F. M. 2008. The vitamin D receptor is a Wnt effector that controls hair follicle differentiation and specifies tumor type in adult epidermis. *PLoS One,* 3**,** e1483.

PARI, L. & AMALI, D. R. 2005. Protective role of tetrahydrocurcumin (THC) an active principle of turmeric on chloroquine induced hepatotoxicity in rats. *J Pharm Pharm Sci,* 8**,** 115-23.

PARK, H. Y., KOSMADAKI, M., YAAR, M. & GILCHREST, B. A. 2009. Cellular mechanisms regulating human melanogenesis. *Cell Mol Life Sci,* 66**,** 1493-506.

PATTISON, D. I. & DAVIES, M. J. 2006. Actions of ultraviolet light on cellular structures. *EXS***,** 131-57.

PELLETIER, G. & REN, L. 2004. Localization of sex steroid receptors in human skin. *Histol Histopathol,* 19**,** 629-36.

PENDAS-FRANCO, N., GARCIA, J. M., PENA, C., VALLE, N., PALMER, H. G., HEINANIEMI, M., CARLBERG, C., JIMENEZ, B., BONILLA, F., MUNOZ, A. & GONZALEZ-SANCHO, J. M. 2008. DICKKOPF-4 is induced by TCF/beta-catenin and upregulated in human colon cancer, promotes tumour cell invasion and angiogenesis and is repressed by 1alpha,25-dihydroxyvitamin D3. *Oncogene,* 27**,** 4467-77.

PEUS, D., VASA, R. A., BEYERLE, A., MEVES, A., KRAUTMACHER, C. & PITTELKOW, M. R. 1999. UVB activates ERK1/2 and p38 signaling pathways via reactive oxygen species in cultured keratinocytes. *J Invest Dermatol,* 112**,** 751-6.

PFEIFER, G. P. & BESARATINIA, A. 2012. UV wavelength-dependent DNA damage and human non-melanoma and melanoma skin cancer. *Photochem Photobiol Sci,* 11**,** 90-7.

POLAKIS, P. 2000. Wnt signaling and cancer. *Genes Dev,* 14**,** 1837-51.

POLIAKOV, S. 2009. *Photoprotection by a potential vitamin D analog.* Bachelor of Medical Science (Hons), University of Sydney.

PRESTON, D. S. & STERN, R. S. 1992. Nonmelanoma cancers of the skin. *N Engl J Med,* 327**,** 1649-62.

RANGWALA, S. & TSAI, K. Y. 2011. Roles of the immune system in skin cancer. *Br J Dermatol,* 165**,** 953-65.

RASTOGI, R. P., RICHA, KUMAR, A., TYAGI, M. B. & SINHA, R. P. 2010. Molecular mechanisms of ultraviolet radiation-induced DNA damage and repair. *J Nucleic Acids,* 2010**,** 592980.

RAVANAT, J. L., DOUKI, T. & CADET, J. 2001. Direct and indirect effects of UV radiation on DNA and its components. *J Photochem Photobiol B,* 63**,** 88-102.

REEVE, V. E. 2002. Ultraviolet radiation and the contact hypersensitivity reaction in mice. *Methods,* 28**,** 20-4.

REEVE, V. E., ALLANSON, M., CHO, J. L., ARUN, S. J. & DOMANSKI, D. 2009. Interdependence between heme oxygenase-1 induction and estrogen-receptor-beta signaling mediates photoimmune protection by UVA radiation in mice. *J Invest Dermatol,* 129**,** 2702-10.

REEVE, V. E., ALLANSON, M., DOMANSKI, D. & PAINTER, N. 2012. Gender differences in UV-induced inflammation and immunosuppression in mice

reveal male unresponsiveness to UVA radiation. *Photochem Photobiol Sci,* 11**,** 173-9.

REEVE, V. E., NISHIMURA, N., BOSNIC, M., MICHALSKA, A. E. & CHOO, K. H. 2000. Lack of metallothionein-I and -II exacerbates the immunosuppressive effect of ultraviolet B radiation and cis-urocanic acid in mice. *Immunology,* 100**,** 399-404.

RIIS, J. L., JOHANSEN, C., GESSER, B., MOLLER, K., LARSEN, C. G., KRAGBALLE, K. & IVERSEN, L. 2004. 1alpha,25(OH)(2)D(3) regulates NF-kappaB DNA binding activity in cultured normal human keratinocytes through an increase in IkappaBalpha expression. *Arch Dermatol Res,* 296**,** 195-202.

ROBERTSON, A. B., KLUNGLAND, A., ROGNES, T. & LEIROS, I. 2009. DNA repair in mammalian cells: Base excision repair: the long and short of it. *Cell Mol Life Sci,* 66**,** 981-93.

ROZA, L., VAN DER WULP, K. J., MACFARLANE, S. J., LOHMAN, P. H. & BAAN, R. A. 1988. Detection of cyclobutane thymine dimers in DNA of human cells with monoclonal antibodies raised against a thymine dimer-containing tetranucleotide. *Photochem Photobiol,* 48**,** 627-33.

RYAN, A. 2010. *Photoprotection by vitamin D-like compounds.* Bachelor of Medical Science (Honours), University of Sydney.

RYBCHYN, M. S., SLATER, M., CONIGRAVE, A. D. & MASON, R. S. 2011. An Akt-dependent increase in canonical Wnt signaling and a decrease in sclerostin protein levels are involved in strontium ranelate-induced osteogenic effects in human osteoblasts. *J Biol Chem,* 286**,** 23771-9.

SAMUEL, S. & SITRIN, M. D. 2008. Vitamin D's role in cell proliferation and differentiation. *Nutr Rev,* 66**,** S116-24.

SEGDITSAS, S. & TOMLINSON, I. 2006. Colorectal cancer and genetic alterations in the Wnt pathway. *Oncogene,* 25**,** 7531-7.

SEIDENARI, S., PAGNONI, A., DI NARDO, A. & GIANNETTI, A. 1994. Echographic evaluation with image analysis of normal skin: variations according to age and sex. *Skin Pharmacol,* 7**,** 201-9.

SEQUEIRA, V. B. 2011. Doctor of Philosophy, University of Sydney.

SEQUEIRA, V. B., RYBCHYN, M. S., GORDON-THOMSON, C., TONGKAO-ON, W., MIZWICKI, M. T., NORMAN, A. W., REEVE, V. E., HALLIDAY, G. M. & MASON, R. S. 2012a. Opening of Chloride Channels by 1alpha,25-Dihydroxyvitamin D(3) Contributes to Photoprotection against UVR-Induced Thymine Dimers in Keratinocytes. *J Invest Dermatol*.

SEQUEIRA, V. B., RYBCHYN, M. S., TONGKAO-ON, W., GORDON-THOMSON, C., MALLOY, P. J., NEMERE, I., NORMAN, A. W., REEVE, V. E., HALLIDAY, G. M., FELDMAN, D. & MASON, R. S. 2012b. The role of the vitamin D receptor and ERp57 in photoprotection by 1alpha,25-dihydroxyvitamin D3. *Mol Endocrinol,* 26**,** 574-82.

SHIVJI, M. K., PODUST, V. N., HUBSCHER, U. & WOOD, R. D. 1995. Nucleotide excision repair DNA synthesis by DNA polymerase epsilon in the presence of PCNA, RFC, and RPA. *Biochemistry,* 34**,** 5011-7.

SHUSTER, S., BLACK, M. M. & MCVITIE, E. 1975. The influence of age and sex on skin thickness, skin collagen and density. *Br J Dermatol,* 93**,** 639-43.

SJOSTROM, L., SMITH, U., KROTKIEWSKI, M. & BJORNTORP, P. 1972. Cellularity in different regions of adipose tissue in young men and women. *Metabolism,* 21**,** 1143-53.

SKOBOWIAT, C., DOWDY, J. C., SAYRE, R. M., TUCKEY, R. C. & SLOMINSKI, A. 2011. Cutaneous hypothalamic-pituitary-adrenal axis homolog: regulation by ultraviolet radiation. *Am J Physiol Endocrinol Metab,* 301**,** E484-93.

SLOMINSKI, A., ERMAK, G. & MIHM, M. 1996. ACTH receptor, CYP11A1, CYP17 and CYP21A2 genes are expressed in skin. *J Clin Endocrinol Metab,* 81**,** 2746-9.

SLOMINSKI, A., JANJETOVIC, Z., TUCKEY, R. C., NGUYEN, M. N., BHATTACHARYA, K. G., WANG, J., LI, W., JIAO, Y., GU, W., BROWN, M. & POSTLETHWAITE, A. E. 2013. 20S-hydroxyvitamin D3, noncalcemic product of CYP11A1 action on vitamin D3, exhibits potent antifibrogenic activity in vivo. *J Clin Endocrinol Metab,* 98**,** E298-303.

SLOMINSKI, A., SEMAK, I., ZJAWIONY, J., WORTSMAN, J., LI, W., SZCZESNIEWSKI, A. & TUCKEY, R. C. 2005. The cytochrome P450scc system opens an alternate pathway of vitamin D3 metabolism. *FEBS J,* 272**,** 4080-90.

SLOMINSKI, A., ZJAWIONY, J., WORTSMAN, J., SEMAK, I., STEWART, J., PISARCHIK, A., SWEATMAN, T., MARCOS, J., DUNBAR, C. & R, C. T. 2004. A novel pathway for sequential transformation of 7-dehydrocholesterol and expression of the P450scc system in mammalian skin. *Eur J Biochem,* 271**,** 4178-88.

SLOMINSKI, A. T., JANJETOVIC, Z., FULLER, B. E., ZMIJEWSKI, M. A., TUCKEY, R. C., NGUYEN, M. N., SWEATMAN, T., LI, W., ZJAWIONY, J., MILLER, D., CHEN, T. C., LOZANSKI, G. & HOLICK, M. F. 2010. Products of vitamin D3 or 7-dehydrocholesterol metabolism by cytochrome P450scc show anti-leukemia effects, having low or absent calcemic activity. *PLoS One,* 5**,** e9907.

SLOMINSKI, A. T., KIM, T. K., CHEN, J., NGUYEN, M. N., LI, W., YATES, C. R., SWEATMAN, T., JANJETOVIC, Z. & TUCKEY, R. C. 2012. Cytochrome P450scc-dependent metabolism of 7-dehydrocholesterol in placenta and epidermal keratinocytes. *Int J Biochem Cell Biol,* 44**,** 2003-18.

SOMPARN, P., PHISALAPHONG, C., NAKORNCHAI, S., UNCHERN, S. & MORALES, N. P. 2007. Comparative antioxidant activities of curcumin and its demethoxy and hydrogenated derivatives. *Biol Pharm Bull,* 30**,** 74-8.

SONG, E. J. 2014.

SONG, E. J., GORDON-THOMSON, C., COLE, L., STERN, H., HALLIDAY, G. M., DAMIAN, D. L., REEVE, V. E. & MASON, R. S. 2012. 1alpha,25-Dihydroxyvitamin D(3) reduces several types of UV-induced DNA damage and contributes to photoprotection. *J Steroid Biochem Mol Biol*.

SOULTANAKIS, R. P., MELAMEDE, R. J., BESPALOV, I. A., WALLACE, S. S., BECKMAN, K. B., AMES, B. N., TAATJES, D. J. & JANSSEN-HEININGER, Y. M. 2000. Fluorescence detection of 8-oxoguanine in nuclear and mitochondrial DNA of cultured cells using a recombinant Fab and confocal scanning laser microscopy. *Free Radic Biol Med,* 28**,** 987-98.

SPEED, N. & BLAIR, I. A. 2011. Cyclooxygenase- and lipoxygenase-mediated DNA damage. *Cancer Metastasis Rev,* 30**,** 437-47.

ST-ARNAUD, R. 2008. The direct role of vitamin D on bone homeostasis. *Arch Biochem Biophys,* 473**,** 225-30.

STAPLES, M., MARKS, R. & GILES, G. 1998. Trends in the incidence of non-melanocytic skin cancer (NMSC) treated in Australia 1985-1995: are primary prevention programs starting to have an effect? *Int J Cancer,* 78**,** 144-8.

STAPLES, M. P., ELWOOD, M., BURTON, R. C., WILLIAMS, J. L., MARKS, R. & GILES, G. G. 2006. Non-melanoma skin cancer in Australia: the 2002 national survey and trends since 1985. *Med J Aust,* 184**,** 6-10.

STEIN, R. C. & WATERFIELD, M. D. 2000. PI3-kinase inhibition: a target for drug development? *Mol Med Today,* 6**,** 347-57.

SUGIYAMA, Y., KAWAKISHI, S. & OSAWA, T. 1996. Involvement of the beta-diketone moiety in the antioxidative mechanism of tetrahydrocurcumin. *Biochem Pharmacol,* 52**,** 519-25.

SURJANA, D., HALLIDAY, G. M. & DAMIAN, D. L. 2013. Nicotinamide enhances repair of ultraviolet radiation-induced DNA damage in human keratinocytes and ex vivo skin. *Carcinogenesis,* 34**,** 1144-9.

TADOKORO, T., KOBAYASHI, N., ZMUDZKA, B. Z., ITO, S., WAKAMATSU, K., YAMAGUCHI, Y., KOROSSY, K. S., MILLER, S. A., BEER, J. Z. & HEARING, V. J. 2003. UV-induced DNA damage and melanin content in human skin differing in racial/ethnic origin. *FASEB J,* 17**,** 1177-9.

TEICHERT, A. E., ELALIEH, H., ELIAS, P. M., WELSH, J. & BIKLE, D. D. 2011. Overexpression of hedgehog signaling is associated with epidermal tumor formation in vitamin D receptor-null mice. *J Invest Dermatol,* 131**,** 2289-97.

THOMAS-AHNER, J. M., WULFF, B. C., TOBER, K. L., KUSEWITT, D. F., RIGGENBACH, J. A. & OBERYSZYN, T. M. 2007. Gender differences in UVB-induced skin carcinogenesis, inflammation, and DNA damage. *Cancer Res,* 67**,** 3468-74.

THOMPSON, B. C., SURJANA, D., HALLIDAY, G. M. & DAMIAN, D. L. 2014. Nicotinamide enhances repair of ultraviolet radiation-induced DNA damage in primary melanocytes. *Exp Dermatol,* 23**,** 509-11.

THORNTON, M. J., TAYLOR, A. H., MULLIGAN, K., AL-AZZAWI, F., LYON, C. C., O'DRISCOLL, J. & MESSENGER, A. G. 2003a. The distribution of estrogen receptor beta is distinct to that of estrogen receptor alpha and the androgen receptor in human skin and the pilosebaceous unit. *J Investig Dermatol Symp Proc,* 8**,** 100-3.

THORNTON, M. J., TAYLOR, A. H., MULLIGAN, K., AL-AZZAWI, F., LYON, C. C., O'DRISCOLL, J. & MESSENGER, A. G. 2003b. Oestrogen receptor beta is the predominant oestrogen receptor in human scalp skin. *Exp Dermatol,* 12**,** 181-90.

TOBIN, D. J. 2006. Biochemistry of human skin-our brain on the outside. *Chemical Society Reviews,* 35**,** 52-67.

TONGKAO-ON, W. 2014.

TONGKAO-ON, W., GORDON-THOMSON, C., RYAN, A., HALLIDAY, G. M., REEVE, V. E. & MASON, R. S. 2012. Photoimmune modulation by 1,25dihydroxyvitaminD is not specific to species or test protocol but may be regulated by gender. University of Sydney.

TUCKEY, R. C., LI, W., ZJAWIONY, J. K., ZMIJEWSKI, M. A., NGUYEN, M. N., SWEATMAN, T., MILLER, D. & SLOMINSKI, A. 2008a. Pathways and products for the metabolism of vitamin D3 by cytochrome P450scc. *FEBS J,* 275**,** 2585-96.

TUCKEY, R. C., NGUYEN, M. N. & SLOMINSKI, A. 2008b. Kinetics of vitamin D3 metabolism by cytochrome P450scc (CYP11A1) in phospholipid vesicles and cyclodextrin. *Int J Biochem Cell Biol,* 40**,** 2619-26.

TUR, E. 1997. Physiology of the skin--differences between women and men. *Clin Dermatol,* 15**,** 5-16.

VAN LAETHEM, A., CLAERHOUT, S., GARMYN, M. & AGOSTINIS, P. 2005. The sunburn cell: regulation of death and survival of the keratinocyte. *Int J Biochem Cell Biol,* 37**,** 1547-53.

VAN LAETHEM, A., GARMYN, M. & AGOSTINIS, P. 2009. Starting and propagating apoptotic signals in UVB irradiated keratinocytes. *Photochem Photobiol Sci,* 8**,** 299-308.

VANTIEGHEM, K., DE HAES, P., BOUILLON, R. & SEGAERT, S. 2006. Dermal fibroblasts pretreated with a sterol Delta7-reductase inhibitor produce 25-hydroxyvitamin D3 upon UVB irradiation. *J Photochem Photobiol B,* 85**,** 72-8.

VERTINO, A. M., BULA, C. M., CHEN, J. R., ALMEIDA, M., HAN, L., BELLIDO, T., KOUSTENI, S., NORMAN, A. W. & MANOLAGAS, S. C. 2005. Nongenotropic, anti-apoptotic signaling of 1alpha,25(OH)2-vitamin D3 and analogs through the ligand binding domain of the vitamin D receptor in osteoblasts and osteocytes. Mediation by Src, phosphatidylinositol 3-, and JNK kinases. *J Biol Chem,* 280**,** 14130-7.

VILLIOTOU, V. & DELICONSTANTINOS, G. 1995. Nitric oxide, peroxynitrite and nitroso-compounds formation by ultraviolet A (UVA) irradiated human squamous cell carcinoma: potential role of nitric oxide in cancer prognosis. *Anticancer Res,* 15**,** 931-42.

WAN, Y. S., WANG, Z. Q., SHAO, Y., VOORHEES, J. J. & FISHER, G. J. 2001. Ultraviolet irradiation activates PI 3-kinase/AKT survival pathway via EGF receptors in human skin in vivo. *Int J Oncol,* 18**,** 461-6.

WANG, H. Q., QUAN, T., HE, T., FRANKE, T. F., VOORHEES, J. J. & FISHER, G. J. 2003. Epidermal growth factor receptor-dependent, NF-kappaB-independent activation of the phosphatidylinositol 3-kinase/Akt pathway inhibits ultraviolet irradiation-induced caspases-3, -8, and -9 in human keratinocytes. *J Biol Chem,* 278**,** 45737-45.

WANG, J., SLOMINSKI, A., TUCKEY, R. C., JANJETOVIC, Z., KULKARNI, A., CHEN, J., POSTLETHWAITE, A. E., MILLER, D. & LI, W. 2012a. 20-hydroxyvitamin D(3) inhibits proliferation of cancer cells with high efficacy while being non-toxic. *Anticancer Res,* 32**,** 739-46.

WANG, W. H., LI, L. F., ZHANG, B. X. & LU, X. Y. 2004. Metallothionein-null mice exhibit reduced tolerance to ultraviolet B injury in vivo. *Clin Exp Dermatol,* 29**,** 57-61.

WANG, X., CHEN, W. R. & XING, D. 2012b. A pathway from JNK through decreased ERK and Akt activities for FOXO3a nuclear translocation in response to UV irradiation. *J Cell Physiol,* 227**,** 1168-78.

WANG, Y., ZHU, J. & DELUCA, H. F. 2012c. Where is the vitamin D receptor? *Arch Biochem Biophys,* 523**,** 123-33.

WARIN, A. P. 1978a. THE ULTRAVIOLET ERYTHEMAS IN MAN. *British Journal of Dermatology,* 98**,** 473-477.

WARIN, A. P. 1978b. The ultraviolet erythemas in man. *Br J Dermatol,* 98**,** 473-7.

WHITACRE, C. C., REINGOLD, S. C. & O'LOONEY, P. A. 1999. A gender gap in autoimmunity. *Science,* 283**,** 1277-8.

WIDYARINI, S., DOMANSKI, D., PAINTER, N. & REEVE, V. E. 2006. Estrogen receptor signaling protects against immune suppression by UV radiation exposure. *Proc Natl Acad Sci U S A,* 103**,** 12837-42.

WILGUS, T. A., BREZA, T. S., JR., TOBER, K. L. & OBERYSZYN, T. M. 2004. Treatment with 5-fluorouracil and celecoxib displays synergistic regression of ultraviolet light B-induced skin tumors. *J Invest Dermatol,* 122**,** 1488-94.

WILGUS, T. A., ROSS, M. S., PARRETT, M. L. & OBERYSZYN, T. M. 2000. Topical application of a selective cyclooxygenase inhibitor suppresses UVB mediated cutaneous inflammation. *Prostaglandins Other Lipid Mediat,* 62**,** 367-84.

WILLIAMS, C. S., MANN, M. & DUBOIS, R. N. 1999. The role of cyclooxygenases in inflammation, cancer, and development. *Oncogene,* 18**,** 7908-16.

WILLIAMS, I. R. & KUPPER, T. S. 1996. Immunity at the surface: homeostatic mechanisms of the skin immune system. *Life Sci,* 58**,** 1485-507.

WONG, G., GUPTA, R., DIXON, K. M., DEO, S. S., CHOONG, S. M., HALLIDAY, G. M., BISHOP, J. E., ISHIZUKA, S., NORMAN, A. W., POSNER, G. H. & MASON, R. S. 2004. 1,25-Dihydroxyvitamin D and three low-calcemic analogs decrease UV-induced DNA damage via the rapid response pathway. *J Steroid Biochem Mol Biol,* 89-90**,** 567-70.

WOOD, A. W., CHANG, R. L., HUANG, M. T., USKOKOVIC, M. & CONNEY, A. H. 1983. 1 alpha, 25-Dihydroxyvitamin D3 inhibits phorbol ester-dependent chemical carcinogenesis in mouse skin. *Biochem Biophys Res Commun,* 116**,** 605-11.

WU, J. C., LAI, C. S., BADMAEV, V., NAGABHUSHANAM, K., HO, C. T. & PAN, M. H. 2011. Tetrahydrocurcumin, a major metabolite of curcumin, induced autophagic cell death through coordinative modulation of PI3K/Akt-mTOR and MAPK signaling pathways in human leukemia HL-60 cells. *Mol Nutr Food Res,* 55**,** 1646-54.

WU, J. C., TSAI, M. L., LAI, C. S., WANG, Y. J., HO, C. T. & PAN, M. H. 2013. Chemopreventative effects of tetrahydrocurcumin on human diseases. *Food Funct,* 5**,** 12-7.

YOSHIZAWA, T., HANDA, Y., UEMATSU, Y., TAKEDA, S., SEKINE, K., YOSHIHARA, Y., KAWAKAMI, T., ARIOKA, K., SATO, H., UCHIYAMA, Y., MASUSHIGE, S., FUKAMIZU, A., MATSUMOTO, T. & KATO, S. 1997. Mice lacking the vitamin D receptor exhibit impaired bone formation, uterine hypoplasia and growth retardation after weaning. *Nat Genet,* 16**,** 391-6.

YU, C., FEDORIC, B., ANDERSON, P. H., LOPEZ, A. F. & GRIMBALDESTON, M. A. 2011. Vitamin D(3) signalling to mast cells: A new regulatory axis. *Int J Biochem Cell Biol,* 43**,** 41-6.

ZANELLO, L. P. & NORMAN, A. 2006. 1alpha,25(OH)2 vitamin D3 actions on ion channels in osteoblasts. *Steroids,* 71**,** 291-7.

ZANELLO, L. P. & NORMAN, A. W. 1996. 1 alpha,25(OH)2 vitamin D3-mediated stimulation of outward anionic currents in osteoblast-like ROS 17/2.8 cells. *Biochem Biophys Res Commun,* 225**,** 551-6.

ZANELLO, L. P. & NORMAN, A. W. 1997. Stimulation by 1alpha,25(OH)2-vitamin D3 of whole cell chloride currents in osteoblastic ROS 17/2.8 cells. A structure-function study. *J Biol Chem,* 272**,** 22617-22.

ZANELLO, L. P. & NORMAN, A. W. 2003. Multiple molecular mechanisms of 1 alpha,25(OH)2-vitamin D3 rapid modulation of three ion channel activities in osteoblasts. *Bone,* 33**,** 71-9.

ZANELLO, L. P. & NORMAN, A. W. 2004a. Electrical responses to 1alpha,25(OH)2-Vitamin D3 and their physiological significance in osteoblasts. *Steroids,* 69**,** 561-5.

ZANELLO, L. P. & NORMAN, A. W. 2004b. Rapid modulation of osteoblast ion channel responses by 1alpha,25(OH)2-vitamin D3 requires the presence of a functional vitamin D nuclear receptor. *Proc Natl Acad Sci U S A,* 101**,** 1589-94.

ZBYTEK, B., JANJETOVIC, Z., TUCKEY, R. C., ZMIJEWSKI, M. A., SWEATMAN, T. W., JONES, E., NGUYEN, M. N. & SLOMINSKI, A. T. 2008a. 20-Hydroxyvitamin D3, a Product of Vitamin D3 Hydroxylation by Cytochrome P450scc, Stimulates Keratinocyte Differentiation. *J Invest Dermatol,* 128**,** 2271-2280.

ZBYTEK, B., JANJETOVIC, Z., TUCKEY, R. C., ZMIJEWSKI, M. A., SWEATMAN, T. W., JONES, E., NGUYEN, M. N. & SLOMINSKI, A. T. 2008b. 20-Hydroxyvitamin D3, a product of vitamin D3 hydroxylation by cytochrome P450scc, stimulates keratinocyte differentiation. *J Invest Dermatol,* 128**,** 2271-80.

ZINSER, G. M., SUNDBERG, J. P. & WELSH, J. 2002. Vitamin D(3) receptor ablation sensitizes skin to chemically induced tumorigenesis. *Carcinogenesis,* 23**,** 2103-9.